On the Cycling of Sulfur and Mercury in the St. Louis River Watershed, Northeastern Minnesota

An Environmental and Natural Trust Fund Final Report

August 15, 2012

Michael Berndt
and
Travis Bavin

Minnesota Department of Natural Resources
500 Lafayette Rd.
St. Paul, MN 55455

Contents

Summary

The biologic reduction of sulfate to sulfide plays an important role in the conversion of mercury to methylmercury (MeHg), a toxic form of the element that is known to accumulate in fish. This study investigates release of sulfate from Minnesota's taconite mining region in the St. Louis River watershed and evaluates its impact on dissolved MeHg concentrations. Extensive sampling and stream gaging were combined three times throughout the watershed while weekly to biweekly samples were collected for more than a year from a site located just upstream from Scanlon Dam in Cloquet, Minnesota, where the United States Geological Survey monitors stream flow. Samples collected periodically throughout the watershed were then compared to samples collected upstream to help identify and quantify the dominant sources of sulfate and to determine if and how it impacts dissolved MeHg concentrations in areas upstream from the Scanlon Dam.

Isotopic methods were used to evaluate sulfur cycling processes. Mine-waters in taconite pits and in wells near the mines were found to contain dissolved sulfate with sulfur and oxygen isotope ratios distinct from those observed in waters collected in the rest of the watershed. Changes in isotope ratios observed in streams leading from the mines reveal that considerable biologic reduction of the sulfate occurs in some, but not all, of the mining watersheds. This sulfate reduction is mostly confined to wetlands or small lakes closest to the mines. An additional unidentified exchange process, also likely biologically controlled, modifies oxygen isotope ratios for dissolved sulfate without changing the sulfur isotope ratios as the mine waters move downstream and mix with low-sulfate non-mining waters in tributaries leading to the St. Louis River. Sulfur and oxygen isotopes in dissolved sulfate for waters collected near Scanlon Dam were consistent with the simple mixing and no evidence of sulfate reduction in the river itself.

The average daily mining and non-mining $SO_4^=$ contributions to the St. Louis River, as determined from measurements at the Scanlon Dam site, are about 35 and 15 metric tons, respectively. Flow versus concentration plots for sulfate and other dissolved components indicate that this loading is highly episodic, rarely reaching a steady state. Rather, the sulfate accumulates relatively slowly in the watershed during winter and dry periods, and is then flushed rapidly downstream during snowmelt and precipitation events. The non-mining waters that flush the St. Louis River during summer high-flow periods have low sulfate, but elevated dissolved aluminum, iron, and manganese. The presence of these dissolved components is consistent with river recharge through oxygen-depleted, organic-rich, soils and sediments. Sulfate concentrations become elevated under dry conditions while iron and aluminum concentrations decrease. These effects are due to reduced recharge from the non-mining regions and possibly also to deposition of colloidally transported iron and aluminum.

Methylmercury, total mercury (THg), and dissolved organic carbon (DOC) concentrations for mining and non-mining streams, measured following a major storm event, were compared to similar non-event data reported for 2007 to 2009. THg/DOC ratios remained constant while MeHg/DOC and DOC concentrations became elevated following the rain event. These chemical trends are interpreted as a natural consequence of stream recharge through oxygen-depleted, organic rich materials.

MeHg/DOC and THg/DOC ratios of waters recharging the rivers is established initially in waters recharged through reduced sediments and soils. Subsequently, demethylation processes under oxidizing conditions decreases MeHg/DOC while preserving the primary THg/DOC ratio. Similarity in MeHg, THg, and DOC relationships for mining and non-mining streams, respectively, suggest that mercury cycling processes are insensitive to sulfate concentration in the central stream. However, elevated MeHg/DOC ratios have been found locally in some wetlands and lakes that directly receive mining waters, particularly when sulfate reduction leads to H_2S generation in amounts that upset the cycling of iron or when sulfate addition takes place in wetlands or peatlands prone to flooding.

Introduction

The St. Louis River basin is well known for its vast mineral resources. The Biwabik Iron Formation, which lies along the northern fringe of the basin (Fig. 1), supports a world class mining district that has supplied iron to the US continuously since the 1890s and could continue to do so for another century or more.   In addition, undeveloped Cu-Ni sulfide/ precious metal deposits can be found along the eastern edge of the St. Louis River watershed, and these are sufficiently large to be considered an important future US mineral resource.

Reports of elevated sulfate ($SO_4^=$) concentrations in the St. Louis River date back at least to the 1940s and 1960s (Maderak, 1963; Moyle and Kenyon, 1947). A previous report by the Minnesota Department of Natural Resources found that $SO_4^=$ loading to the river was variable and seasonal, increasing from approximately 25 tons/day under relatively dry conditions to more than 200 tons/day under relatively wet conditions (Berndt and Bavin, 2009). $SO_4^=$ concentrations were also found to be seasonally variable, highest during dry periods and lowest when water flow in the river was elevated by precipitation and snow melt. However, the detailed SO_4 loading characteristics were not well known, particularly the relative contribution from mining and non-mining sources.

$SO_4^=$ release became a concern on the Iron Range when a growing body of research began supporting a link between bacterial $SO_4^=$ reduction and conversion of mercury (Hg) to methylmercury (MeHg) (Benoit et al., 1999; Gilmour et al., 1992; Jeremiason et al., 2006). MeHg is the type of Hg that accumulates in fish. High Hg concentrations in fish have led to issuance of fish consumption advisories throughout the state, including the St. Louis River and its estuary on Lake Superior.

The stream survey presented here is a part of a more comprehensive effort funded by Minnesota's Environmental and Natural Resources Trust Fund. Other studies conducted by this effort evaluated sulfur isotope distributions in drill core from the Biwabik Iron Formation (Theriault et al., 2011), Hg and $SO_4^=$ cycling in sediments from the St. Louis River's estuary on Lake Superior (Johnson and Beck, 2012), and cycling of iron (Fe), calcium (Ca), and magnesium (Mg) in high- $SO_4^=$ pit water when $SO_4^=$ reduction to sulfide was promoted by addition of a variety of organic carbon and Fe sources (Johnson and Zhu, 2012).   Together with these documents, this reports adds much detail to what was previously a limited understanding of how and when $SO_4^=$ is added to the St. Louis River and how it behaves in reference to production and transport of MeHg.

Stream gaging was combined in this case with chemical analysis at many points along mining streams to help provide information on $SO_4^=$ loading and sulfur cycling processes on a sub-watershed scale. Major cation and anion concentrations were analyzed along with the isotopic compositions of sulfur and oxygen in dissolved $SO_4^=$ ($\delta^{34}S_{SO4}$ and $\delta^{18}O_{SO4}$, respectively). Samples were also collected weekly to biweekly from July 2010 to November 2011 from a site located well downstream from the mining region in the St. Louis River. This sampling site, referred to as Site 001, was located several miles upstream from the Scanlon Dam where flow is monitored continuously by the United States Geological Survey (USGS). Thus, measurements on waters collected from this site provide a near continuous record of loading and sulfur cycling processes at the scale of the watershed north of Cloquet.

Additionally, an extensive set of samples was collected following a relatively large summer rain event that was mostly focused over the mining district. Total mercury (THg), MeHg, and DOC were analyzed during this period to allow comparison with previously reported results for these elements from the same area for samples that were collected under less extreme flow conditions (Berndt and Bavin, 2011, 2012). This data set also allowed comparison of event driven MeHg release in this watershed, where elevated $SO_4^=$ levels are common, with MeHg release observed following a major runoff event in two low-$SO_4^=$ streams in east central Minnesota (Balogh et al., 2004).

Special emphasis in this report is also placed on Fe transport. Fe available is particularly important in determining the impacts of $SO_4^=$ reduction on wetland processes (Berndt and Bavin, 2011; Geurts et al., 2009; Lamers et al., 2002; Lamers et al., 1998). In particular, concentrations of hydrogen sulfide (H_2S), a species that can be toxic to plants and which may promote MeHg transport as a volatile bisulfide species ($MeHgHS^0$) (Gray and Hines, 2009; Jonsson et al., 2010), is limited by the presence or absence of a reduced Fe source (Chapelle et al., 2009). Moreover, iron oxides and oxy-hydroxides are important phases that control transport of phosphorus (P), an element that is often rate-limiting for algae growth in surface waters. If H_2S combines with all available Fe^{++} in a pore fluid environment, then an important control on eutrophication can be lost (Geurts et al., 2009; Lamers et al., 2002; Lamers et al., 1998).

Finally, although a legal standard exists in Minnesota for $SO_4^=$ in water bodies where wild rice can grow (10 mg/L, currently under review), no such standard exists to regulate the potential for this species to affect dissolved methyl mercury or mercury in fish. This report does not determine whether a standard of this type should or should not exist, but simply provides data and interpretations that may be used by future decision makers tasked with deciding this issue.

Methods

Sampling Site Selection

Prior to sampling, the Minnesota Department of Natural Resources analyzed maps, air photos, and reports to identify likely $SO_4^=$ sources in the mining region. The sites identified were then visited in the field prior to the start of sampling activities. Sites were selected, in some cases, to permit direct comparison of upstream and downstream samples. Mixing and chemical processes taking place

between the sites could then be determined.   Two sites were also sampled to allow characterization of inputs from the two large non-mining watersheds in the region (Whiteface and Cloquet Rivers).   Surface water samples were collected and water flow measurements were made at all or some of these sampling locations on three separate occasions: August 10 to 12 and September 14 to 16 in 2010 and March 8 in 2011. Locations for these sites are provided in Appendix A1. Site 001 was located on the St. Louis River in Cloquet which is downstream from all of the other sites, as described earlier.   Samples at this site were collected weekly to biweekly beginning July 2010 until November 2011.

An additional set of samples was collected and analyzed for Hg, MeHg, and dissolved organic carbon (DOC) during the August 2010 sampling trip. This sampling occurred eight to ten days after a major precipitation event in the mining region. As mentioned previously, these samples were collected to allow comparison with similar data from a previous study that was conducted when smaller storms and drier conditions prevailed in the watershed (Berndt and Bavin, 2012) and also for comparison against similar data from a precipitation event in a low $SO_4^=$ watershed (Balogh et al., 2004).

Chemical Analysis

All chemical analyses were made on grab samples collected from shore using either a Teflon sampling cup (always used for Hg and MeHg sample collection) or a plastic sampling bottle. The temperature and pH of each sample collected during the watershed surveys was measured in the field using a portable temperature probe and pH meter (Beckman Model 255).   Conductivity was also determined for those samples using a portable conductivity meter (Myron L Conductivity Meter, Model EP-10).

For cation and anion analysis, 60 mL samples were filtered in the field using a portable vacuum pump and acid-washed, 0.45 μm Nalgene filters. The cation samples were preserved with nitric acid and both cation and anion samples were shipped cold to the University of Minnesota – Geochemistry Laboratory (Minneapolis, MN) for analysis by ICP –AES and ion-chromatography, respectively.   Samples from the Scanlon Dam site were refrigerated for periods varying between a few weeks to two months prior to analysis. Comparison of analyses conducted on same samples analyzed immediately following and up to several months after sample collection indicated that storage time made no difference for the major cation and anion concentrations analyzed at this site.

Mercury samples were always collected using a Teflon sampling cup and were processed using clean hands/dirty hands techniques. All Hg samples were filtered in the field by pulling ~500 ml of water through a pre-packaged, 0.45 μm, sterile Nalgene filter and were stored in Nalgene sterile square media bottles after preserving with HCl in the field. Sample blanks and duplicates were also included with this set of samples to ensure the sampling method was not introducing any appreciable Hg or MeHg to the samples. These samples were shipped cold to the Minnesota Department of Health Laboratory (St. Paul, MN) within a few days of their collection and were analyzed using US EPA Method 1631, Revision E for total mercury (THg) and US EPA Method 1630 for MeHg.

Sulfur and Oxygen Isotopes in Dissolved Sulfate ($\delta^{34}S_{SO4}$ and $\delta^{18}O_{SO4}$)

One liter samples were collected and shipped to the University of Waterloo Environmental Isotope Laboratory (Waterloo, CA) where they were analyzed for $\delta^{34}S$ and $\delta^{18}O$ in dissolved $SO_4^=$ ($^{34}S_{SO4}$ and $\delta^{18}O_{SO4}$, respectively). The samples collected at the beginning of the season were filtered at the isotope laboratory while the samples collected after September 15th were filtered at the DNR lab in Hibbing, MN using 0.7 µm filter paper. This change in procedures was requested by the analytical facility because the DNR was better facilitated to filter large samples. Low-$SO_4^=$ samples were either evapo-concentrated using a hot plate or were passed through an anion exchange column containing 5.0 mL of resin (BIO-Rad AG-1-X8 anion exchange resin). The $SO_4^=$ was then precipitated from the samples with excess $BaCl_2 \cdot 2H_2O$. Relative ^{34}S and ^{32}S abundances for the precipitates were determined using an Isochrom Continuous Flow Stable Isotope Ratio Mass Spectrometer (GV Instruments, Micromass, UK) coupled to a Costech Elemental Analyzer (CNSO 2010, UK). Relative ^{18}O and ^{16}O abundances for the precipitate were determined using a GVI Isoprime Mass Spectrometer coupled to a Hekatech High Temperature Furnace and a Euro Vector Elemental Analyzer.

$\delta^{34}S_{SO4}$ and $\delta^{18}O_{SO4}$ values are reported in this document using standard per mil notation (‰) which is a convenient means for reporting small ratios that vary by small amounts. For sulfur, the reported value represents the difference between the $^{34}S/^{32}S$ ratio measured in the sample and an accepted standard value (FeS in Canyon Diablo meteorite) multiplied by a factor of $1000/(^{34}S/^{32}S$ in the standard). A $\delta^{34}S_{SO4}$ value of 1‰ means, for example, that the $^{34}S/^{32}S$ ratio in the sample is 0.1% higher than the measured standard value. For $\delta^{18}O_{SO4}$ the reported values represent the difference between $^{18}O/^{16}O$ ratio measured in the sample and the $^{18}O/^{16}O$ ratio for H_2O in Standard Mean Ocean Water (SMOW), also multiplied by a factor of $1000/(^{18}O/^{16}O$ in the standard).

Stream Gaging

Flow gaging was included during the August and September sampling rounds and also, less extensively, during the March sampling round. The DNR uses standard flow meters for stream gaging, including Price AA and Pygmy meters, Acoustic Doppler Current Profilers, and Acoustic Velocity Meters, depending on equipment availability and stream size. The DNR Division of Waters follows the standards and quality control procedures for discharge measurement and computation provided in Rantz (1982).

Results

Watershed Survey

Measured flow rates are presented along with $SO_4^=$ and other cation and anion concentrations, as well as pH, temperature, and $\delta^{34}S_{SO4}$ and $\delta^{18}O_{SO4}$ values in Appendix A2 at the end of this report. Flow rates, $SO_4^=$ concentration, calculated $SO_4^=$ loading rates, and $\delta^{34}S_{SO4}$ and $\delta^{18}O_{SO4}$ values are also provided graphically in Figures 3 to 5. A network "stick-and-ball" representation is used to provide geographical context for the data at each of the sites. In each case, the values plotted at the base of the plot represent the value obtained at the St. Louis River near the Scanlon Dam (Site 001) at the same time that the samples were collected throughout the watershed. The values plotted at levels above this are

for samples collected in the tributaries just upstream from their confluence with the St. Louis River. Results for samples collected from stream sites closer to the mining region are represented at progressively higher levels in each plot with a line connecting them to the downstream site that it drains into.

The total flow from the seven mining tributaries is typically only a small fraction of the total flow in the St. Louis River at Cloquet (Figure 3). Swan and Embarrass rivers were the largest water sources among the mining tributaries. Progressively smaller flows were measured in West Two, East Two, and Partridge Rivers, respectively. Elbow and Long Lake Creeks provided relatively limited water input from the mining watersheds. The direct mining inputs typically accounted for a relatively small fraction of the total water entering the St. Louis River at the mining stream's confluence with the St. Louis River. Thus, flow volumes continue to build downstream from the mining region in each watershed as water from other sources, generally non-mining, entered and mixed with waters from the mines. Mixing between mining and non-mining waters is an important process not just in the St. Louis River, but even within the mining watersheds themselves.

Mining stream confluence $SO_4^=$ concentrations ranged from 15 to 151 mg L^{-1} during the August sampling round (Figure 4A, left side) and between 17 and 121 mg L^{-1} during the September sampling round (Figure 4B, left side), but increased to 28 to 241 mg L^{-1} during the March 2011 sampling round (Figure 4A, left side). The winter increases in $SO_4^=$ concentration may result from the exclusion of salts during partial freezing of mining waters within the watershed. There may also be less input of low-sulfate surface waters from non-mining areas during this time period. No winter samples were collected from Cloquet or Whiteface rivers, but summer $SO_4^=$ concentrations were 2 to 4 mg L^{-1} in the samples collected in August and September 2010. The highest measured concentration within the watershed was 1080 mg L^{-1} in Second Creek near its confluence with the Partridge River (Site 021). Concentration, downstream from this site, decreased greatly because it is mixed into a large amount of low-$SO_4^=$ water from the main branch of the Partridge River.

In contrast to $SO_4^=$ concentrations, $SO_4^=$ loading stayed about the same or increased downstream in mining streams. East Two River was the exception during the surveys. Its load appeared to decrease downstream during the August and March sampling periods. As will be shown below, $SO_4^=$ isotopic data suggest that little, if any, net $SO_4^=$ reduction occurred in this stream south of Lake Manganika's outlet (Site 073). Thus, this stream's loading rates were apparently not at a steady state. Primary $SO_4^=$ sources appeared to be widespread in the St. Louis River system, with $SO_4^=$ loading from the five largest mining tributaries each delivering from 4.8 to 11 metric tons/day of $SO_4^=$ to the stream in August (total = 38.7 metric tons/day) and 3.8 to 9.3 metric tons/day during the September sampling round (34.2 metric tons/day total). March $SO_4^=$ loads for these same five tributaries decreased to between 2.2 and 7.1 metric tons/day (Total = 20.7 metric tons/day) owing to the greatly reduced flow rates.

The total $SO_4^=$ load in the mining streams during the August sampling round exceeded that measured at the same time for the St. Louis River in Cloquet showing that (1) most of the $SO_4^=$ in the stream during this period was being provided to the river from the sampled mining streams (rather than from other streams that were not sampled) and (2) the river is not at steady state from a daily $SO_4^=$ mass

loading perspective. The $SO_4^=$ load in water passing through the Scanlon Dam changes rapidly from day to day. The waters with high $SO_4^=$ concentrations observed in mining watersheds and in the St. Louis River during dry periods are flushed rapidly downstream by waters entering the St. Louis River when wetter conditions prevail.

The isotopic data set (Figure 5A-C) provides clues on how $SO_4^=$ is produced in the headwaters and how sulfur cycles within the watershed. Dissolved $SO_4^=$ with highly negative $\delta^{18}O_{SO4}$ values were only found far upstream in the headwater areas, closest to where the mines discharge water into the watersheds.   Downstream $\delta^{18}O_{SO4}$ values were commonly shifted upward compared to their upstream values in mining tributaries, particularly when the upstream values were negative. In contrast, $\delta^{34}S_{SO4}$ in many of the rivers changed by only a small amount compared to the observed changes in $\delta^{18}O_{SO4}$. The exception in both cases was the Embarrass River, but only a small fraction of the total load in this river was sampled in its upstream sites. Downstream changes in the isotopic composition of $SO_4^=$ could, in this case, be caused by mixing with $SO_4^=$ from other sources.

$\delta^{34}S_{SO4}$ and $\delta^{18}O_{SO4}$ were both elevated in the samples from Elbow Creek, Long Lake Creek, and the upper Embarrass River.   Simultaneous elevation of both $\delta^{34}S_{SO4}$ and $\delta^{18}O_{SO4}$ suggests bacterial $SO_4^=$ reduction is active in the areas upstream of the sample collection sites. Bacteria preferentially process the lighter isotopes during $SO_4^=$ reduction, so any $SO_4^=$ remaining in the stream is enriched in the heavier isotopes (Brunner et al., 2005; Detmers et al., 2001).   Isotopic systematic for $SO_4^=$ during reduction to sulfide in five wetlands and a lake on the iron range were evaluated previously by Berndt and Bavin (2011) although formation of elemental sulfur was also suspected in several locations. Elemental sulfur formation and its subsequent disproportionation into H_2S and $SO_4^=$ can affect isotopic systematics for dissolved $SO_4^=$ (Bottcher and Thamdrup, 2001; Canfield et al., 1998; Wu et al., 2011; Zerkle et al., 2009; Zerkle et al., 2010). However, in this paper sulfur cycling is discussed in terms of two end-member processes, $SO_4^=$ reduction to sulfide and sulfide oxidation to $SO_4^=$. Current ongoing studies at specific sites are expected to provide a more detailed accounting of the isotopic systematic in sites were elemental S is specifically identified.

Dissolved THg and MeHg are plotted against dissolved organic carbon concentrations for the high flow (August-2010) sampling period (Fig 6). Total Hg forms a linear relationship with DOC. MeHg, on the other hand, appears to show almost no relationship with respect to DOC. This difference in behavior between MeHg and THg is enigmatic because MeHg makes up a considerable fraction of the THg measured in these samples.

Scanlon Site

Flow rates and $SO_4^=$ concentrations for July 2010 to November 2011 at Site 001 are presented in the appendix (Appendices A2 and A3) and plotted in Figure 7. Eight high flow periods were recognized, including an extended spring runoff event in April and May 2011.   Water levels in this river are characterized by periods of relative dryness, where flow rates are well below the stream average, and comparatively high flow events following storms, general wet periods, or snowmelt.   Storms in the watershed can cause flows in the river to quickly increase by 10 to 30 times what they are under dry

conditions.   Flow rates almost never stay close to their long term average flow rates except under winter base flow conditions.

$SO_4^=$ concentrations at the Scanlon site ranged from approximately 5 mg L^{-1} during high flow periods up to over 30 mg L^{-1} during an extended dry period at the end of the study.   Conditions were sufficiently dry from September to December 2011, that the river was augmented by addition of water from mine pits. This additional source of water, likely with elevated $SO_4^=$, may help to explain why concentrations varied at the Scanlon site during two periods of similar dryness (21 mg L^{-1} in August 2011 versus 32 mg L^{-1} in November 2012).   Winter base flow $SO_4^=$ concentrations were approximately 15 mg L^{-1}. The un-weighted average $SO_4^=$ concentration for samples collected at this site for the whole period was 13.7 mg L^{-1}.

$\delta^{34}S_{SO4}$ and $\delta^{18}O_{SO4}$ for water sampled at the Scanlon site are included in Appendix A2 and also are plotted in Figure 9. Waters sampled from Site 001 during the two extremely high flow periods generally had $\delta^{34}S_{SO4}$ and $\delta^{18}O_{SO4}$ values both approaching +6 ‰. The extended summer drought at the end of 2011 produced waters with higher-than-average $\delta^{34}S_{SO4}$ and lower-than-average $\delta^{18}O_{SO4}$ values, respectively, of +9 and 0 to 1, respectively. The $\delta^{18}O_{SO4}$ values during this period, in particular, are consistent with additional input of a relatively unaltered mining load to the normal river's load, probably related to upstream augmentation from a mine pit.

Winter base flow values for $\delta^{34}S_{SO4}$ ranged from about +7 ‰ to slightly over +8 ‰, a range that is intermediate to the high values observed during drought periods and low compared to values observed during peak runoff events. $\delta^{18}O_{SO4}$ values in winter were between +3 and +4, which was also intermediate to values found under drought and peak runoff conditions. However, unlike $\delta^{34}S_{SO4,}$ peak runoff produced waters high $\delta^{18}O_{SO4}$ values at Site 001, and drought conditions low values. Thus, $\delta^{34}S_{SO4}$ and $\delta^{18}O_{SO4}$ values in the main river vary in directions opposite to each other, which is not typical of a $SO_4^=$ reduction process. $SO_4^=$ reduction processes should produce simultaneous increases in both $\delta^{34}S_{SO4}$ and $\delta^{18}O_{SO4}$. This implies that simple mixing of waters from two isotopically distinct sources, broadly termed mining and non-mining here, may account for the majority of isotopic variation at this site.

Discussion

Sulfate Concentrations and Loading

Surface waters obtain their chemistry by interaction with minerals and microbial populations in the biosphere. Although $SO_4^=$ is present in precipitation at around 1 mg L^{-1} (NADP, 2012), the majority of $SO_4^=$ entering streams on the Iron Range is generated when small amounts of iron sulfide present in waste rock and mine tailings are exposed to oxygen in air (Berndt and Bavin, 2009; Theriault, 2011). The sulfide in iron sulfides is converted to soluble $SO_4^=$ that is easily rinsed into surface waters while the iron is converted to insoluble ferric oxy-hydroxide phases. Reactions with the other phases typically present in iron formation rocks, particularly the Fe- and Mg-rich carbonates, creates water with distinctly elevated pH, where the elevated $SO_4^=$ and HCO_3^- anion concentrations are balanced mostly by divalent cations, Mg^{++} and Ca^{++}, but also, to a lesser extent, Na^+ and K^+ (Berndt and Bavin, 2009).

An important clue to how $SO_4^=$ loading occurs to the St. Louis River can be found by examination of a plot of $SO_4^=$ load at the Scanlon site as a function of flow rate (Figure 9). The plot reveals a relatively linear trend with a slope of approximately 0.015 (metric tons/day)/(cfs) and intercept of 20.1 metric tons/day. Such a trend might be expected for a base flow containing somewhat greater than 20.1 tons of $SO_4^=$ from mining to which is added a much greater source of water containing approximately 6 mg L^{-1} derived from the rest of the watershed.   However, the actual case is more complicated than this. Actual watershed inputs from streams where no mining is taking place in this area rarely carry water with 6 mg L^{-1} or more of dissolved $SO_4^=$. The averaged $SO_4^=$ concentrations for the two non-mining streams sampled in this study (Cloquet and Whiteface rivers) were 2.0 and 2.9 mg L^{-1} $SO_4^=$, respectively. Moreover, Berndt and Bavin (2011) systematically sampled the Cloquet and Whiteface Rivers seven times at their confluences and also the St. Louis River upstream from the mining regions. They reported $SO_4^=$ concentrations (mg L^{-1}) as follows: Cloquet River, 2.9 ± 0.4; Whiteface River, 4.1 ± 1.5; St. Louis River sampled upstream from the mining region, 2.9 ± 1.4.

 Thus, the average $SO_4^=$ concentrations in this region for streams with no mining influence appears to be close to 3 mg L^{-1}, a value that is approximately half that implied by the relatively steep slope displayed in Figure 9. Mining-and non-mining sourced loads at Site 001 increase together during periods of high flow in such a way that a total slope equivalent to 6 mg L^{-1} is maintained through event periods. This suggests that the $SO_4^=$ accumulated in the river during periods of low flow is generally flushed downstream through Site 001 during periods of high flow.

 The degree to which this $SO_4^=$ is rinsed from the system on a seasonal basis is illustrated in Figure 10, which allocates $SO_4^=$ at the Scanlon site to its original source, mining or non-mining. If an average value of approximately 3 mg L^{-1} $SO_4^=$ is applied for waters not impacted by mining, then the mining load can be estimated by assigning all $SO_4^=$ above 3 mg L^{-1} as arising from mining. This method will likely under-estimate mining load during wet periods (when non-mining streams frequently have less that 3 mg L^{-1}) and overestimate it during dry periods (when non-mining streams have higher $SO_4^=$ concentrations). Nevertheless, this simple model allows clear illustration of the general relationship between flow rate and sources to the St. Louis River (Figure 10). The mining load typically varies between about 20 and 40 tons per day (average = 35 tons/day) but can easily and quickly increase to over 100 tons/day when the river is flushed out by waters from the non-mining portions of the watershed. Non-mining $SO_4^=$ is significant (average = 15 tons/day), especially during periods of high flow, when loads can temporarily approach contributions from the mining industry.

Sulfur Cycling ($\delta^{34}S_{SO4}$ and $\delta^{18}O_{SO4}$)

From an environmental health perspective, dissolved $SO_4^=$ is relatively harmless compared to H_2S. Thus, an essential part of assessing the potential environmental effect of $SO_4^=$ is to evaluate when, how, and if it converts to reduced sulfide species such as HS^-, H_2S, or Fe-sulfide phases. Conversion to Fe-sulfide is the preferred reduction product in most cases, but H_2S can form if ferrous Fe^{++} is unavailable to trap it. To evaluate sulfate reduction and other sulfur cycling processes in streams, we rely on the observed changes to $\delta^{34}S_{SO4}$ and $\delta^{18}O_{SO4}$ values.

$\delta^{34}S_{SO4}$ and $\delta^{18}O_{SO4}$ for high-$SO_4^=$ samples collected from mine pits in the area are shown in Table 2. These values are consistent with derivation from iron sulfides in the iron formation (Poulton et al., 2010; Theriault, 2011). There is generally little or no sulfur isotope fractionation associated with Fe-sulfide oxidation under aerobic conditions and only a slight fractionation of approximately -0.7 ‰ if the oxidation takes place under anaerobic conditions (Balci et al., 2007). $\delta^{34}S_{SO4}$ for $SO_4^=$ in wells and mine pits from the west end of the Iron Range (not in the St. Louis River watershed) are lower than those on the east side of the Iron Range and so may have a slightly different heritage than those from the eastern side of the range.

$\delta^{34}S_{SO4}$ and $\delta^{18}O_{SO4}$ values from mine pits and wells in the St. Louis River watershed are plotted in Figure 11, along with weighted-average values for headwater samples from West Two, East Two, and Partridge Rivers. $\delta^{18}O_{SO4}$ values for many of the mine waters and, to some degree, the headwaters for these streams, are negative and approach $\delta^{18}O$ of local meteoric waters (approximately -10‰ in this region). This suggests that the O in $SO_4^=$ may have been derived, largely unfractionated, from H_2O in the environment rather than from atmospheric O_2 ($\delta^{18}O$ of about 23 ‰). Such a process can occur, for example, if the final oxidation step for $SO_4^=$ (e.g., during conversion of $S^=$ or S^0 to $SO_4^=$) is driven by a reaction with another oxidized species such as dissolved Fe^{+3} rather than by the O_2 in the atmosphere (Balci et al., 2007; Toran and Harris, 1989) (See Appendix A4 for a more extended discussion of this).

$\delta^{34}S_{SO4}$ and $\delta^{18}O_{SO4}$ data for samples collected from the West Two, East Two, and Partridge River stream confluences are also plotted in Figure 11. $\delta^{18}O_{SO4}$ values for these streams shift uniformly from headwaters to confluence in a positive direction while the accompanying shifts in $\delta^{34}S_{SO4}$ are small by comparison. Mixing with a different $SO_4^=$ source cannot explain the large shifts in $\delta^{18}O_{SO4}$ observed in the plotted stream segments because the amount of $SO_4^=$ added is insufficient to account for such large changes without appealing to unreasonably high $\delta^{18}O_{SO4}$ values for the added $SO_4^=$. Simple $SO_4^=$ reduction cannot explain this type of change either, because sulfate reduction should lead to increases in both $\delta^{34}S_{SO4}$ and $\delta^{18}O_{SO4}$.

Shifts of this type suggest that many of the $SO_4^=$ molecules in the streams are being stripped of their oxygen atoms and being converted temporarily to either S^0 or to H_2S, but then oxidizing back to dissolved $SO_4^=$. Reduction to S^0 or H_2S followed by an incomplete re-oxidation process would cause a corresponding shift in $\delta^{34}S_{SO4}$ in a distinctly positive direction if the new O atoms were obtained from O_2 rather than from meteoric water. Although some $SO_4^=$ reduction and re-oxidation is known to occur in the wetlands and lakes where $SO_4^=$ from mining is added directly (Berndt and Bavin, 2011). The mechanism for this O exchange in streams is little understood. Studies to identify the mechanism were underway in the watershed at the time this report was being written.

St. Louis River water sampled at Site 001 is also plotted in Figure 11, along with limited isotopic data from non-mining streams (from this study and also from Berndt and Bavin (2009)). Simple mixing explains the majority of the St. Louis River $SO_4^=$ isotope data (Figure 8) whereby periods of high flow correspond to large increases in the percentage of the dissolved $SO_4^=$ arising from non-mining sources. During such periods, non-mining water, containing $SO_4^=$ with $\delta^{34}S_{SO4}$ of about 6‰ and $\delta^{18}O_{SO4}$ also near

6‰ is introduced into the watershed and causes a shift in the river's $\delta^{18}O_{SO4}$ and $\delta^{34}S_{SO4}$ towards those values. On the other hand, when mining $SO_4^=$ dominates the inventory of $SO_4^=$ in the river, the St. Louis River's isotopic characteristics look like the values observed at the mining tributary confluences with the St. Louis River.

The isotopic composition of non-mining waters is likely derived from a number of sources, including, potentially, $SO_4^=$ from acid rain, oxidation of organic sulfur, and also from minor sulfides in bedrock and glacial tills (Eimers et al., 2004; Eimers et al., 2007). $\delta^{34}S_{SO4}$ in non-mining streams is relatively variable suggesting multiple sources, ranging from about +6 to +12 for the samples collected in this study. $\delta^{18}O_{SO4}$ for non-mining streams and for periods of high flow in the St. Louis River, on the other hand, tend towards a value of approximately +6 ‰. The consistency of this value among different watersheds suggest that the $SO_4^=$ molecules in each case are "constructed" under similar environmental conditions. Sulfur cycling and recycling is a continuous and on-going process that involves reduction, uptake by organic carbon, disproportionation, and oxidation so streams draining such areas likely incorporate dissolved $SO_4^=$ with a relatively limited range of $\delta^{18}O_{SO4}$ compared to $\delta^{34}S_{SO4}$ values (Blodau et al., 2007; Mandernack et al., 2000; Novak et al., 2005; Urban et al., 1989). $\delta^{18}O_{SO4}$ reflects the relatively fixed compositions of the water or oxygen in the environment where the sulfur or sulfide was last oxidized to $SO_4^=$. $\delta^{34}S_{SO4}$, on the other hand, can be impacted by the value of $\delta^{34}S_{SO4}$ from a variety of source materials, as well as by $SO_4^=$ cycling processes.

Data from three other mining streams where $SO_4^=$ reduction appears to be important, are shown in Figure 12. This includes Elbow and Long Lake Creeks which were only sampled at their confluences with the St. Louis River, and data from the Embarrass River, which was sampled incompletely in its headwater regions. The load measured in this stream greatly increased downstream likely owing to additional unsampled input of mine waters in the middle region (Site 033 in Figure2), and at its confluence (Site 035). In contrast to $SO_4^=$ in the East Two, West Two, and Partridge River sites, there was abundant evidence for a net $SO_4^=$ reduction process affecting the isotopic composition at these sites. These data were likely derived from similar mining $SO_4^=$ sources as those described above because the pits and tailings in their source regions are from the same Iron Formation. However, the high values suggest that significant $SO_4^=$ reduction must have occurred upstream from the sample locations in each case (Berndt and Bavin, 2011). As mentioned previously, $SO_4^=$ reduction produces an increase in both $\delta^{34}S_{SO4}$ and $\delta^{18}O_{SO4}$ in the residual dissolved $SO_4^=$.

The arrow in Figure 12 shows a simple case where mining $SO_4^=$ with $\delta^{34}S_{SO4}$ = +6 ‰ and $\delta^{18}O_{SO4}$ = -10‰ is reduced by a process that fractionates both S and O by the same amount (e.g., slope = 1.0 on a $\delta^{34}S_{SO4}$ versus $\delta^{18}O_{SO4}$ plot).   This type of fractionation helps to explain the elevated $\delta^{34}S_{SO4}$ and $\delta^{18}O_{SO4}$ measured in these streams. It is important to note, however, that the isotopic composition of $SO_4^=$ at one of the headwater sites, where reduction was evident in the samples collected in the summer (Spring Mine Creek; Site 031), shifted towards more typical, unreduced mine-water values in the winter. This indicates either that a different $SO_4^=$ source was feeding the stream in winter compared to summer, or that reduction upstream from the sampling site is a shallow subsurface process that occurs exclusively during the warmer summer and early autumn months.

Samples at the Embarrass River's confluence with the St. Louis River fall in a relatively narrow range with $\delta^{34}S_{SO4}$ close to 10‰ and $\delta^{18}O_{SO4}$ near 2‰. This is a considerable shift from upstream values and suggests that the reduced mining inputs form only a small fraction of the inputs to the Embarrass River at this location (Site 035). This is consistent with the loading estimates for the Embarrass River (Figure 4) which implied high inputs downstream from the sites visited during the present study.

$^{34}S_{SO4}$ and $\delta^{18}O_{SO4}$ data for the Swan River is unique from that found at the other sites and is shown in Figure 13. This river, located on the western end of the range, appears to have incorporated $SO_4^=$ with a consistently lower $\delta^{34}S_{SO4}$ value (4.0 to 5.1‰) than the other streams in the study area. $\delta^{18}O_{SO4}$ in the headwater regions were already close to 0 ‰. Both $\delta^{34}S_{SO4}$ and $\delta^{18}O_{SO4}$ were slightly elevated at the confluence compared to the corresponding headwaters. While $SO_4^=$ reduction could cause this trend, a more likely explanation is that non-mining water with $\delta^{34}S_{SO4}$ near 6 ‰ and $\delta^{18}O_{SO4}$ also around 6 ‰ produced this shift.   Based on geographical considerations, a large proportion of the water in this watershed originates in non-mining regions. It is also noteworthy that this river is the furthest west of the mining tributaries, where $\delta^{34}S_{SO4}$ in pits and nearby wells were somewhat lower than on the west side of the Iron Range (Table 1). Thus, mixing of SO_4 from mine water with $SO_4^=$ from non-mining watersheds in this region would be expected to produce a positive shift in both $\delta^{34}S_{SO4}$ and $\delta^{18}O_{SO4}$, even though a similar process in the other watersheds generates a negative shift in $\delta^{34}S_{SO4}$ in the other mining watersheds.

Figure 14 superimposes a "sequential framework model" under development by the Minnesota department of Natural Resources on a summary plot of the δ $^{34}S_{SO4}$ and $\delta^{18}O_{SO4}$ data collected from the St. Louis River and surrounding areas prior to June 2011. This figure includes data from this study and also data from samples reported by Berndt and Bavin (2011), as well as data reported from other sources from mines and wells on the Iron Range (Table 2).   The elements of the sequential framework model are described in more detail in Appendix A4, but are reviewed briefly, here.

The frame describes the evolution of $SO_4^=$ that is initially derived through an iron mediated oxidation process that adds oxygen atoms having $\delta^{18}O$ of local meteoric water to sulfur atoms derived from iron sulfide with $\delta^{34}S$ of +5 ‰ (the same as the sulfide mineral undergoing oxidation). The $SO_4^=$ is then reduced by a Rayleigh distillation process that fractionates sulfur and oxygen by 17 ‰, a value which fits estimates based on observations from two sites on the Iron Range where $SO_4^=$ reduction percentage was quantified using an independent method (Berndt and Bavin, 2011). Finally, $\delta^{18}O_{SO4}$ is allowed to equilibrate within the watershed to a value of +8, representing approximately a 3:1 ratio of oxygen atoms derived from oxygen in air (fractionated) and meteoric water (unfractionated), respectively.   These values and mechanisms were selected using the generalized fractionation mechanisms described by Toran and Harris (1989).

By this mechanism, approximately 60% the $SO_4^=$ needs to reduced to sulfide and removed in order to shift $\delta^{34}S_{SO4}$ from a value of +5 ‰ to a value of +20‰ and by more than 80% to shift $\delta^{34}S_{SO4}$ to values above +30‰. Based on this model, it is apparent that a large amount of $SO_4^=$ reduction occurs in some watersheds (e.g., Figure 12). By this same token, it can be seen that net $SO_4^=$ reduction in streams

displayed in Figure 11 must be slight, but the percentage of $\delta^{18}O_{SO4}$ atoms that must re-equilibrate during migration to the confluence must be quite large. With values at the confluence ranging between -2 and +2, the model suggests that about half of the sulfate molecules in the stream were re-equilibrated isotopically with respect to oxygen. Research in progress at the time of this writing is designed to test the components of this framework model (appropriate fractionation factors) and to better identify the source of the observed O-isotope exchange.

Mixing with Non-Mining Water

Mine waters mix and interact with non-impacted waters at highly variable rates that depend on location in the watershed and on the seasonally changing recharge rates. The degree of mixing depends both on geography and on the relative amount of rainfall or snowmelt that occurs downstream from the sites where mines discharge water into the watershed. The flow measurements in Figure 3, and the low $SO_4^=$ concentrations measured at site 001 compared to in the mineland headwaters show that the great majority of the water that enters the St. Louis River is derived from non-mining lands. In general, the potential for $SO_4^=$ to impact water extends to the lakes, flood plains, and riparian regions of streams and rivers that flow directly downstream from where the mines are located. This differs fundamentally from the potential impacts of, say, $SO_4^=$ derived from precipitation, which is spread over the entire watershed.

Though most water in the St. Louis River is derived from non-mining areas, the elevated $SO_4^=$, Mg^{++}, and Ca^{++} in mine water compared to non-mining waters creates a direct relationship between the concentrations of these elements in the St. Louis River and the flow rate of water at the Scanlon Dam (Figure 15). The relationship for these elements is in stark contrast to the positive to flat-lying trends for Al, Mn, and Fe (Figure 16), all of which are derived primarily from the non-mining watersheds. The negativity of the slope on log-log plots such as these is of significance since dilution of mine water inputs by pure water would result in a slope of -1, while a slope of 0 would result when a constituent is buffered by reactions in the watershed (Godsey et al., 2009). The trends for Ca, Mg, and $SO_4^=$ have much shallower slopes than the -1 value that might suggest dilution with pure water. The slopes of -0.22 (R^2=0.79), -0.33 (R^2=0.80), and -0.34 (R^2=0.81), respectively, indicate that the water added to the system during high flow events has significant concentrations of each of these components. The plots for Al, Fe, and Mn, meanwhile, reveal that the mining water, which has a greater presence during periods of low flow, has lower concentrations of these components than does the water added to the stream from non-mining areas during periods of high flow.

Interestingly, Al and Fe, two elements known to be transported colloidally with dissolved organic carbon (Dolfing et al., 1999; Heikkinen, 1994; Sjostedt et al., 2010), had concentrations that fell precipitously when the St. Louis River was at its lowest flow rates. This is consistent with the findings of Berndt et al (2012) who noted that non-mining tributaries of the St. Louis River carried higher DOC levels than mining streams and attributed the difference to the effect of increasing ionic strength on colloidal transport. Colloidal Al and Fe deposition in response to increasing ionic strength has been previously noted in coastal estuaries (Crerar, 1981), and it appears that a similar process may take place in the main channel of the St. Louis River. Alternatively, the low flow rates that prevail under such conditions may promote long residence times that may promote photo-oxidation, biotic degradation, and overall

general settling of organic matter or other compounds in the streams and river during this period (Aiken et al., 2011).

The highest Fe concentrations at Site 001 were found during the month after Event 8 (on August 2, 2011). Up to six inches of precipitation fell almost exclusively onto non-mining portions of the watershed during Event 8 (Figure 17). The mining region, meanwhile, remained in a drought that started long before the rain event occurred and continued through the end of the study period. The drought conditions caused implementation of river augmentation plans upstream, whereby mine waters were pumped into the St. Louis River via the Long Lake Creek watershed, beginning on September 23, 2011. The juxtaposition of a major rain event over the non-mining portion of the region, followed by drought-related augmentation of the river by mine-waters provided an opportunity to examine the regional effect of mixing of mining and non-mining waters on a regional scale. Thus, Fe and $SO_4^=$ concentrations during this period are shown with increased detail in Figure 18.

The rain event precipitated a ten-fold increase in flow at Site 001, from approximately 1000 to 10000 CFS. The immediate response in water chemistry was a decrease in both $SO_4^=$ and Fe concentration, likely due to in-stream dilution, but this decrease was much less than that which would have occurred by a pure dilution process. This is an indication that the water added immediately to the river following the storm already contained considerable quantities of $SO_4^=$ and dissolved Fe. Within a week of the event, the Fe concentrations exceeded their pre-event levels, while the SO_4 concentrations continued declining. For over a month following the event the St. Louis River $SO_4^=$ level remained low compared to its pre-event level while Fe concentrations persisted at elevated concentrations, indicating a sustained above-normal input of non-mining waters in the watershed.

By early to mid September, flow and $SO_4^=$ concentrations were back to their pre-event levels and Fe concentration was declining rapidly. Although flow rates continued to decline slightly after this date, Fe concentrations dropped even faster and never rebounded to their pre-event levels. The augmentation process was of little consequence to the flow levels in the St. Louis River at Site 001, but appears to have driven increases in $SO_4^=$ concentration beginning in early October. Fe concentrations, no longer supported by inputs related to Event 8, declined even further as a result of the increase in ionic strength associated with $SO_4^=$ added during stream augmentation.

Whatever its fate, the elevated Fe that persists throughout the study is in itself of significance for the reduced conditions it represents in its source region. In addition to Fe, the river retains relatively high dissolved Si (about 5 mg L^{-1}) (Figure 19). Elevated Fe and SiO_2 levels, especially during high flow events, suggest that the majority of the water entering the rivers during such periods is emerging from subsurface mineralized zones, rather than by overland flow of un-reacted precipitation. This is consistent with many recent observations of stream chemistry, isotopic characteristics, and event-related flow in other watersheds (Birkel et al., 2012; Godsey et al., 2009; McDonnell et al., 2010). A consistent theme is that water discharged into a stream following a precipitation event is "old-water", which fell on the watershed long before the triggering event occurred. Modeling the complex relationships and relative residence times for surface and subsurface waters following a precipitation event is the subject of active investigations (McDonnell et al., 2010; McGlynn et al., 2003; McGlynn and

McDonnell, 2003; Weiler et al., 2003) but helps to explain how, in this study, the river retains elevated concentrations of Fe and Si, as well, following major rain events.

This observation and interpretation is important when we consider that the waters entering the watershed following rain events, in addition to Fe and Si, also contain elevated DOC, MeHg, and THg (Balogh et al., 2004; Balogh et al., 2006). That the waters that supply MeHg, THg, and DOC to the watershed following an event have elevated dissolved Fe is consistent with derivation in the reduced sediments in streams and wetlands.

Mercury and Methyl Mercury

It has been well established that, in addition to Fe, the concentrations of Hg, MeHg, and DOC can become elevated during events in streams and rivers, especially in and near wetland regions (Balogh et al., 2004; Balogh et al., 2006; Burns et al., 2012).   Although MeHg and Hg production was not the primary focus of the present study, as mentioned previously, there was one round of samples, collected in August 2010, following a major rain event in the mining region (Event 1, August 2, 2011, see Figure 18).   The results from this sampling round are plotted against similar data for samples collected during the summer and early autumn, 2007 to 2009, in the St. Louis River watershed by Berndt and Bavin (2012). The data from Berndt and Bavin (2012) includes four sets of Hg data from the confluences of five mining and five non-mining tributaries with the St. Louis River and also includes data from many sites in the St. Louis River itself. St. Louis River samples were collected from seven sites located upstream from, within, and downstream from the mining region. The primary difference between the present data and that from Berndt and Bavin (2012) is that conditions in the latter study were comparatively dry. The new set of samples was collected to provide a direct means of comparison for MeHg and Hg concentrations in tributaries following a major storm "event" with those collected under relatively normal "non-event" conditions (Figure 20).

Most striking for the new data is that the generally elevated THg and DOC concentrations appear to extend a generally linear relationship for these components found for samples collected under relatively dry conditions. Considering the wide range of conditions and sources represented by the combined set of samples, this linear trend implies that source and transport of these components are linked fundamentally to processes that are relatively insensitive to the season or to $SO_4^=$ concentration in the stream. Furthermore, even though MeHg is one of the species included as part of the THg analysis, the samples containing elevated MeHg have THg values that lie on a similar trend as those samples that have little or no MeHg.   In effect, *the total amount of mercury carried by individual dissolved organic carbon molecules appears to be fixed, while the speciation of the Hg carried by these same particles is a variable.* A higher percentage of event THg carried by the DOC is comprised of MeHg during events than during non-event periods.   Before examining the geochemical mechanisms that might be responsible for this, we examine the distribution of samples with respect to precipitation and also examine the geochemistry of several samples from selected sites in greater detail.

Many of the samples with the highest MeHg concentrations appeared to have been collected in the mining region which, for this storm, was also the focal point for elevated precipitation (Figure 21). This raises the question of whether the high MeHg observed in the streams was related to enhanced

$SO_4^=$ reduction, to the rain event itself, or to both effects. To address this question we compare event and non event data from this watershed with data from Balogh et al. (2004). Balogh et al. (2004) reported data for samples collected biweekly throughout the summer. This included samples from before and following a rain event in what can be characterized a low-$SO_4^=$ watershed (Trott Brook and Cedar Creek, two tributaries to the Rum River in Minnesota). By comparing MeHg/THg ratio, THg, and DOC relationships in the two watersheds (Figure 22), insight can be gained on the geochemical processes lying behind the trends in each watershed.

Maximum MeHg/THg ratios, represented by the size of the symbols were approximately the same for both data sets, suggesting, perhaps that peak mercury methylation efficiencies in the primary mercury source regions for streams in the two areas are similar. On the other hand, two samples appear somewhat anomalous on this plot, one from Lake Manganika and the other from Long Lake Creek at its confluence with the St. Louis River.

The sample with the highest MeHg concentration (2.7 ng/L) is from the Long Lake Creek confluence, which had 33 mg L^{-1} $SO_4^=$ and $^{34}S_{SO4}$ and $\delta^{18}O_{SO4}$ values of +20.9 ‰ and +5.9 ‰, respectively. In comparison, MeHg concentration was only 1.0 ng/L in a sample collected upstream from this site, where $SO_4^=$ concentration, $^{34}S_{SO4}$, and $\delta^{18}O_{SO4}$ were 77 mg L^{-1}, 12.0 ‰, and 0.0 ‰, respectively (Berndt and Bavin, 2011). The lower $SO_4^=$ concentrations and higher $^{34}S_{SO4}$ and $\delta^{18}O_{SO4}$ values at the downstream site compared to the upstream site are indicative of both mixing and $SO_4^=$ reduction having taken place between sample locations. Many other parameters were also analyzed for these fluids and, taking these into account, it appears that approximately two thirds of the water in the stream at the confluence entered the stream between the two sampling sites. Taking into account dilution and also assuming a 17 ‰ fractionation process for sulfur during sulfate reduction, it can be calculated that approximately 1/3 of the $SO_4^=$ in the mixed fluid was reduced to sulfide and lost from the stream. Because MeHg concentration was only 1.0 ng L^{-1} at the upstream site, the majority of the MeHg at the confluence must have been added to the stream between the sites. The MeHg/THg ratio of the bulk sample from Site 051 is close to the maximum observed in non-mining watershed events (Figure 22), even though this water is one third composed of water having a much lower ratio. Thus, either the MeHg/THg of water added between the sites was much higher than that in the bulk fluid, or MeHg was generated in the stream itself. The area between the sampling sites is a ditched peatland prone to flooding and, so, although the data are not yet unequivocal, they suggest that passage of mining water through this type of setting may lead to increased MeHg generation and release following storm events.

Another sample that is relatively anomalous compared to the data of Balogh et al. (2004) and even to the other data in our present sample set is the sample from Lake Manganika's outlet (highlighted on Figure 22). This site was discussed in detail by Berndt and Bavin (2011), who thought the samples were the result of hypereutrophic conditions in the lake, the elevated $SO_4^=$, and the low Fe^{++} concentrations in the lake's inputs. This lake also receives output from a sewage treatment plant. A lack of ferrous iron to trap reduced $SO_4^=$ as iron sulfide results in formation of H_2S at the bottom of this lake which may assist MeHg transport from sediments as the volatile species, MeHgHS^0. A similar mechanism was also used recently to account for high MeHg transport in a highly eutrophic reservoir in

Idaho (Gray and Hines, 2009). Hypereutrophic lakes are another setting where MeHg generation may become accelerated, especially during summer months.

We now turn back to the more general case and attempt to account for the overall consistency of the THg/DOC trend between many samples collected in the St. Louis River watershed shown in Figure 20). Although studies have been conducted to evaluate methylation of mercury in stream sediments (Creswell et al., 2010; Marvin-DiPasquale et al., 2009; Rulik et al., 2000), the dynamic nature of streams and the potential for hyporheic flow (Bencala et al., 2011) make it difficult to fully relate or extrapolate processes directly observed in sediments at a single site and time to that for an entire river or stream. While methylation and $SO_4^=$ may be found in sediments at a specific site, chemistry of the overlying water column is typically set by a conglomeration of processes, potentially unrelated to those at the study site, that occur upstream.

However, just as chemostatic behavior of elements in streams is used to imply consistency in geochemical processes on a watershed scale (Godsey et al., 2009), we suggest that the THg/DOC trend in Figure 20 imply a similarity among processes taking place in the reduced sediments in small streams throughout the region (Figure 23). Based on the high Fe, Al, and DOC, we infer that watershed recharge in non-mining portions is dominated by the passage of stored water through the reduced sediments that line the creeks and streams throughout the watersheds.

Under low flow conditions, when transport rate is slow or non-existent, a higher percentage of water in the streams is sourced from groundwater or, in the case of the mining region, mine water pumped directly into streams. These sources have comparatively low DOC concentrations. While some DOC may still be added from the shallower surface aquifers during non-event periods, the slower flow rate means that the transit times for these components from the reduced zones where MeHg is produced to open water will be long when compared to transit times for event driven flow.

A difference in transit time for event and non-event MeHg transit times will have a direct bearing on MeHg/THg ratios in the streams. While Hg^{++} is stable in oxygenated surface water environments, MeHg is clearly not (Drott et al., 2008; Hammerschmidt and Fitzgerald, 2010; Lehnherr and St. Louis, 2009) and degrade with timescales of hours and days. Elevated MeHg levels can be sustained under reducing conditions in sediment pore fluids by a balance of reactions that result in continuous methylation at a rate equal to the rate of demethylation. This balance is lost when the pore fluid is transferred from reduced to oxidizing conditions when methylation stops but the demethylation process continues. Correspondingly, surface waters that were once pore fluids may contain DOC that preserves its original THg/DOC ratio, even when MeHg/THg and MeHg/DOC ratios decline.

Precipitation events hasten flow through the reduced portions of the sediments and driving the expulsion of pore fluids containing DOC with bound Fe, Al, Hg^{2+}, and MeHg into streams. Because MeHg and oxidized, unmethylated (inorganic) Hg are typically present in sediments at concentrations that are on the order of 10^3 to 10^6 times the concentrations in coexisting pore fluids. Thus, a large amount of water can pass through a methylating zone with only minor impact to sediment MeHg or THg inventories.

A critical component of this model for mining streams involves whether $SO_4^=$ added to a stream is introduced in such a way that it can upset the balance of methylation and demethylation along its own flow path. To do so, $SO_4^=$ would need to access the organic matter in places where it can be reduced to sulfide, and it must do so in an environment where the reduction process doesn't limit Hg^{++} availability by HgS precipitation (Miller et al., 2007). And once the methylation has occurred, the methyl mercury that is produced must have access and transport mechanisms that bring it back into the open water.   Recent studies reveal a clear connection between $SO_4^=$ addition to peat and the level of MeHg in the peat and coexisting pore fluids (Coleman Wasik et al., 2012; Jeremiason et al., 2006). Even in this setting, however, considerable demethylation occurred, affecting transport of MeHg from the wetland.

The consistency of THg/DOC relationships among most mining and non-mining streams displayed in Figures 20 and 22, suggest that MeHg generation and transport in mining and non-mining watersheds are more typically alike than they are different, particularly when viewed on the scale of the mining stream watershed. A major part of this may relate to the fact that little methyl mercury is generated and added to streams during dry periods when mining water represents a proportionately more important part of the total flow. During and following rain events, however, when the highest MeHg concentrations are typically observed, the majority of water added to the mining streams may be derived from the non-mining portions of the watershed.

This does not mean, however, that $SO_4^=$ does not impact MeHg generation and transport at all in places where it comes into contact with organic carbon. Long Lake Creek and Lake Manganika were already mentioned as exceptions.   Similarly, elevated MeHg levels have also been previously reported for Second Creek, a wetland receiving high $SO_4^=$ waters that are commonly dammed by beavers (Barr-Engineering, 2009). The same area and several other wetlands receiving $SO_4^=$ from mines in other areas were studied by Berndt and Bavin (2011) but MeHg levels never reached the levels found during the Barr 2009 study.   Elevated MeHg/DOC ratios are commonly observed in the wetland settings themselves, most likely because they are close to the sources where methylation takes place and where release is too recent for demethylation to impact the chemistry.

The general case implied by Figures 20 and 22 are that the impacts from high-SO_4 mining waters on MeHg distribution in the distribution are small when viewed on a regional basis such as at the confluence of major rivers; sporadic but measurable in water collected from localized settings such as in wetlands and peatlands temporarily flooded by mining waters; and considerable in hypereutrophic lakes such as Lake Manganika, where MeHg is actively produced and transported into the open water column at rates sufficient to impact the stream chemistry for long periods of time.

Conclusions

Several geochemical trends were identified for the sulfur concentration and isotopic data, cation and anion chemistry, and the ratios of total mercury and methylmercury to dissolved organic carbon in the St. Louis River and its many tributaries. Relationships among dissolved species, isotopes, and flow rate, considered together as a package rather than separately and in isolation from each another, imply

that a relatively few fundamental hydrologic and geochemical processes control much of the chemistry in the region.   In the most general sense, water chemistry in the river at different sites and under different flow conditions can be considered as differing primarily in the ratio of mining and non-mining waters in the mixture they represent. Whereas "mine waters" are derived during the oxidative weathering of rocks exposed to air during mining, so called "non-mining waters" were derived primarily under reducing conditions where iron, dissolved organic carbon, and methylmercury are mobilized. Waters from these two primary sources mix throughout the watershed under a range of hydrologic conditions and it is the result of this mixing process that produces much of the observed variability in chemistry of waters in the region.

As a slightly more detailed level a series of other smaller conclusions were reached, some of which add detail to the general state above, but others of which add complexity in certain settings. These are, as follows:

(1) The St. Louis River receives a relatively small percentage of its water from the mining industry, but this water has high pH, and contains elevated sulfate, magnesium, calcium, sodium, and potassium compared to the bulk of the water that feeds the St. Louis River.

(2) The sulfate in the mining pits and in the headwater streams for rivers receiving direct input from the mines has isotopic composition consistent with derivation by Fe^{+3}-mediated oxidation of sulfides found in the iron formation.

(3) Flow in the system is highly variable such that the mining inputs that accumulate in the river during periods of low flow are mixed with and flushed downstream by waters from the non-mining watersheds.

(4) Sulfate reduction, as evidenced by simultaneous enrichment of $\delta^{34}S_{SO4}$ and $\delta^{18}O_{SO4}$, appears to be generally confined to areas nearest the mining region where sulfate comes into direct contact with reduced organic carbon. There is little change in $\delta^{34}S_{SO4}$ in the channelized streams, suggesting that little or no net sulfate reduction takes place in the streams themselves, at least not at the level that can be measured by this method.   However, considerable re-equilibration of $\delta^{18}O_{SO4}$ appears to occur, beyond that which can be explained by mixing, when mining and non-mining waters mingle within the watershed.

(5) The waters added to the river following precipitation events contain iron, aluminum, dissolved organic carbon, and methylmercury, the levels of which were probably determined when pore fluids were pushed into and through the submerged, reduced sediments that surround streams, rivulets, and ditches throughout this highly forested and wetland-rich area.

(6) During periods of extreme low flow in the St. Louis River or in upstream regions where the percentage of mine water in a stream is elevated, the capacity of the stream to transport dissolved organic carbon and associated metals such as iron and aluminum is diminished. This effect is believed to be related to colloid deposition at elevated ionic strengths.

(7) Total mercury to dissolved organic carbon ratios are similar in surface waters derived under many conditions and in many regions throughout the region. This suggests there is a relative similarity in the geochemical processes, pervasive throughout the region, affecting

production and transport of both components into surface waters. By contrast, the methylmercury to dissolved organic carbon ratio is highly variable, and may reflect differences in the amount of time since the water in the stream last resided in the reduced pore-fluid environment where the methylmercury is produced. Demethylation following transport into the open waters reduces the ratio of methylmercury to total mercury and also the ratio of methyl mercury to dissolved organic carbon, but does not affect the ratio of total mercury to dissolved organic carbon.

(8) Shear geographical consideration demands that the vast majority of MeHg in this watershed is generated in the non-mining regions, although the inventories of MeHg may be increased sporadically and locally by sulfate added to wetlands prone to flooding or when sulfate reduction processes lead to hydrogen sulfide generation in sediments. An important consideration relates to the availability of ferrous iron which, if present in sufficient quantity, can trap hydrogen sulfide as iron sulfide. In some situations, where hydrogen sulfide is generated, there may be enhanced transport of methyl mercury as the volatile species methylmercury-bisulfide (MeHgHS^0).

Acknowledgements

Tables

Table 1. $SO_4^=$ concentrations and isotopic data for waters collected from wells and pits on or near mining properties.

| Site Description	$SO_4^=$ mg L^{-1}	$\delta^{34}S_{SO4}$	$\delta^{18}O_{SO4}$	$\delta^{18}O_{H2O}$	*Source
Mesabi Nuggest/Former LTV Site					
Pit 1 – Surface Water	384	8.8	-7.3		1
Pit 9N – Surface Water	350	6.5	-9.7		1
St. James – Surface Water	285	6.5	-8.8		1
Pit 6 – Surface Water	951	5.4	-9.6		1
Well GW01 - South of Pit 1	100	6.3	-10	-11.5	1
Well GW02 - South of Pit 1	387	4.6	-10.2	-11.4	1
Well GW03 - South of Pit 1	289	3.9	-4.9	-11.2	1
Well GW04 - South of Pit 9N	357	6.6	-6.5	-10.5	1
Well GW05 - Between Pit 9S and Pit 6	1240	6.2	-10.5	-9.2	1
Well GW06 - North of St. James Pit	152	6.5	-8.9	-12.1	1
Minntac Area					
Mott Mine Pit Lake (South of Minntac)	100	6.4	-2.1	-7.1	2
Iroquois Mine Pit Lake (South of Minntac)	101	11.2	0.2	-6.8	2
Minntac Mtn. Iron Pit Lake (Minntac Source water)	342	6.3	-7.4	-9.8	2
Minntac Admin. Bldg. Well	284	5.3	-6.5	-10.0	2
Mtn Iron Well 1	62	10.3	-0.5	-8.9	2
Mtn Iron Well 2	32	10.8	-1.2	-11.1	2
West Iron Range Area					
Bovey Well 1	316	-10.4	-4.3		3
Canisteo Pit	106	1.4	-0.3		4
West Hill Pit	100	2.9	0.9		4
Lind Pit	110	3.4	1.0		4

*Sources:

1 = Mesabi Nugget Data Sent to the Minnesota DNR in 2008 during EIS scoping.

2 = James Walsh, Minnesota Pollution Control Agency, 2010 Personal Communication.

3 = James Walsh, Minnesota Pollution Control Agency, 2011 Personal Communication.
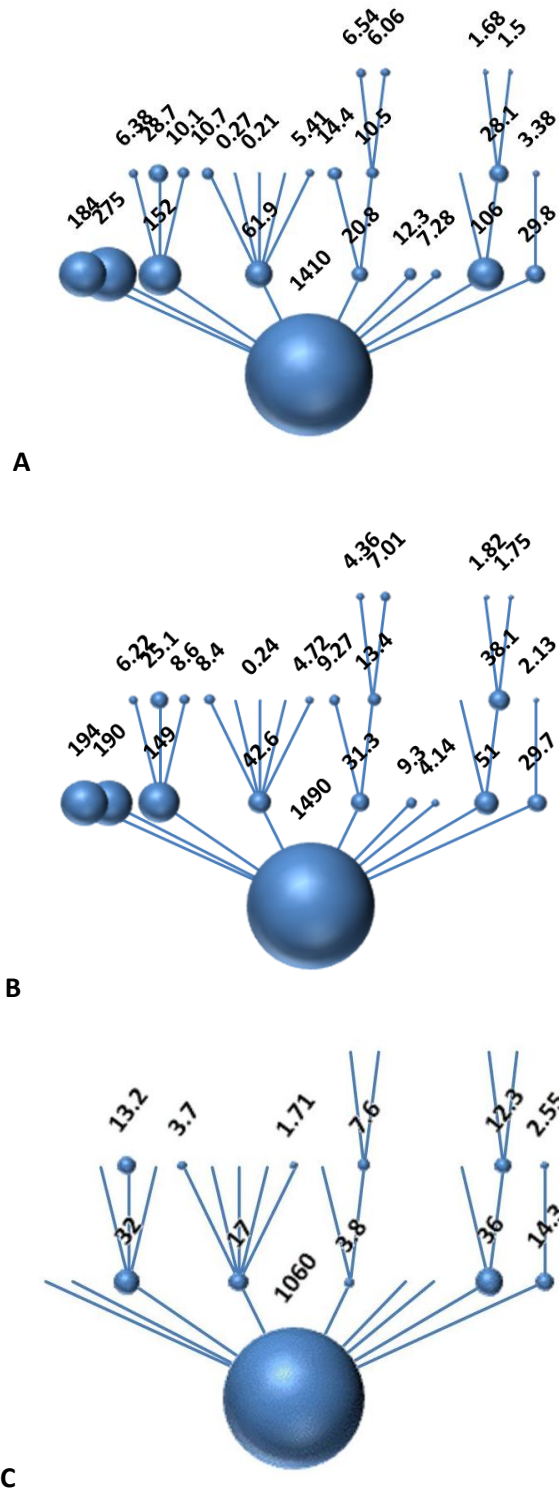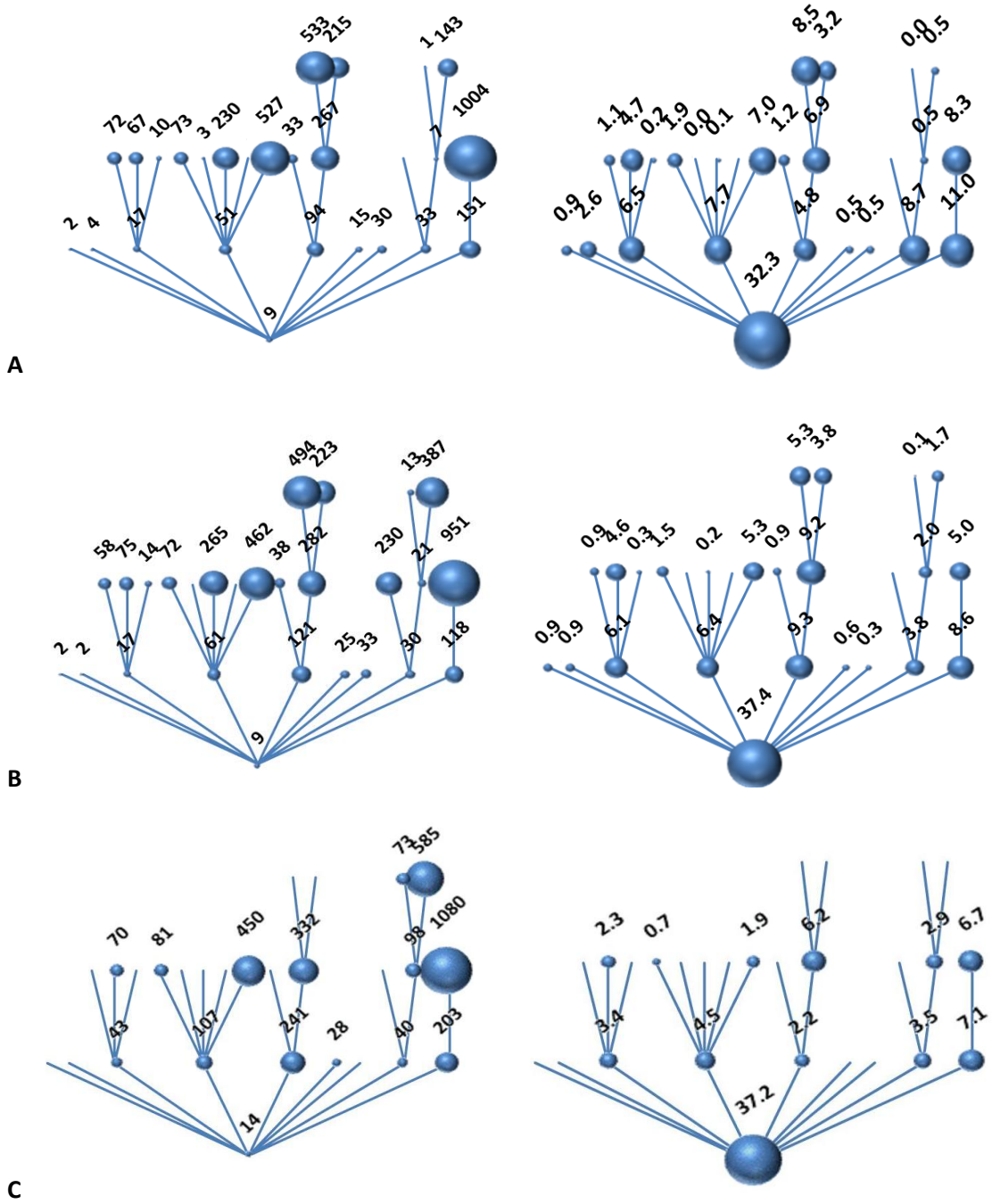
4 = This study.

Figures
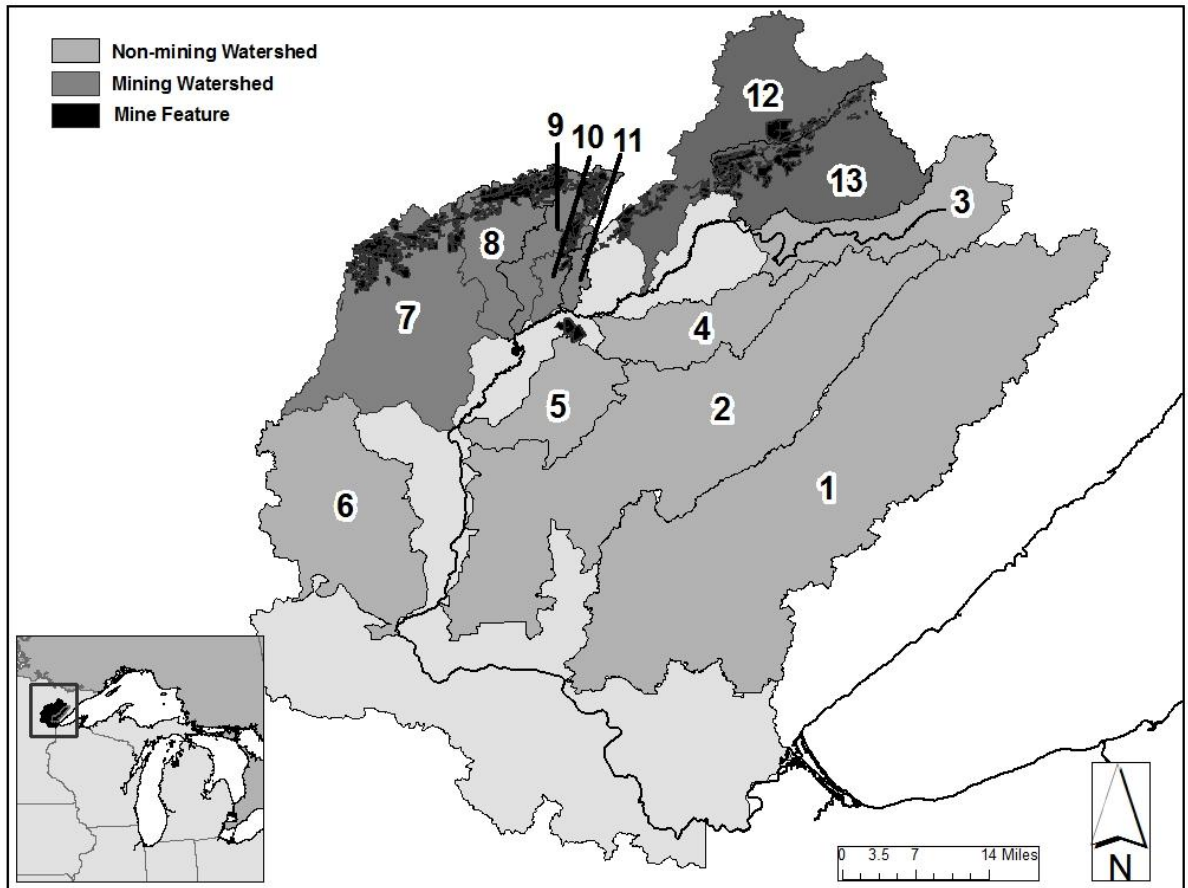
Figure 1. St. Louis River basin and major sub-watersheds within the basin (From Berndt and Bavin, 2012). These include: (1) Cloquet, (2) Whiteface, (3) Upper St. Louis (upstream from the mining region), (4) Mudhen Creek, (5) Stony Creek, (6) Floodwood, (7) Swan, (8) West Two, (9) East Two, (10) Long Lake, (11) Elbow, (12) Embarrass, and (13) Partridge Rivers.   Taken from Berndt and Bavin, 2012.
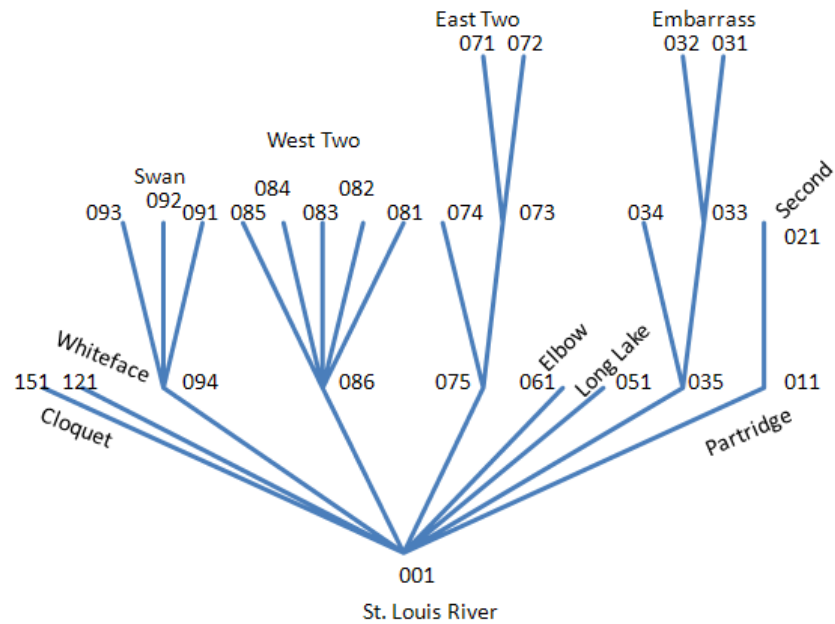
Figure 2. Watershed-wide network and site representation used in this report. All of the streams shown as tributaries deliver water to the St. Louis River and, thus, contribute to the $SO_4^=$ load at Site MSRS 001 (e.g., the St. Louis River in Cloquet). The numbers at each node represent the sampling sites and are described in Table 1.

Figure 3. Water flow rates (CFS) for sites evaluated in this study in August (A), September (B), and March (C). Limited flow data are available for March owing to limited access and ice formation in the region.

Figure 4. SO$_4^=$ concentrations (mg L^{-1}, on left) and loads (metric tons/day, on right) determined in this study for August (A), September (B), and March (C).
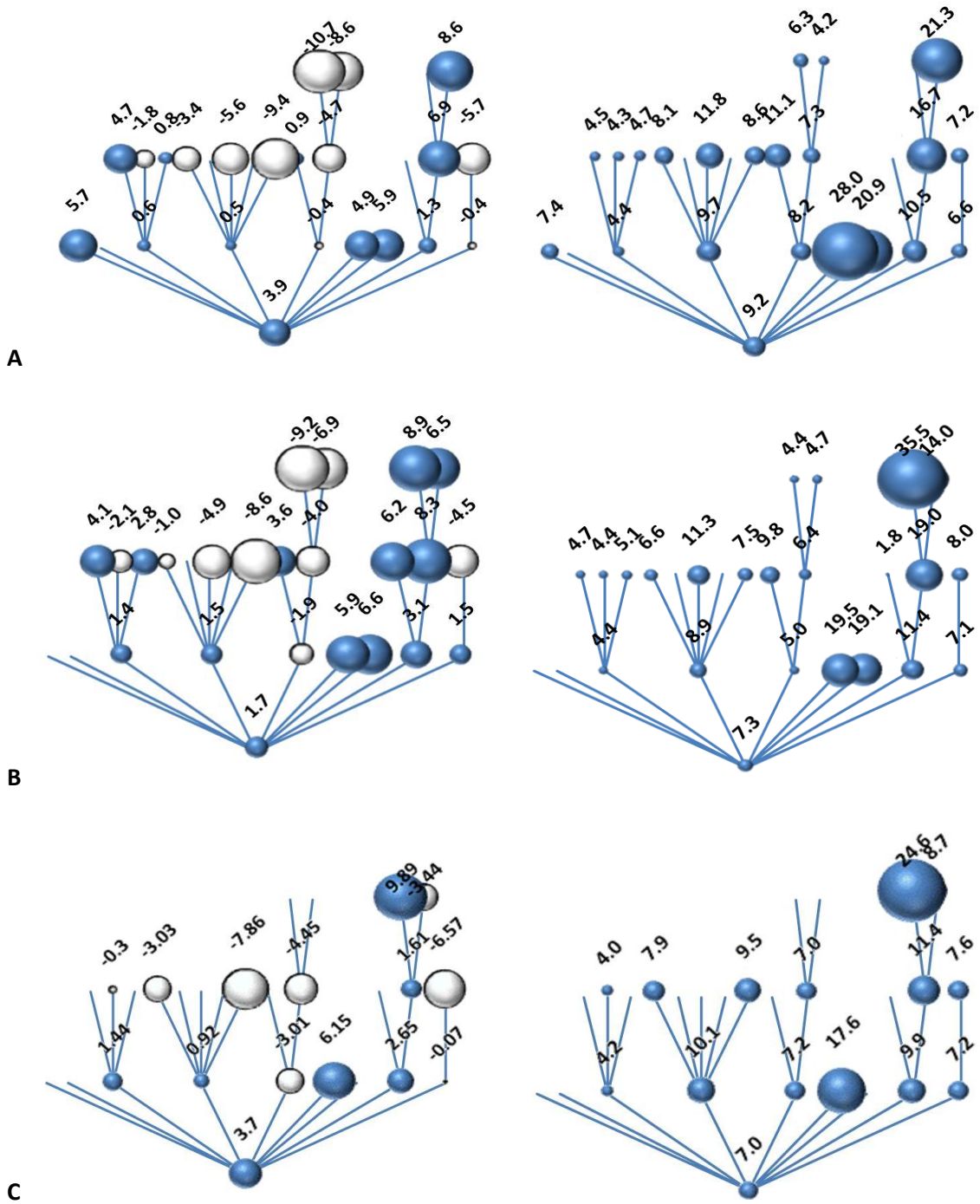
Figure 5. $\delta^{18}O_{SO4}$ (‰ relative to SMOW, on left) and $\delta^{34}S_{SO4}$ (‰ relative to Canyon Diablo Troilite, on right) for samples collected in this study in August (A), September (B), and March (C).
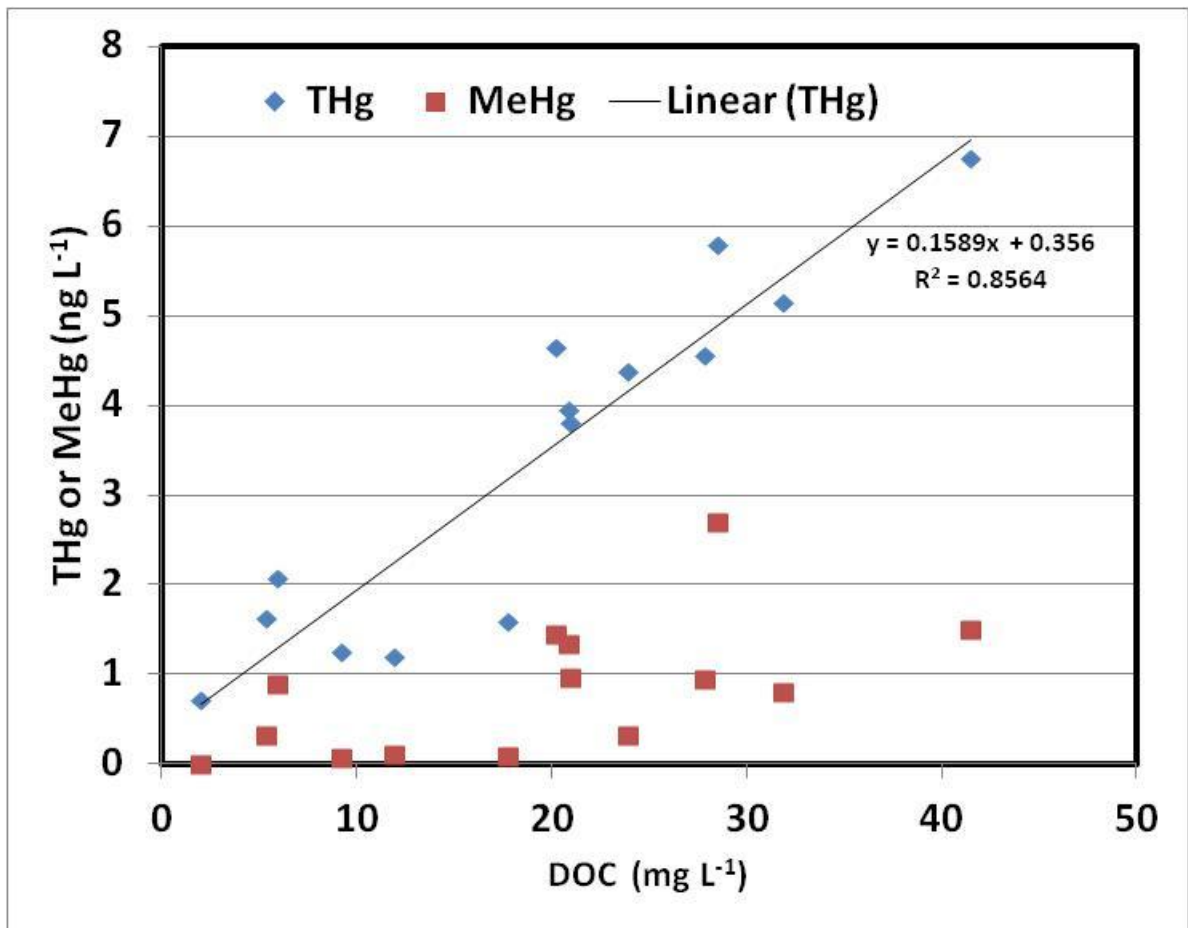
Figure 6. THg and MeHg versus dissolved organic carbon (DOC) in filtered samples collected at our study sites in the St. Louis River watershed from August 10 to August 12, 2010, after a major rain event in early August.
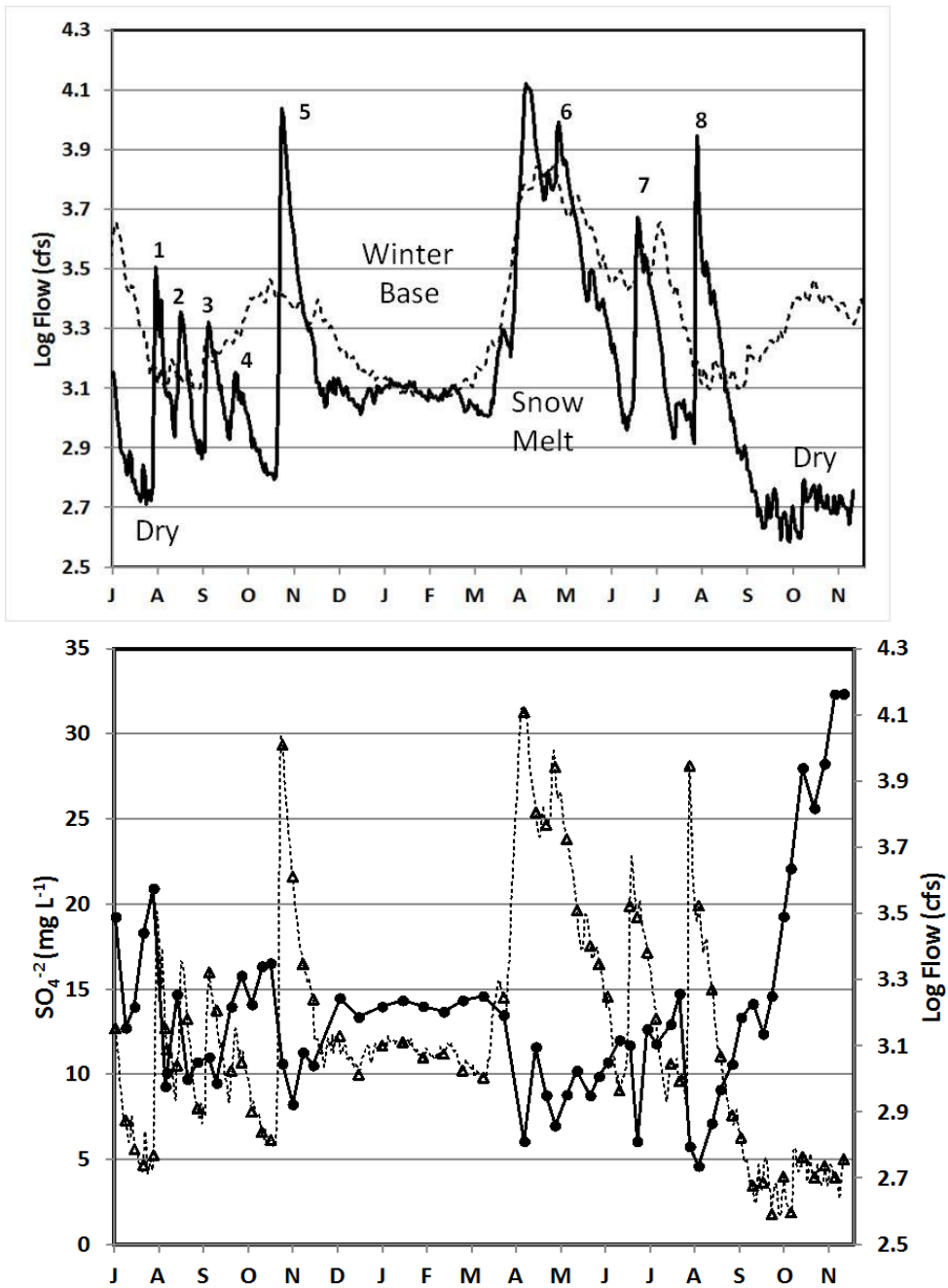
Figure 7. The top graph shows measured (solid line) versus 30 year average flow (dashed) at the Scanlon site from July 2010 to November 2011. High runoff events are numbered for reference. The bottom graph compares flow (triangles-dashed) to dissolved $SO_4^=$ concentration (black circles- solid line) measured at the same time. $SO_4^=$ varies inversely to flow owing to watershed dilution of mine inputs. Winter base-flow $SO_4^=$ concentration is approximately 14 mg L^{-1}, but concentrations reached over 30 mg L^{-1} following a late summer and fall drought period.
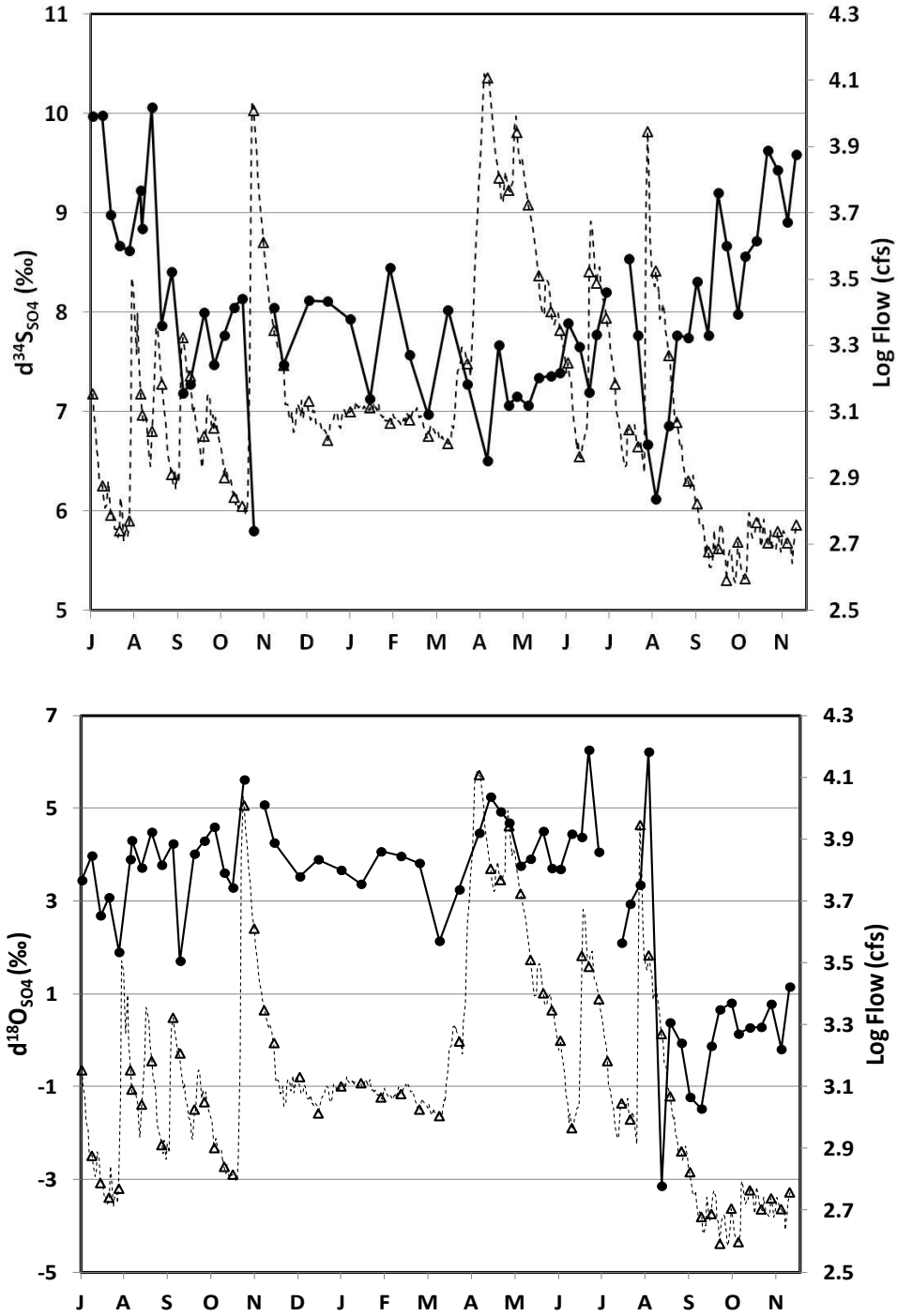
Figure 8. $\delta^{34}S_{SO4}$ and $\delta^{18}O_{SO4}$ values (black circles – solid lines) compared to flow (triangles/dashed line) at the Scanlon site (001) from July 2010 to November 2011.
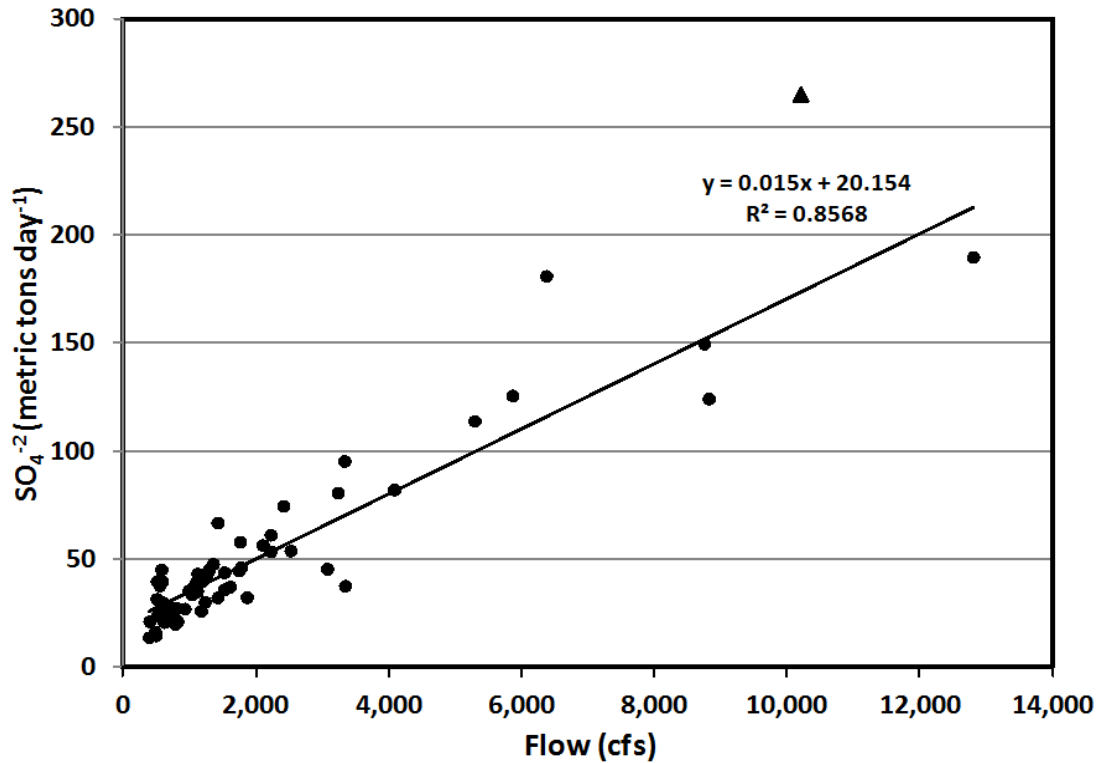
Figure 9. $SO_4^=$ loading as a function of flow for the St. Louis River. Dry periods were characterized with loading rates between 10 and 40 metric tons per day. These values increased to as high as 260 tons per day. Note that the slope of 0.015 on this plot corresponds to addition of water containing an average of about 6 mg L^{-1} to the watershed during high flow periods. This slope represents the combined input of new $SO_4^=$ from non-mining portions of the watershed, the flushing downstream of mining $SO_4^=$ that collected previously in the watershed during dry periods, and possibly to increased pumping of mine waters in response to increased rainfall on mine properties.

Figure 10. SO$_4^=$ load from mining and non-mining sources estimated using an assumption that anything above 3 mg L^{-1} was contributed from the mining industry. In actuality, SO$_4^=$ concentrations in streams from non-mining watersheds tend to have values above 3 mg L^{-1} during dry periods and less than 3 mg L^{-1} during wet periods. Thus, this method likely underestimates non-mining contributions slightly during dry periods and over-estimates them during wet periods. Based on this model, the SO$_4^=$ loading to the St. Louis River is dominated by mining inputs, except during periods of high flow. The mining load increases rapidly in the watershed during wet periods because water that fills the stream during dry periods is flushed downstream. However, additional loading from the mines themselves cannot be eliminated. The increase in mining load at the end of the study period occurred owing to drought-related augmentation of the St. Louis River with water containing elevated SO$_4^=$ from an existing mine pit.

Figure 11. $\delta^{18}O_{SO4}$ (‰ relative to SMOW) and $\delta^{34}S_{SO4}$ (‰ relative to Canyon Diablo Troilite) for samples from mines and mining streams where little or no $SO_4^=$ reduction appears to occur in the headwater regions (West Two River, East Two River, Partridge River). Isotopic data for non-mining streams and the St. Louis River are also shown.   Lines connect headwater and river confluence values for samples collected from mining streams during single mining trips.   When multiple streams were sampled in a headwater region, only the load-weighted isotopic data are shown. $\delta^{18}O_{SO4}$ changes much more rapidly than $\delta^{34}S_{SO4}$ in these streams, suggesting there is a process that causes $SO_4^=$ oxygen to re-equilibrate during flow. Exchange thereafter can be explained by variable mixing of mining and non-mining $SO_4^=$, with little or no net $SO_4^=$ reduction.
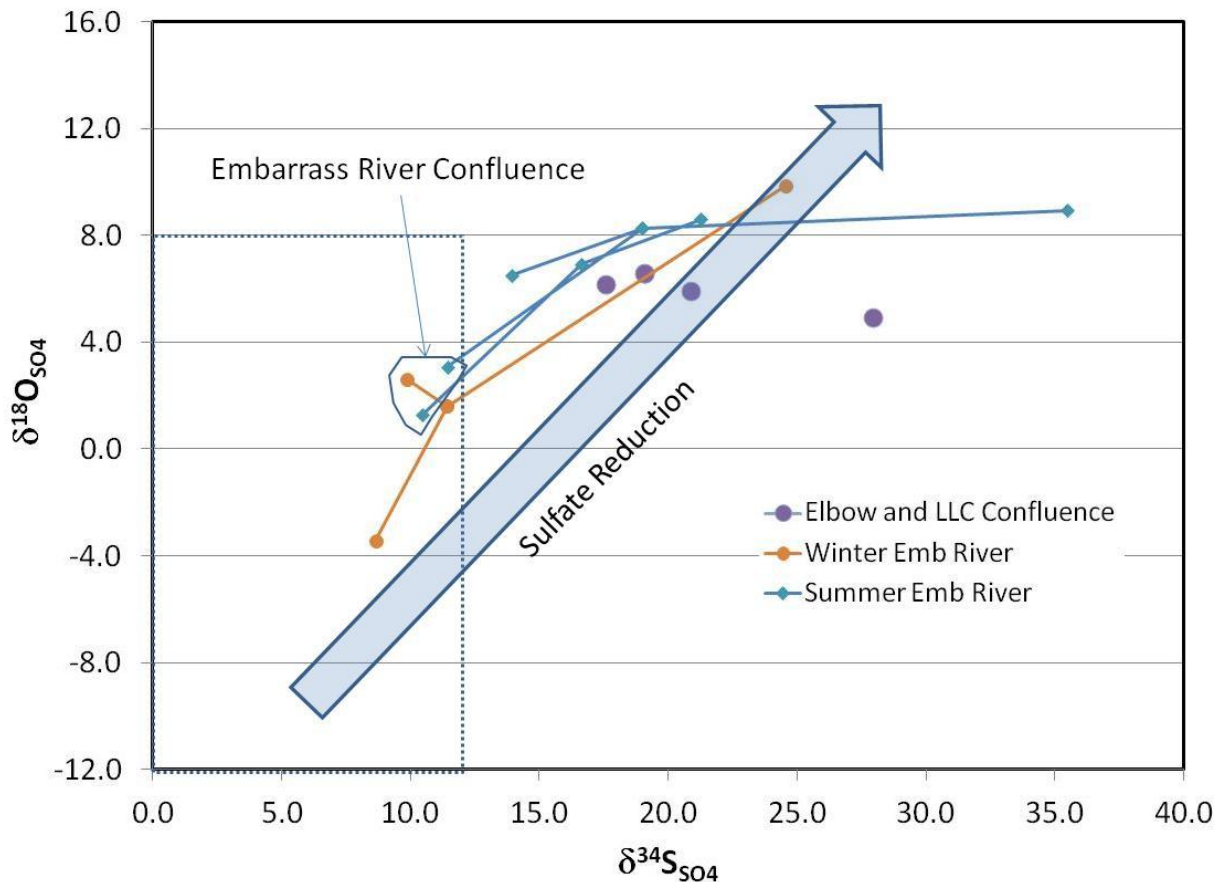
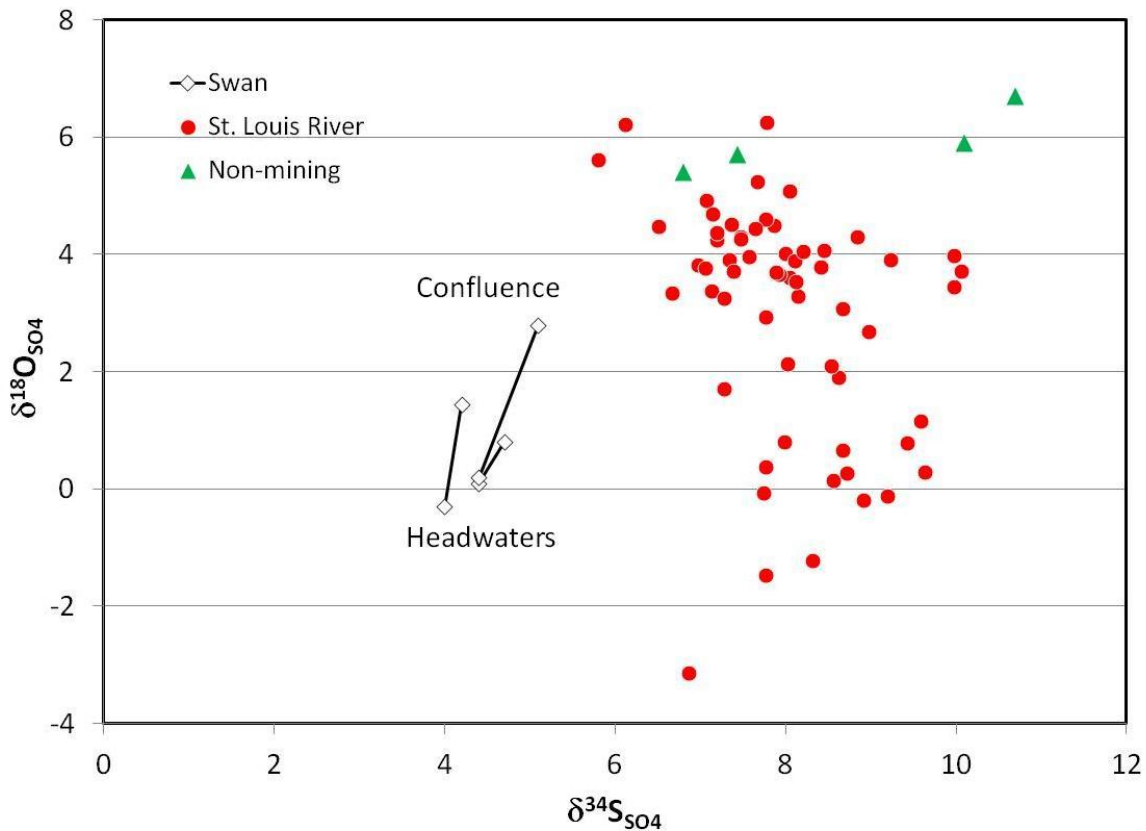**Figure 12.** $\delta^{18}O_{SO4}$ (‰ relative to SMOW) and $\delta^{34}S_{SO4}$ (‰ relative to Canyon Diablo Troilite) for samples from mining streams where extensive SO_4 reduction occurs upstream from sampling sites in the watershed (Elbow, Long Lake Creek, and Embarrass River). The dotted box outline represents the region shown in Figure 11. The shaded arrow represents the trend for $SO_4^{=}$ reduction expected if fractionation for sulfur and oxygen isotopes is equal in magnitude and is the only process affecting the isotopic ratio for the residual $SO_4^{=}$. The arrow begins at $\delta^{34}S_{SO4}$ = +6 ‰ and $\delta^{18}O_{SO4}$ = -10‰ which is chosen to represent $SO_4^{=}$ derived by ferric iron (Fe^{+++}) mediated oxidation of Fe-sulfide. The Fe-sulfide in this case is assumed to have $\delta^{34}S$ = +6 ‰, similar to dissolved $SO_4^{=}$ commonly observed on the Iron Range.

Figure 13. $\delta^{18}O_{SO4}$ (‰ relative to SMOW) and $\delta^{34}S_{SO4}$ (‰ relative to Canyon Diablo Troilite) for samples from the Swan River headwaters (weighted) and its confluence. The data are compared to samples from Site 001 in the St. Louis River and non-mining watersheds.   Most of the downstream isotopic variation in the watershed is thought to be related to mixing with non-mining waters, although a small amount of $SO_4^{=}$ reduction or $\delta^{18}O_{SO4}$ re-equilibration cannot be ruled out in this case.
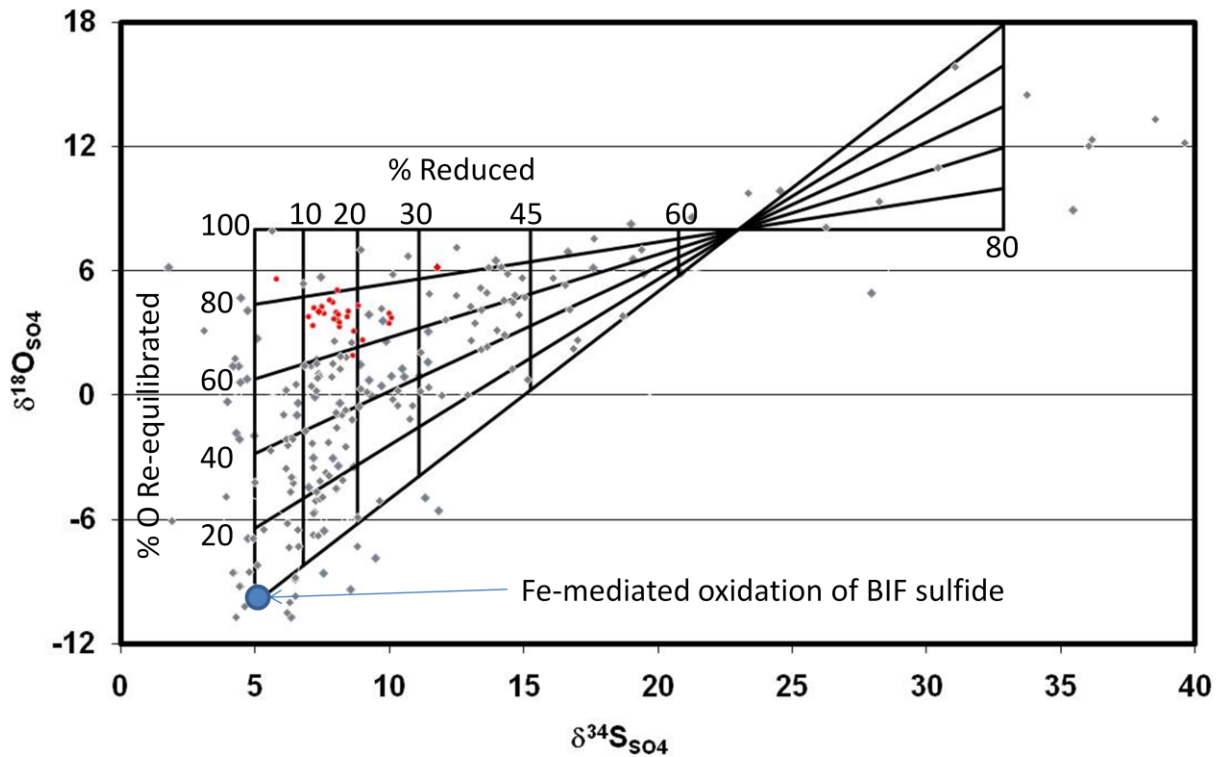
Figure 14. Sequential framework model for $\delta^{34}S_{SO4}$ and $\delta^{18}O_{SO4}$ data developed by the DNR for mining $SO_4^=$ evolution compared to $\delta^{34}S_{SO4}$ and $\delta^{18}O_{SO4}$ values measured in or near the St. Louis River watershed through July 2011. Dark gray points are assorted data from lakes, streams, rivers, and wells. Red points are from the St. Louis River and include abundant $SO_4^=$ from non-mining regions. Note that non-mining $SO_4^=$, with $\delta^{34}S_{SO4}$ from about +6 to +10 and $\delta^{18}O_{SO4}$ around +6 ‰ is also abundant in the watershed. The framework is only provided as a reference to illustrate the relative consequences of $SO_4^=$ reduction and re-equilibration in the watershed on $SO_4^=$ derived from mining. See text for explanation.
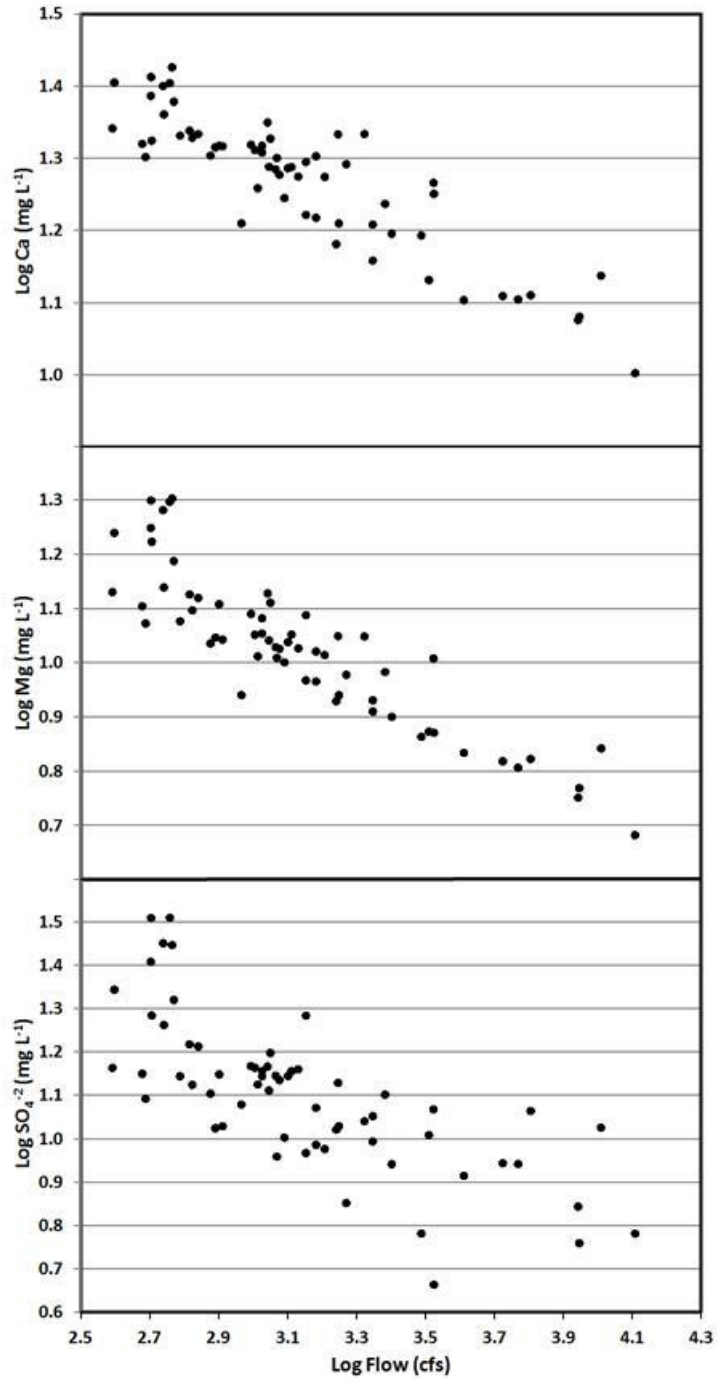
Figure 15. Calcium, magnesium, and $SO_4^=$ concentrations as a function of flow rate for the St. Louis River at Site 001 and Scanlon Dam. Under low flow conditions, the St. Louis River has a disproportionate amount of water containing these components, which are elevated in streams that originate in the mining region. Similar negatively sloping trends are observed for chloride, fluoride, strontium, and sodium (provided in Appendix A3).
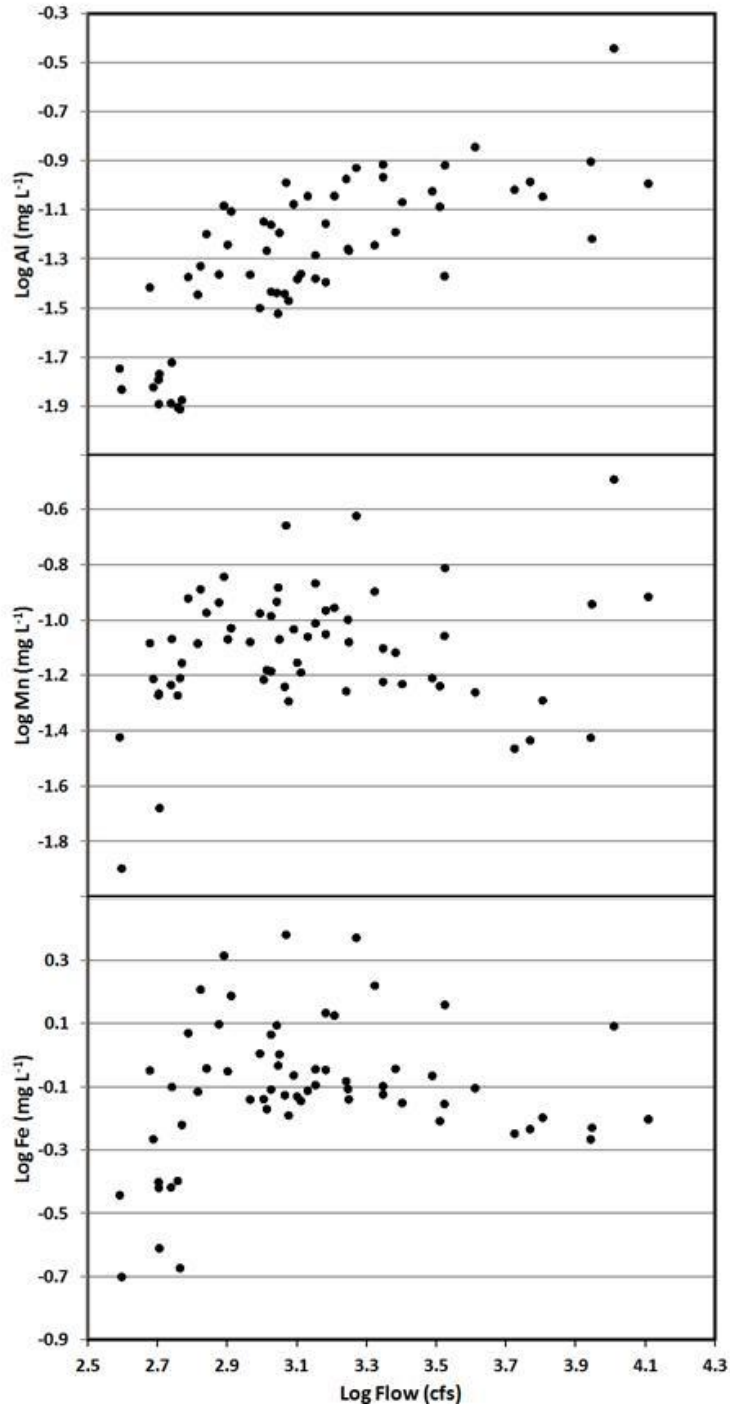
Figure 16.   Dissolved aluminum, manganese, and iron concentrations as a function of flow rate for the St. Louis River at the Scanlon Dam. These components likely originate from chemical reactions occurring in reduced soils and sediments throughout the watershed.
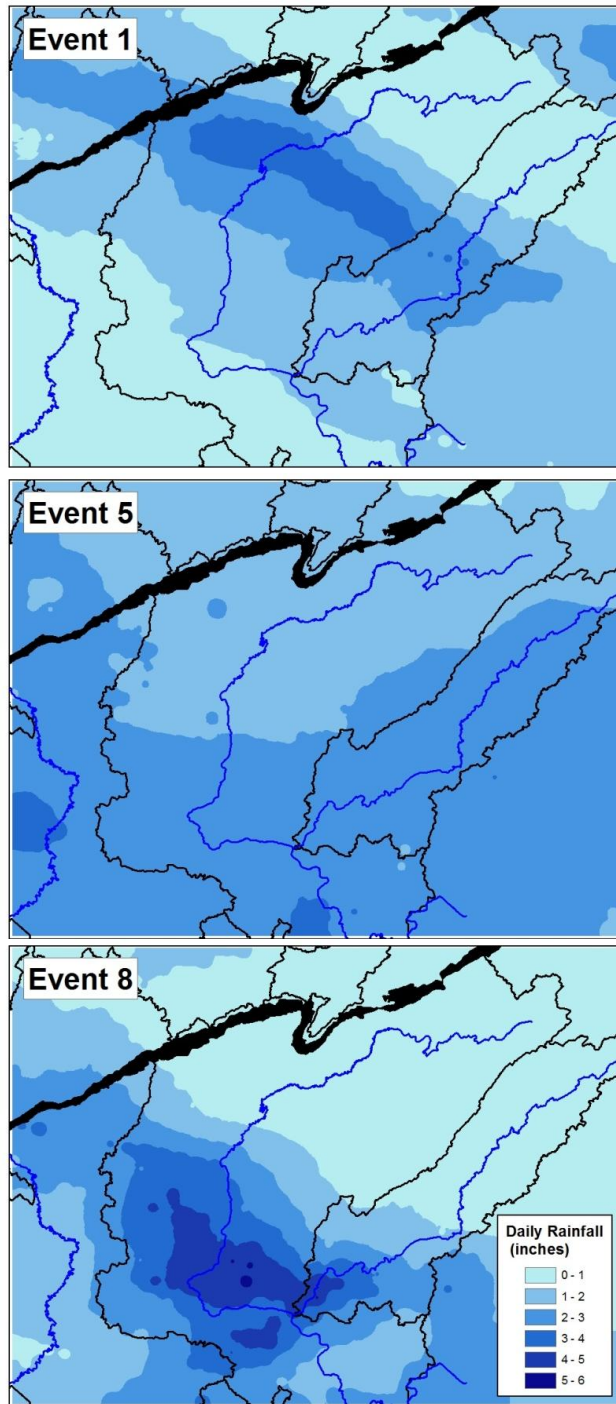
Figure 17. Precipitation distribution (interpolated from National Weather Service radar-based estimates) for Events 1, 5, and 8 (see Figure 7). These events occurred on August 2, 2010, October 27, 2010, and August 2, 2011, respectively. All other events had relatively even precipitation distributions and so are not shown.
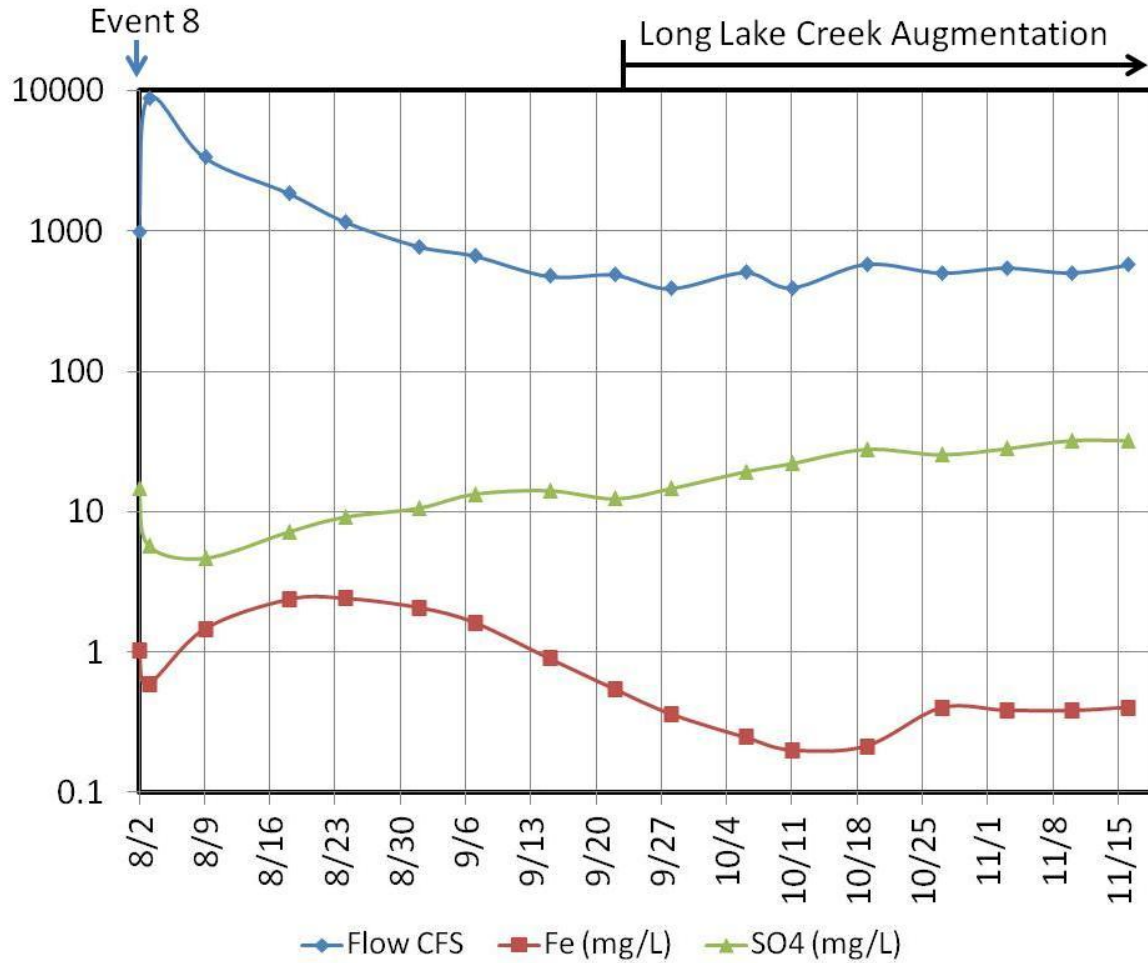
Figure 18. $SO_4^=$ and Fe concentrations in the St. Louis River following a major rain event over the southern portion of the region (Event 8) that was followed by drought conditions throughout the region. The river was eventually augmented by pumping of mine water through the Long Lake Creek watershed beginning on Sept. 23.   This resulted in a further increase in $SO_4^=$ concentration which precipitated an increase in ionic strength and a decrease in Fe concentrations. The further decrease in Fe is thought to represent deposition of colloidal iron.
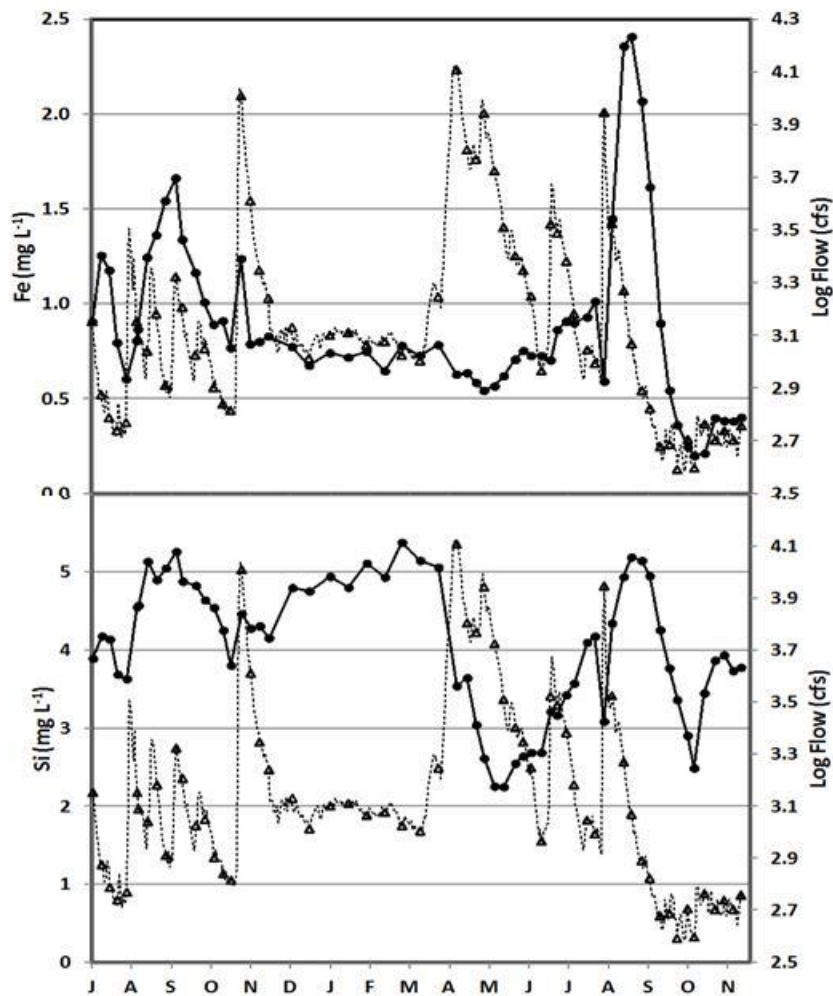
Figure 19. Fe and Si concentrations (solid lines, circles) for the 001 site compared to flow (dotted line, triangles) measured at Scanlon from July 2010 to November 2011.   Fe concentrations remained above about 0.5 mg L^{-1} in the St. Louis River throughout the study, except during the extreme drought period when non-mining inputs were low, ionic strength in the stream became elevated, and colloidal transport of iron became less efficient.   The highest Fe and Si concentrations were observed following summer rain events, suggesting that most event water was previously stored and reacting in reduced soils and sediments before being expelled into the river.
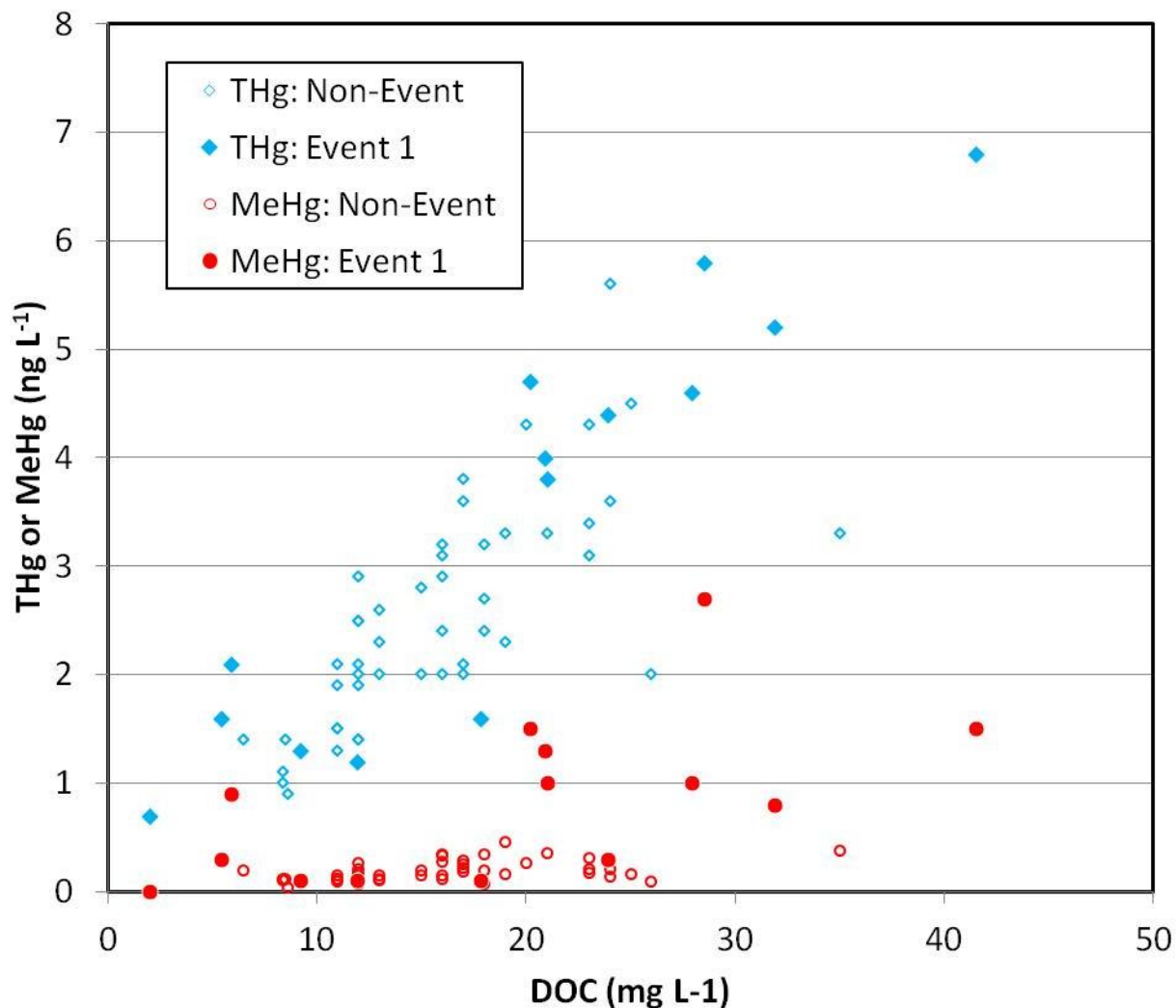
Figure 20. Comparison of THg and MeHg concentrations measured in this study with those reported previously for the same watershed by Berndt and Bavin (2012). Snowmelt runoff samples from Berndt and Bavin (2012) were not plotted. The data from the present data set were collected following a major rain event over part of the region (Fig 21). Those from the previous data set were collected when comparatively dry conditions prevailed in the watershed. THg vs DOC relations are similar for the two data sets, but many waters from the present study have elevated MeHg compared to those from the previous study. We suggest that DOC containing similar amounts of MeHg and THg emerge from pore fluids following rainfall events (Figure 23). Methylmercury is unstable so the MeHg/DOC ratio decreases with time of transit (from reduced pore fluid to sample location). THg/DOC ratio is preserved during demethylation while, obviously, the MeHg concentration is not.
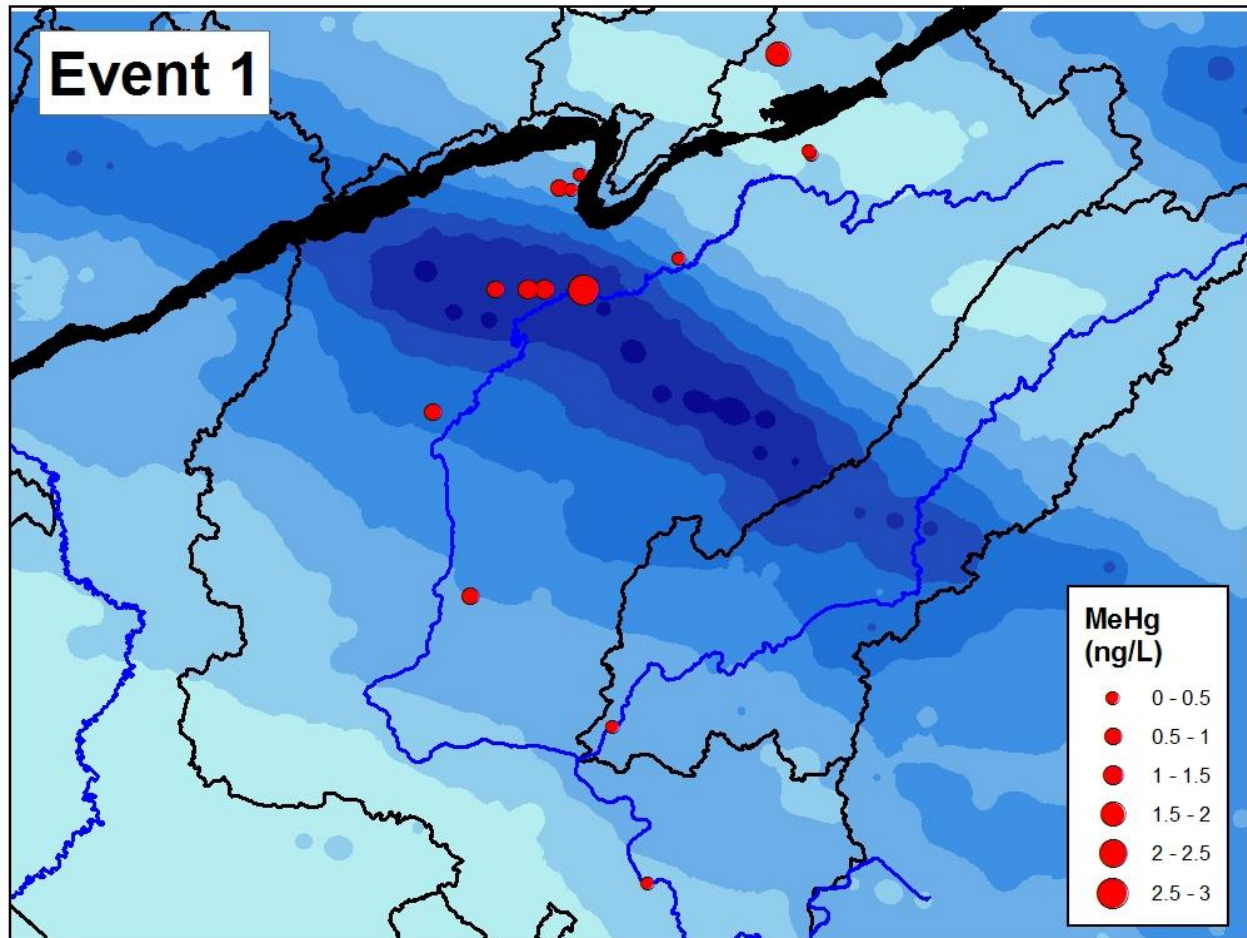
Figure 21. MeHg concentrations superimposed on precipitation map for Event 1. High rainfall likely expelled pore-fluids with elevated methylmercury from reduced soils and sediments into nearby streams.
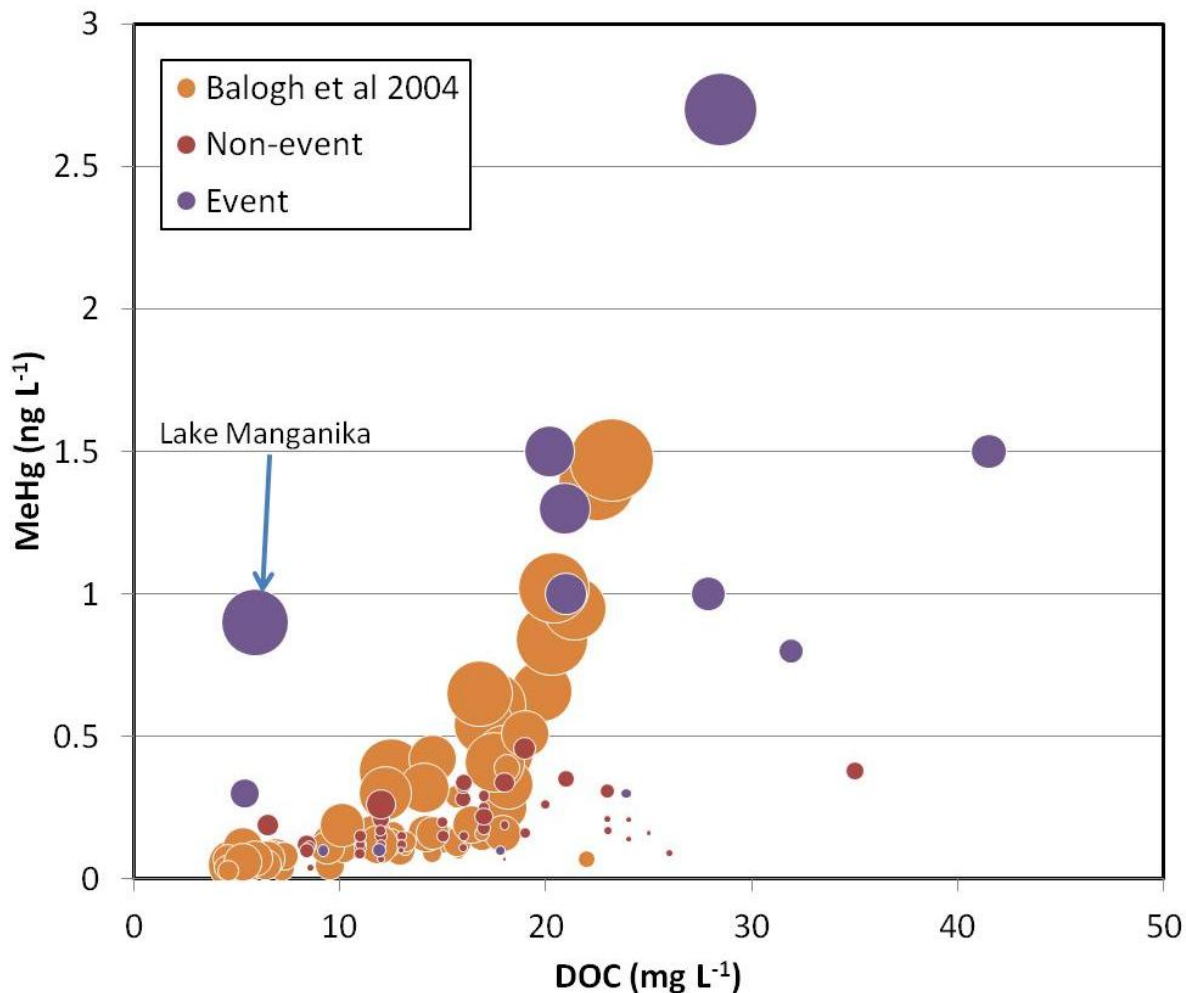
Figure 22. Bubble plot comparing MeHg and DOC relationships in the St. Louis River and Rum River watersheds during event and non/event sampling periods. The width of the bubble is proportional to MeHg/THg ratio. Many factors control the MeHg concentration in streams, including the amount and sources of DOC and the amount of time that passes once the DOC leaves the source zone. Lake Manganika outlet is highlighted because this stream's MeHg source is derived internally within the lake (See Berndt and Bavin, 2011). In most cases, the MeHg is probably generated in the reduced sediments that surrounds small streams and wetlands throughout the region. It is transported with DOC out into oxygenated waters where demethylation (and methylation stops). High MeHg/THg ratios and MeHg concentrations are found when the DOC has been freshly transported from the reducing to oxidizing portions of the watershed, such as the time period directly following a precipitation event. The waters sampled in Balogh's 2004 study were collected during a variety of flow conditions (event and non-event) from two low-SO_4 streams in Minnesota. MeHg ratios and MeHg concentrations are largely similar to those in the St. Louis River watershed, with the exception of Lake Manganika outlet waters (very low DOC, but elevated MeHg) or where high DOC levels were encountered in the St. Louis River watershed.
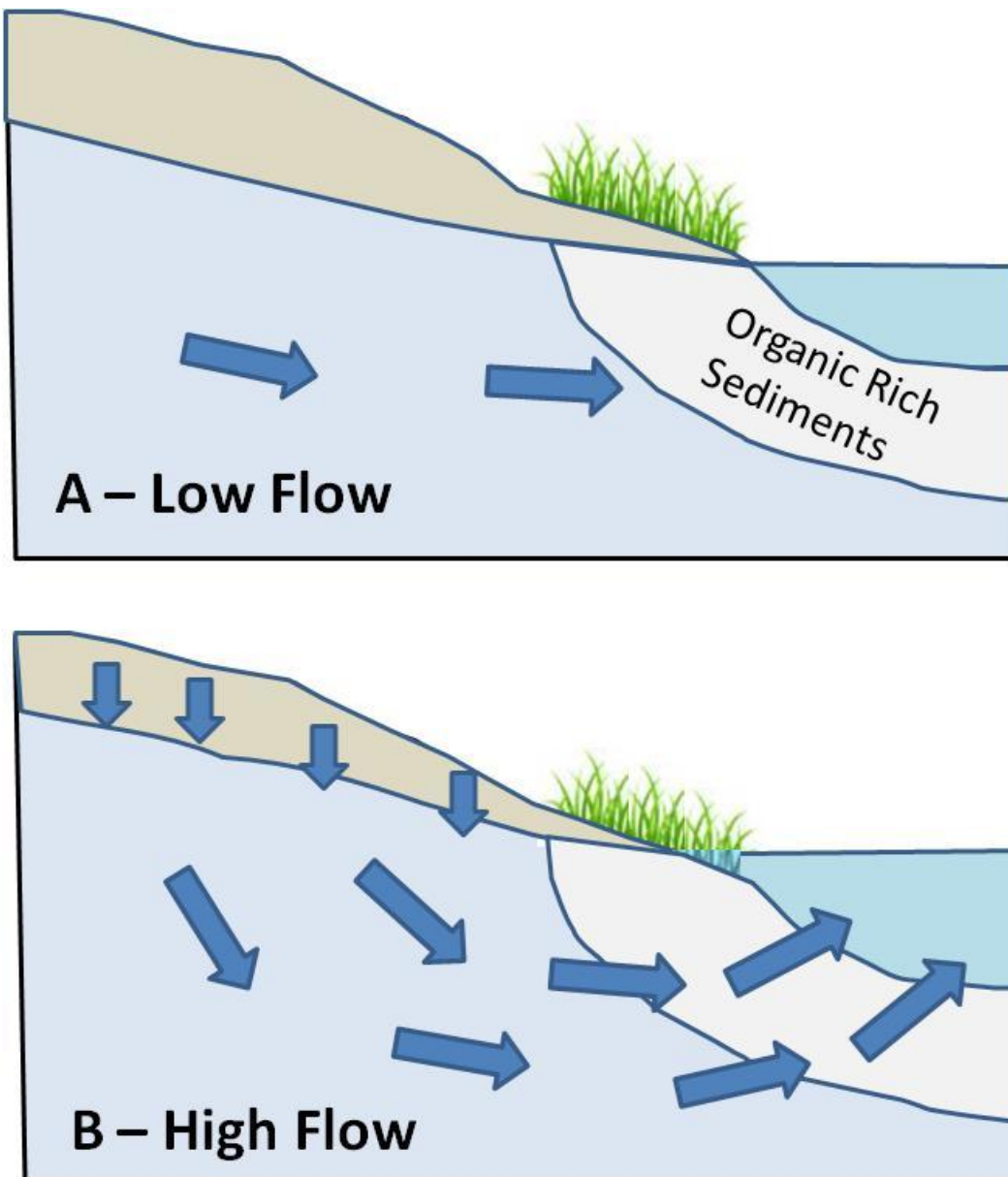
Figure 23. Model hypothesized to account for Fe, Mn, Al, SiO_2, DOC, MeHg and THg data in this study. Rainfall events are followed by periods of enhanced transport of these components. The enhanced transport is caused by increasing flow rate of water through reduced soils and sediments into the openly flowing water column.

References

Aiken, G.R., Hsu-Kim, H., Ryan, J.N., 2011. Influence of dissolved organic matter on the environmental fate of metals, nanoparticles, and colloids. Environmental Science and Technology 45, 3196-3201.

Balci, N., Shanks III, W.C., Mayer, B., Mandernack, K.W., 2007. Oxygen and sulfur isotope systematics of sulfate produced by bacterial and abiotic oxidation of pyrite. Geochimica et Cosmochimica Acta 71, 3796-3811.

Balogh, S.J., Nollet, Y.H., Swain, E.B., 2004. Redox chemistry in Minnesota streams during episodes of increased methylmercury discharge. Environmental Science and Technology 38, 4921-4927.

Balogh, S.J., Swain, E.B., Nollet, Y.H., 2006. Elevated methylmercury concentrations and loadings during flooding in Minnesota rivers. Science of The Total Environment 368, 138-148.

Barr-Engineering, 2009. Sulfate, Mercury, and Methyl Mercury in Second Creek, Submitted to the Minnesota Department of Natural Resources, 62 p.

Bencala, K.E., Gooseff, M.N., Kimball, B.A., 2011. Rethinking hyporheic flow and transient storage to advance understanding of stream-catchment connections. Water Resources Research 47.

Benoit, J.M., Gilmour, C.C., Mason, R.P., Heyes, A., 1999. Sulfide Controls on Mercury Speciation and Bioavailability to Methylating Bacteria in Sediment Pore Waters. Environmental Science & Technology 33, 951-957.

Berndt, M.E., Bavin, T.K., 2009. Sulfate and mercury chemistry of the St. Louis River in Northeastern Minnesota: A Report to the Minerals Coordinating Committee. Minnesota Department of Natural Resources, Division of Lands and Minerals, St. Paul, MN, 83 p.

Berndt, M.E., Bavin, T.K., 2011. Sulfate and Mercury Cycling in Five Wetlands and a Lake Receiving Sulfate from Taconite Mines in Northeastern Minnesota: A Report to Iron Ore Cooperative Research Program., Minnesota Department of Natural Resources, Division of Lands and Minerals, St. Paul, MN, 77p.

Berndt, M.E., Bavin, T.K., 2012. Methylmercury and dissolved organic carbon relationships in a wetland-rich watershed impacted by elevated sulfate from mining. Environmental Pollution 161, 321-327.

Birkel, C., Soulsby, C., Tetzlaff, D., Dunn, S., Spezia, L., 2012. High-frequency storm event isotope sampling reveals time-variant transit time distributions and influence of diurnal cycles. Hydrological Processes 26, 308-316.

Blodau, C., Mayer, B., Peiffer, S., Moore, T.R., 2007. Support for an anaerobic sulfur cycle in two Canadian peatland soils. Journal of Geophysical Research G: Biogeosciences 112.

Bottcher, M.E., Thamdrup, B., 2001. Oxygen and sulfur isotope fractionation during anaerobic bacterial disproportionation of elemental sulfur. Geochimica et Cosmochimica Acta 65, 1601-1609.

Brunner, B., Bernasconi, S.M., Kleikemper, J., Schroth, M.H., 2005. A model for oxygen and sulfur isotope fractionation in sulfate during bacterial sulfate reduction processes. Geochimica et Cosmochimica Acta 69, 4773-4785.

Burns, D.A., Riva-Murray, K., Bradley, P.M., Aiken, G.R., Brigham, M.E., 2012. Landscape controls on total and methyl Hg in the upper Hudson River basin, New York, USA. Journal of Geophysical Research G: Biogeosciences 117.

Canfield, D.E., Thamdrup, B., Fleischer, S., 1998. Isotope fractionation and sulfur metabolism by pure and enrichment cultures of elemental sulfur-disproportionating bacteria. Limnology and Oceanography 43, 253-264.

Chapelle, F.H., Bradley, P.M., Thomas, M.A., McMahon, P.B., 2009. Distinguishing iron-reducing from sulfate-reducing conditions. Ground Water 47, 300-305.

Coleman Wasik, J., Mitchell, C.P.J., Engstrom, D.R., Swain, E.B., Monson, B.A., Balogh, S.J., Jeremiason, J.D., Branfireun, B.A., Eggert, S.L., Kolka, R.K., Almendinger, J.E., 2012. Methylmercury Declines in a Boreal Peatland When Experimental Sulfate Deposition Decreases. Environmental Science & Technology in press.

Crerar, D.A., 1981. Hydrogeochemistry of the New Jersey Coastal Plain. 2. Transport and deposition of iron, aluminum, dissolved organic matter, and selected trace elements in stream, ground- and estuary water. Australian Journal of Soil Research 33, 23-44.

Creswell, J.E., Kerr, S.C., Meyer, M.H., Babiarz, C.L., Shafer, M.M., Armstrong, D.E., Roden, E.E., 2010. Factors controlling temporal and spatial distribution of total mercury and methylmercury in hyporheic sediments of the Allequash Creek wetland, northern Wisconsin. Journal of Geophysical Research - Part G - Biogeosciences 115, 00-02.

Detmers, J., Bruchert, V., Habicht, K.S., Kuever, J., 2001. Diversity of sulfur isotope fractionations by sulfate-reducing prokaryotes. Applied and Environmental Microbiology 67, 888-894.

Dolfing, J., Chardon, W.J., Japenga, J., 1999. Association between colloidal iron, aluminum, phosphorus, and humic acids. Soil Science 164, 171-179.

Drott, A., Lambertsson, L., Bjorn, E., Skyllberg, U., 2008. Potential demethylation rate determinations in relation to concentrations of MeHg, Hg and pore water speciation of MeHg in contaminated sediments. Marine Chemistry 112, 93-101.

Eimers, M.C., Dillon, P.J., Schiff, S.L., 2004. A S-isotope approach to determine the relative contribution of redox processes to net SO4 export from upland, and wetland-dominated catchments. Geochimica et Cosmochimica Acta 68, 3665-3674.

Eimers, M.C., Watmough, S.A., Buttle, J.M., Dillon, P.J., 2007. Drought-induced sulphate release from a wetland in south-central Ontario. Environmental Monitoring and Assessment 127, 399-407.

Geurts, J.J.M., Sarneel, J.M., Willers, B.J.C., Roelofs, J.G.M., Verhoeven, J.T.A., Lamers, L.P.M., 2009. Interacting effects of sulphate pollution, sulphide toxicity and eutrophication on vegetation development in fens: A mesocosm experiment. Environmental Pollution 157, 2072-2081.

Gilmour, C.C., Henry, E.A., Mitchell, R., 1992. Sulfate stimulation of mercury methylation in freshwater sediments. Environmental Science & Technology 26, 2281-2287.

Godsey, S.E., Kirchner, J.W., Clow, D.W., 2009. Concentration-discharge relationships reflect chemostatic characteristics of US catchments. Hydrological Processes 23, 1844-1864.

Gray, J.E., Hines, M.E., 2009. Biogeochemical mercury methylation influenced by reservoir eutrophication, Salmon Falls Creek Reservoir, Idaho, USA. Chemical Geology 258, 157-167.

Hammerschmidt, C.R., Fitzgerald, W.F., 2010. Iron-Mediated Photochemical Decomposition of Methylmercury in an Arctic Alaskan Lake. Environmental Science & Technology 44, 6138-6143.

Heikkinen, K., 1994. Organic matter, iron and nutrient transport and nature of dissolved organic matter in the drainage basin of a boreal humic river in northern Finland. Science of The Total Environment 152, 81-89.

Jeremiason, J.D., Engstrom, D.R., Swain, E.B., Nater, E.A., Johnson, B.M., Almendinger, J.E., Monson, B.A., Kolka, R.K., 2006. Sulfate addition increases methylmercury production in an experimental wetland. Environmental Science and Technology 40, 3800-3806.

Johnson, N., Beck, B., 2012. Sulfur and carbon controls on methyl mercury in St. Louis River Estuary sediment, Report Submitted to the Minnesota Department of Natural Resources, p. 45.

Johnson, N., Zhu, X., 2012. Carbon and iron additions to stimulate in-pit sulfate reduction and removal, Report to the Minnesota Department of Natural Resources, p. 24.

Jonsson, S., Skyllberg, U., Bjorn, E., 2010. Substantial emission of gaseous monomethylmercury from contaminated water-sediment microcosms. Environmental Science and Technology 44, 278-283.

Lamers, L.P.M., Sarah-J, F., Samborska, E.M., Van Dulken, I.A.R., Van Hengstum, G., Roelofs, J.G.M., 2002. Factors controlling the extent of eutrophication and toxicity in sulfate-polluted freshwater wetlands. Limnology and Oceanography 47, 585-593.

Lamers, L.P.M., Tomassen, H.B.M., Roelofs, J.G.M., 1998. Sulfate-induced eutrophication and phytotoxicity in freshwater wetlands. Environmental Science and Technology 32, 199-205.

Lehnherr, I., St. Louis, V.L., 2009. Importance of Ultraviolet Radiation in the Photodemethylation of Methylmercury in Freshwater Ecosystems. Environmental Science & Technology 43, 5692-5698.

Maderak, M.L., 1963. Quality of waters, Minnesota, A compilation, 1955-1962. State of Minnesota Department of Conservation Division of Waters, St. Paul, MN.

Mandernack, K.W., Lynch, L., Krouse, H.R., Morgan, M.D., 2000. Sulfur cycling in wetland peat of the New Jersey Pinelands and its effect on stream water chemistry. Geochimica et Cosmochimica Acta 64, 3949-3964.

Marvin-DiPasquale, M., Lutz, M.A., Brigham, M.E., Krabbenhoft, D.P., Aiken, G.R., Orem, W.H., Hall, B.D., 2009. Mercury Cycling in Stream Ecosystems. 2. Benthic Methylmercury Production and Bed Sediment–Pore Water Partitioning. Environmental Science & Technology 43, 2726-2732.

McDonnell, J.J., McGuire, K., Aggarwal, P., Beven, K.J., Biondi, D., Destouni, G., Dunn, S., James, A., Kirchner, J., Kraft, P., Lyon, S., Maloszewski, P., Newman, B., Pfister, L., Rinaldo, A., Rodhe, A., Sayama, T., Seibert, J., Solomon, K., Soulsby, C., Stewart, M., Tetzlaff, D., Tobin, C., Troch, P., Weiler, M., Western, A., Worman, A., Wrede, S., 2010. How old is streamwater? Open questions in catchment transit time conceptualization, modelling and analysis. Hydrological Processes 24, 1745-1754.

McGlynn, B., McDonnell, J., Stewart, M., Seibert, J., 2003. On the relationships between catchment scale and streamwater mean residence time. Hydrological Processes 17, 175-181.

McGlynn, B.L., McDonnell, J.J., 2003. Role of discrete landscape units in controlling catchment dissolved organic carbon dynamics. Water Resources Research 39, SWC31-SWC318.

Miller, C.L., Mason, R.P., Gilmour, C.C., Heyes, A., 2007. Influence of dissolved organic matter on the complexation of mercury under sulfidic conditions. Environmental Toxicology and Chemistry 26, 624-633.

Moyle, J.B., Kenyon, W.A., 1947. A biologic survey and fishery management plan for the streams of the Saint Louis River basin. Minnesota Department of Conservation Report.

NADP, 2012. National Atmospheric Deposition Program (website at http://nadp.sws.uiuc.edu/).

Novak, M., Vile, M.A., Bottrell, S.H., tepanova, M., Jackova, I., Buzek, F., Prechova, E., Newton, R.J., 2005. Isotope systematics of sulfate-oxygen and sulfate-sulfur in six European peatlands. Biogeochemistry 76, 187-213.

Poulton, S.W., Fralick, P.W., Canfield, D.E., 2010. Spatial variability in oceanic redox structure 1.8 billion years ago. Nature Geoscience 3, 486-490.

Rantz, S.E., 1982. Measurement and computation of streamflow. Volume 1. Measurement of stage and discharge. Volume 2. Computation of discharge. US Geological Survey Water-Supply Paper 2175.

Rulik, M., Cap, L., Hlavacova, E., 2000. Methane in hyporheic zone of a small lowland stream (Sitka, Czech Republic). Limnologica 30, 359-366.

Sjostedt, C.S., Gustafsson, J.P., Kohler, S.J., 2010. Chemical equilibrium modeling of organic acids, pH, Aluminum, and iron in Swedish surface waters. Environmental Science and Technology 44, 8587-8593.

Theriault, S.A., 2011. Mineralogy, Spatial Distribution, and Isotope Geochemistry of Sulfide Minerals in the Biwabik Iron Formation, Geology. University of Minnesota, 165 p.

Theriault, S.A., Miller, J.D., Berndt, M.E., Ripley, E.M., 2011. The mineralogy, spatial distribution, and isotope geochemistry of sulfide minerals in the Biwabik Iron Formation, Institute for Lake Superior Geology, Abstract.

Toran, L., Harris, R.F., 1989. Interpretation of sulfur and oxygen isotopes in biological and abiological sulfide oxidation. Geochimica et Cosmochimica Acta 53, 2341-2348.

Urban, N.R., Eisenreich, S.J., Grigal, D.F., 1989. Sulfur cycling in a forested Sphagnum bog in northern Minnesota. Biogeochemistry 7, 81-109.

Weiler, M., McGlynn, B.L., McGuire, K.J., McDonnell, J.J., 2003. How does rainfall become runoff? A combined tracer and runoff transfer function approach. Water Resources Research 39, SWC41-SWC413.

Wu, S., Jeschke, C., Dong, R., Paschke, H., Kuschk, P., Knoller, K., 2011. Sulfur transformations in pilot-scale constructed wetland treating high sulfate-containing contaminated groundwater: A stable isotope assessment. Water Research 45, 6688-6698.

Zerkle, A.L., Farquhar, J., Johnston, D.T., Cox, R.P., Canfield, D.E., 2009. Fractionation of multiple sulfur isotopes during phototrophic oxidation of sulfide and elemental sulfur by a green sulfur bacterium. Geochimica et Cosmochimica Acta 73, 291-306.

Zerkle, A.L., Kamyshny, A., Kump, L.R., Farquhar, J., Oduro, H., Arthur, M.A., 2010. Sulfur cycling in a stratified euxinic lake with moderately high sulfate: Constraints from quadruple S isotopes. Geochimica et Cosmochimica Acta 74, 4953-4970.

Appendix A1 Sampling Location Map and Descriptions
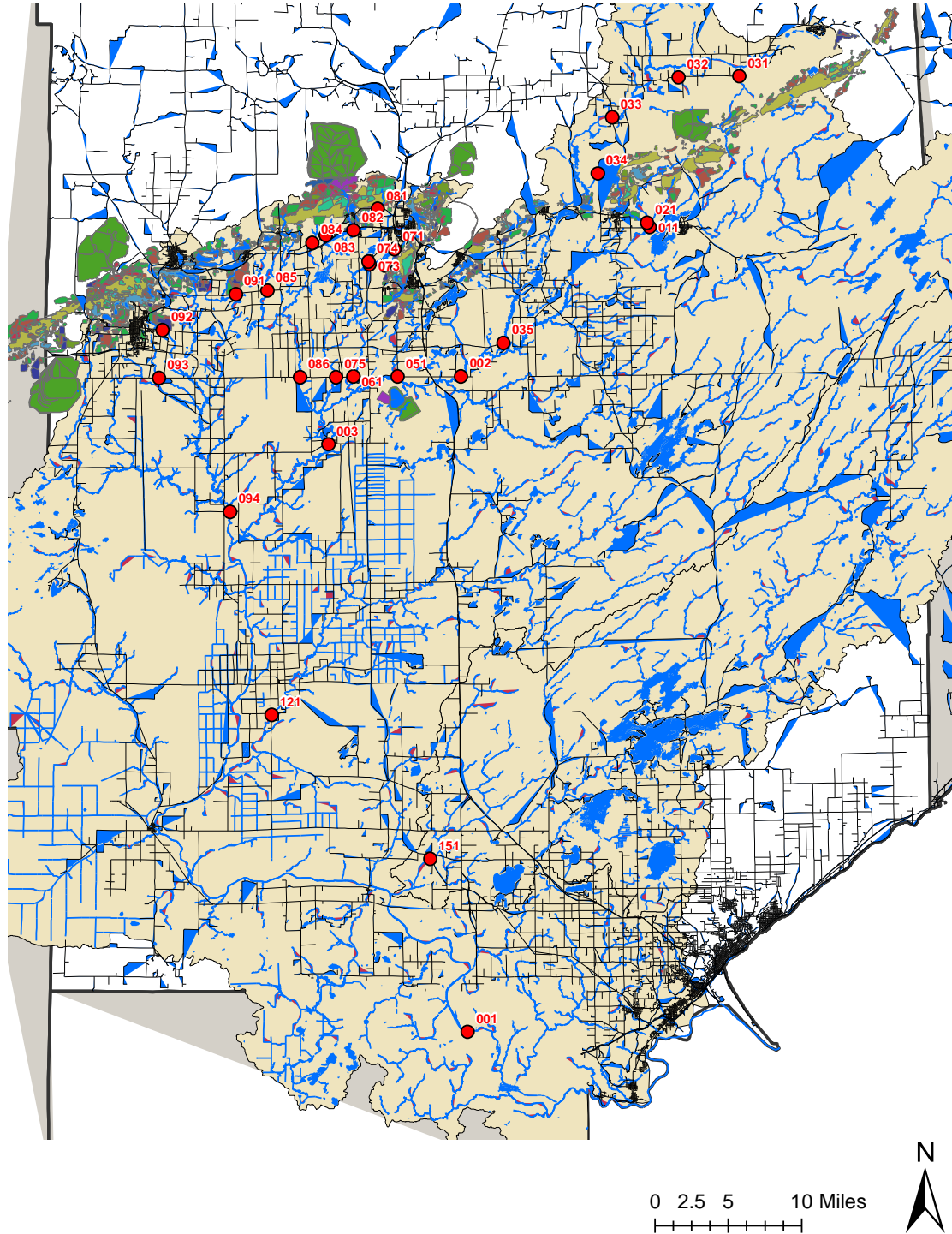
Figure A-1. Sampling locations, St. Louis River watershed (brown shaded).

Table A-1. Sample site descriptions.

ID	Site Description	Location
001	St. Louis River in Cloquet	Dock north of Hwy 33 bridge
002	St. Louis River upstream of Forbes Plant at mile 135	CR 957; Town Line Road
003	St. Louis River downstream of Forbes Plant at mile 115	HW 27; Zim canoe access
011	Partridge River downstream of Second Creek near confluence with St. Louis River	HW 110
021	Second Creek near confluence with Partridge River	N of HW 110 near Partridge River bridge
031	Spring Mine Creek	CR 620; Salo Road
032	Trimble Creek	Cr 615; Salo Road
033	Embarrass River downstream of tailngs basin	HW 135
034	Unnamed creek flowing W towards Wynne Lake from Mesabi Nugget property	HW 135
035	Embarrass River downstream of Embarrass Chain of Lakes near confluence with St. Louis River	HW 336; Bodas Road
051	Long Lake Creek near confluence with St. Louis River	HW 16; Town Line Road
061	Elbow Creek near confluence with St. Louis River	HW 16; Town Line Road
071	East Two River upstream of Lake Manganika, downstream of City of Virginia WWTF	CN Railroad right-of-way at CR 103 S of Virginia
072	Creek flowing into E side Lake Manganika from Utac	
073	East Two River downstream of Lake Manganika	HW 7 south of Virginia
074	East Two River downstream of Lake Mashkinode	CR 102 near intersection with HW 7 south of Virginia
075	East Two River near confluence with St. Louis River	HW 16; Town Line Road
081	Minntac discharge to West Two Rivers	Old HW 169; near Minntac main gate
082	Minntac discharge to West Two Rivers (diverted to Mtn. Iron Pit during this study)	HW 169 S of Mt. Iron
083	Minntac discharge to West Two Rivers	CR 768; Otto Rd? N of HW 169, W of Mountain Iron – eastern side
084	Minntac discharge to West Two Rivers	CR 768; Otto Rd? N of HW 169, W of Mountain Iron – west of 083
085	Minntac discharge to West Two Rivers	CR 625; W of HW 25 E of CR 453
086	West Two Rivers near confluence with St. Louis River	HW 16; Town Line Road
091	East Swan River near historical mining feature S of Buhl	CR 642 near intersection with CR 461; E of CR 5
092	Hibtac Hull Rust Pit discharge	CR 63 E of Hibbing
093	East Swan River near Hibbing S WWTF	HW 16; Town Line Road; near CR 444
094	Swan River near confluence with St. Louis River	CR 750
121	Whiteface River near confluence with St. Louis River	HW 5 near intersection with CR 29
151	Cloquet River near confluence with St. Louis River	CR 694 NE of Brookston; S of HW 7

Appendix A2: Data Tables for Samples Collected During the Survey

Table A-1-1: Sample identifiers, dates, flow rates and field parameters from the August 2010 $SO_4^=$ survey.   The three digit number identifies the site while the single digit following identifies the round number (see Table 1 in the text). If no sample was collected during that round, the table parameters are left blank.   Other parameters for these samples can be found in Tables A-2-1 and A-3-2.

ID	Date	Time	Flow (cfs)	Flow (mgd)	pH	Cond	T
MSRS-001-1	8/10/2010	8:59	1420	917.55	7.3	500	24.3
MSRS-002-1	8/11/2010	13:55	190	122.77	8.0	250	25.9
MSRS-003-1	8/10/2010	11:45	344	222.28	7.4	500	25.2
MSRS-011-1	8/12/2010	9:00	29.8	19.26	7.6	700	24.5
MSRS-021-1	8/12/2010	8:30	3.4	2.18	7.4	2050	24.4
MSRS-031-1	8/12/2010	12:45	1.5	0.97	8.7	550	22.6
MSRS-032-1	8/12/2010	12:30	1.7	1.09	8.3	550	22.5
MSRS-033-1	8/12/2010	11:43	28.1	18.16	8.6	160	24.1
MSRS-034-1							
MSRS-035-1	8/11/2010	14:10	106	68.49	8.1	245	28.2
MSRS-051-1	8/10/2010	12:45	7.3	4.70	7.5	400	24.4
MSRS-061-1	8/10/2010	13:00	12.3	7.95	7.3	500	24.3
MSRS-071-1	8/11/2010	11:00	6.1	3.92	8.1	1150	21.6
MSRS-072-1	8/11/2010	12:10	6.5	4.23	8.5	1600	22.6
MSRS-073-1	8/11/2010	12:00	10.5	6.78	9.1	1000	26.4
MSRS-074-1	8/11/2010	11:40	14.4	9.30	8.0	450	25.1
MSRS-075-1	8/10/2010	13:15	20.8	13.44	7.5	850	26.1
MSRS-081-1	8/11/2010	9:20	5.4	3.50	8.2	1300	18.7
MSRS-082-1							
MSRS-083-1	8/11/2010	8:55	0.21	0.14	7.8	1200	19.7
MSRS-084-1	8/11/2010	8:48	0.27	0.17	7.8	130	22.1
MSRS-085-1	8/11/2010	8:30	10.7	6.91	7.6	510	23
MSRS-086-1	8/10/2010	13:45	61.9	40.00	7.5	600	24.6
MSRS-091-1	8/11/2010	8:00	10.1	6.53	7.1	240	24
MSRS-092-1	8/10/2010	14:45	28.7	18.54	7.5	800	23.7
MSRS-093-1	8/10/2010	15:34	6.4	4.12	7.2	550	22.1
MSRS-094-1	8/10/2010	11:15	152	98.22	7.3	500	23.2
MSRS-121-1	8/10/2010	10:20	275	177.70	7.4	400	24.1
MSRS-151-1	8/10/2010	9:30	184	118.89	7.6	600	24.8

Table A-1-2: Sample identifiers, dates, flow rates and field parameters from the September 2010 $SO_4^=$ survey.   The three digit number identifies the site while the single digit following identifies the round number (see Table 1 in the text). If no sample was collected during that round, the table parameters are left blank. Other parameters for these samples can be found in Tables A-2-2 and A-3-2.

ID	Date	Time	Flow (cfs)	Flow (mgd)	pH	Cond	T
MSRS-001-2	9/14/2010	9:16	1610	1040.32	7.3	150	15.3
MSRS-002-2	9/14/2010	11:56	125	80.77	8.0	350	14.4
MSRS-003-2	9/14/2010	11:15	264	170.59	7.8	315	14.2
MSRS-011-2	9/15/2010	9:00	29.7	19.19	8.5	400	13
MSRS-021-2	9/15/2010	8:45	2.13	1.38	7.7	1725	12.00
MSRS-031-2	9/15/2010	11:49	1.75	1.13	7.9	900	11.5
MSRS-032-2	9/15/2010	11:32	1.82	1.18	7.7	500	10
MSRS-033-2	9/15/2010	11:15	38.1	24.62			
MSRS-034-2	9/15/2010	11:00			8.2	1000	10.7
MSRS-035-2	9/14/2010	12:10	51	32.95	8.0	245	15.5
MSRS-051-2	9/14/2010	11:42	4.1	2.68	8.0	290	14
MSRS-061-2	9/14/2010	12:46	9.3	6.01	8.0	270	15
MSRS-071-2	9/15/2010	13:15	7.0	4.53	8.1	1600	15.1
MSRS-072-2	9/15/2010	14:45	4.4	2.82	8.7	1600	12.8
MSRS-073-2	9/15/2010	14:32	13.4	8.66	9.3	1100	13.5
MSRS-074-2	9/15/2010	14:20	9.3	5.99	8.2	500	14.6
MSRS-075-2	9/14/2010	12:56	31.3	20.22	7.7	610	15
MSRS-081-2	9/16/2010	8:45	4.7	3.05	8.7	1225	10.2
MSRS-082-2							
MSRS-083-2	9/16/2010	8:33	0.24	0.16	8.6	1300	8.9
MSRS-084-2							
MSRS-085-2	9/16/2010	8:20	8.4	5.4	7.2	475	10.4
MSRS-086-2	9/14/2010	13:07	42.6	27.5	8.1	400	15.8
MSRS-091-2	9/16/2010	8:07	8.6	5.6	6.2	278	12
MSRS-092-2	9/14/2010	13:45	25.1	16.2	8.1	590	15.6
MSRS-093-2	9/14/2010	13:20	6.2	4.0	7.8	510	16.2
MSRS-094-2	9/14/2010	10:50	149	96	7.4	220	13.6
MSRS-121-2	9/14/2010	10:30	190	123	7.6	125	14.5
MSRS-151-2	9/14/2010	9:47	194	125	7.6	120	14.5

Table A-1-3: Sample identifiers, dates, flow rates and field parameters from the March 2011 SO$_4^=$ survey.   The three digit number identifies the site while the single digit following identifies the round number (see Table 1 in the text). If no sample was collected during that round, the table parameters are left blank. Thermometer was not working during this round, but most temperatures were close to 0 C as all sites were ice covered. Other parameters for these samples can be found in Tables A-2-3 and A-3-3.

ID	Date	Time	Flow (cfs)	Flow (mgd)	pH	Cond	T
MSRS-011-3	3/8/2011	11:45	14.3	9.24	7.8	600	
MSRS-021-3	3/8/2011	12:00	2.6	1.65	7.7	2400	
MSRS-031-3	3/8/2011	12:50			8.1	1400	
MSRS-032-3	3/8/2011	12:40			7.7	900	
MSRS-033-3	3/8/2011	12:10	12.3	7.95	7.9	600	
MSRS-035-3	3/8/2011	10:30	36.0	23.26	7.7	390	
MSRS-061-3	3/8/2011	10:05			8.0	490	
MSRS-073-3	3/8/2011	14:00	7.6	4.91	8.3	1900	
MSRS-075-3	3/8/2011	9:45	3.8	2.46	7.7	1590	
MSRS-081-3	3/8/2011	13:40	1.7	1.10	8.3	1490	
MSRS-085-3	3/8/2011	14:20	3.7	2.39	8.3	710	
MSRS-086-3	3/8/2011	9:28	17.0	10.98	7.7	695	
MSRS-092-3	3/8/2011	15:00	13.2	8.53	8.2	900	
MSRS-094-3	3/8/2011	8:50	32	20.68	7.0	490	

Table A-2-1: Cation chemistry for the August 2010 $SO_4^=$ survey.   Times, dates, and field parameters are provided in Table A-1-1, while anion, Hg, and DOC chemistry for these samples is provided in Table A-3-1.

ID	Al	Ba	Ca	Fe	K	Mg	Mn	Na	Si	Sr
MSRS-001-1	0.05	0.02	16.7	0.81	1.9	9.3	0.10	6.2	4.6	0.05
MSRS-002-1	0.03	0.02	21.9	0.30	2.4	17.8	0.07	10.5	3.9	0.09
MSRS-003-1	0.06	0.02	22.6	0.09	3.4	22.2	0.17	13.8	4.1	0.09
MSRS-011-1	0.03	0.02	30.3	0.56	3.1	39.2	0.14	11.6	4.1	0.21
MSRS-021-1	0.01	0.03	62.2	0.04	17.2	266	0.30	50	4.7	0.27
MSRS-031-1	0.01	0.01	27.7	0.16	10.2	44.1	0.07	20.1	8.1	0.11
MSRS-032-1	0.01	0.09	46.4	1.38	2.9	37.3	0.43	44.3	10.7	0.22
MSRS-033-1	0.13	0.04	19.7	5.9	1.5	11.5	0.32	7.5	7.7	0.08
MSRS-034-1										
MSRS-035-1	0.01	0.03	21.0	0.08	2.6	15.2	0.03	11.4	4.4	0.08
MSRS-051-1	0.17	0.02	28.1	1.91	2.7	21.7	0.28	10.9	5.1	0.10
MSRS-061-1	0.01	0.02	30.2	0.49	3.8	20.8	2.48	20.3	6.9	0.11
MSRS-071-1	0.06	0.01	41.3	0.04	14.6	99	0.15	74	5.3	0.13
MSRS-072-1	0.01	0.01	23.1	0.01	25.7	209	0.02	104	5.2	0.09
MSRS-073-1	0.01	0.01	14.6	0.01	15.0	114	0.06	79	5.2	0.04
MSRS-074-1	0.01	0.02	36.2	0.06	3.9	31.9	0.46	23.6	1.9	0.12
MSRS-075-1	0.08	0.02	27.9	0.60	7.3	53	0.18	37.8	4.7	0.09
MSRS-081-1	0.00	0.04	81.0	0.03	19.1	163	0.32	38.7	8.4	0.51
MSRS-082-1										
MSRS-083-1	0.01	0.05	60.4	0.10	21.9	147	0.09	55	5.0	0.26
MSRS-084-1	0.03	0.03	11.5	1.89	0.7	9.9	2.67	3.7	5.9	0.05
MSRS-085-1	0.02	0.04	35.0	0.29	10.8	44.0	0.15	19.5	4.3	0.15
MSRS-086-1	0.07	0.04	25.2	1.49	5.4	28.1	0.37	14.5	4.0	0.10
MSRS-091-1	0.01	0.02	24.5	0.31	2.7	15.2	0.19	10.2	4.1	0.08
MSRS-092-1	0.01	0.01	44.2	0.02	3.9	46.5	0.07	16.8	4.8	0.11
MSRS-093-1	0.06	0.02	53.6	0.10	6.3	23.4	0.21	55	8.4	0.16
MSRS-094-1	0.09	0.03	27.3	2.30	2.2	16.4	0.38	10.6	5.5	0.08
MSRS-121-1	0.07	0.02	15.8	1.3	1.6	8.7	0.22	5.6	4.6	0.06
MSRS-151-1	0.01	0.01	15.8	0.31	0.7	6.4	0.10	3.6	4.2	0.04

Table A-2-2: Cation chemistry for the September 2010 $SO_4^{=}$ survey.   Times, dates, and field parameters are provided in Table A-1-2 and the anion chemistry is provided in Table A-3-2.

ID	Al	Ba	Ca	Fe	K	Mg	Mn	Na	Si	Sr
MSRS-001-2	0.09	0.02	18.8	1.3	1.5	10.4	0.11	6.2	4.9	0.06
MSRS-002-2	0.03	0.02	23.7	0.33	2.7	26.4	0.07	11.0	4.0	0.10
MSRS-003-2	0.06	0.02	23.7	0.72	3.6	25.9	0.08	15.7	4.3	0.09
MSRS-011-2	0.02	0.01	32.5	0.29	2.7	28.9	0.08	11.5	3.8	0.23
MSRS-021-2	0.01	0.03	65.7	0.08	15.0	254.5	0.15	46.8	4.7	0.26
MSRS-031-2	0.01	0.02	44.4	0.13	21.1	91.4	0.10	41.7	7.6	0.17
MSRS-032-2	0.01	0.06	41.1	0.42	2.8	36.5	0.08	47.8	10.3	0.19
MSRS-033-2	0.06	0.03	16.6	1.4	2.1	12.2	0.09	9.5	7.0	0.06
MSRS-034-2	0.01	0.05	36.4	0.15	11.4	106	0.22	45.1	2.0	0.16
MSRS-035-2	0.01	0.03	23.2	0.15	2.7	16.1	0.05	13.1	4.4	0.08
MSRS-051-2	0.12	0.02	28.1	1.3	2.7	23.6	0.14	11.2	6.4	0.10
MSRS-061-2	0.01	0.01	24.1	0.14	2.4	16.6	0.02	17.9	5.3	0.08
MSRS-071-2	0.08	0.02	56.4	0.05	15.7	112	0.16	188	6.4	0.17
MSRS-072-2	0.01	0.00	23.2	0.03	25.8	205	0.01	103	5.0	0.09
MSRS-073-2	0.02	0.01	25.6	0.04	15.9	126	0.03	83	5.6	0.08
MSRS-074-2	0.01	0.02	39.3	0.03	4.0	34.1	0.12	23.3	4.2	0.12
MSRS-075-2	0.03	0.02	29.0	0.31	7.8	60.7	0.06	40.9	5.1	0.09
MSRS-081-2	0.01	0.04	76.1	0.01	16.8	144	0.04	39.1	6.3	0.44
MSRS-082-2										
MSRS-083-2	0.00	0.05	74.1	0.07	23.1	170	0.04	59.2	5.2	0.29
MSRS-084-2										
MSRS-085-2	0.01	0.04	34.9	0.14	9.2	41.1	0.06	18.2	3.2	0.14
MSRS-086-2	0.04	0.03	26.7	0.51	5.6	30.7	0.10	15.4	3.1	0.10
MSRS-091-2	0.01	0.02	31.2	0.11	2.6	17.7	0.09	10.8	2.8	0.10
MSRS-092-2	0.00	0.01	45.8	0.01	4.3	52.4	0.01	19.0	5.2	0.11
MSRS-093-2	0.05	0.02	46.8	0.13	5.5	20.0	0.04	48.4	6.8	0.14
MSRS-094-2	0.07	0.02	23.2	1.3	2.0	14.7	0.07	10.2	5.1	0.07
MSRS-121-2	0.11	0.01	15.2	1.4	1.2	7.9	0.11	6.0	4.4	0.05
MSRS-151-2	0.02	0.09	15.7	0.39	0.7	6.6	0.06	3.9	4.7	0.04

Table A-2-3: Cation chemistry for the March 2011 $SO_4^=$ survey.   Times, dates, and field parameters are provided in Table A-1-3 and the anion chemistry is provided in Table A-3-3.

ID	Al	Ba	Ca	Fe	K	Mg	Mn	Na	Si	Sr
MSRS-011-3	0.06	0.01	40.4	0.61	3.8	51	0.46	15.4	7.2	0.25
MSRS-021-3	0.01	0.02	69.6	0.15	14.4	291	2.27	50.6	7.4	0.25
MSRS-031-3	0.01	0.03	58.3	0.12	24.1	127	0.27	52.8	7.7	0.20
MSRS-032-3	0.01	0.11	60.5	0.83	4.7	59	0.51	67.2	10.4	0.26
MSRS-033-3	0.02	0.04	33.8	1.3	4.9	35.6	0.30	24.0	8.9	0.13
MSRS-035-3	0.01	0.03	29.4	0.35	3.1	19.9	0.11	14.8	6.1	0.11
MSRS-061-3	0.01	0.01	30.4	0.35	3.6	19.7	0.74	20.6	5.5	0.11
MSRS-073-3	0.02	0.02	50.6	0.04	15.9	139	0.16	122	6.0	0.17
MSRS-075-3	0.00	0.02	45.9	0.08	12.5	106	0.18	102	6.5	0.15
MSRS-081-3	0.04	0.03	85.1	0.02	9.4	136	0.13	26.3	5.6	0.51
MSRS-085-3	0.00	0.04	48.6	0.10	9.2	48	0.22	20.4	7.3	0.18
MSRS-086-3	0.01	0.04	44.6	0.21	7.9	50	0.27	22.7	6.1	0.18
MSRS-092-3	0.00	0.01	50.6	0.02	3.7	44	0.08	65.7	4.9	0.13
MSRS-094-3	0.02	0.02	44.2	0.63	3.4	28.9	0.08	21.5	6.4	0.12

Table A-3-1: Anion chemistry and DOC, THg, and MeHg concentrations for samples collected during the August 2010 $SO_4^=$ survey.   Times, dates, and field parameters are provided in Table A-1-1, while cation chemistry for these samples is provided in Table A-2-1.

ID	F	Cl	Br	SO4=	$^{34}S_{SO4}$	$^{18}O_{SO4}$	DOC	THg	MeHg
MSRS-001-1	0.13	6.3	0.01	9.3	9.2	3.9	23.9	4.4	0.3
MSRS-002-1	0.15	6.6	0.01	46.6	9.2	0.7			
MSRS-003-1	0.17	11.6	0.01	42.7	10.6	0.9			
MSRS-011-1	0.18	6.8	0.02	151	6.6	-0.4	17.8	1.6	0.1
MSRS-021-1	0.26	9.1	0.03	1004	7.2	-5.7	9.2	1.3	0.1
MSRS-031-1	0.10	1.7	0.02	143	21.3	8.6			
MSRS-032-1	0.96	11.4	0.14	1.1					
MSRS-033-1	0.18	3.8	0.03	7.2	16.7	6.9	41.5	6.8	1.5
MSRS-034-1									
MSRS-035-1	0.15	6.7	0.01	33.3	10.5	1.3		<0.4	0.1
MSRS-051-1	0.10	12.9	0.01	29.7	20.9	5.9	28.5	5.8	2.7
MSRS-061-1	0.19	32.2	0.02	15.3	28.0	4.9	20.2	4.7	1.5
MSRS-071-1	0.41	69.3	0.08	215	4.2	-8.6	5.4	1.6	0.3
MSRS-072-1	0.12	27.4	0.04	533	6.3	-10.7	2.0	0.7	<0.05
MSRS-073-1	0.26	73.2	0.07	267	7.3	-4.7	5.9	2.1	0.9
MSRS-074-1	0.18	38.8	0.06	33.1	11.1	0.9			
MSRS-075-1	0.19	42.4	0.04	94.1	8.2	-0.4	20.9	4.0	1.3
MSRS-081-1	0.19	15.3	0.12	527	8.6	-9.4			
MSRS-082-1									
MSRS-083-1	0.15	6.3	0.04	230	11.8	-5.6			
MSRS-084-1	0.08	3.2	0.01	2.6					
MSRS-085-1	0.16	7.5	0.02	72.5	8.1	-3.4			
MSRS-086-1	0.12	10.7	0.02	50.6	9.7	0.5	21.0	3.8	1.0
MSRS-091-1	0.13	10.0	0.01	9.9	4.7	0.8			
MSRS-092-1	0.20	22.8	0.06	66.9	4.3	-1.8			
MSRS-093-1	0.74	77.7	0.05	71.6	4.5	4.7			
MSRS-094-1	0.14	13.6	0.02	17.4	4.4	0.6	27.9	4.6	1.0
MSRS-121-1	0.26	2.8	0.01	3.8			31.9	5.2	0.8
MSRS-151-1	0.10	4.4	0.01	2.0	7.4	5.7	11.9	1.2	0.1

Table A-3-2: Anion chemistry for samples collected during the September 2010 $SO_4^=$ survey. Times, dates, and field parameters are provided in Table A-1-2, while cation chemistry for these samples is provided in Table A-2-2.

ID	F	Cl	Br	SO4$^=$	$^{34}S_{SO4}$	$^{18}O_{SO4}$
MSRS-001-2	0.10	6.3	0.01	9.5	7.3	1.7
MSRS-002-2	0.13	6.5	0.01	77.5		
MSRS-003-2	0.17	13.6	0.01	51.2	9.3	0.0
MSRS-011-2	0.18	8.9	0.02	118	7.1	1.5
MSRS-021-2	0.23	8.5	0.02	951	8.0	-4.5
MSRS-031-2	0.11	2.7	0.01	387	14.0	6.5
MSRS-032-2	0.90	13.5	0.12	13.0	35.5	8.9
MSRS-033-2	0.15	4.9	0.02	21.0	19.0	8.3
MSRS-034-2	0.12	82	0.01	230	1.8	6.2
MSRS-035-2	0.14	7.3	0.01	30.1	11.4	3.1
MSRS-051-2	0.10	12.3	0.01	32.8	19.1	6.6
MSRS-061-2	0.15	27.7	0.02	24.6	19.5	5.9
MSRS-071-2	0.42	235	0.08	223	4.7	-6.9
MSRS-072-2	0.10	27.3	0.04	494	4.4	-9.2
MSRS-073-2	0.25	66	0.06	282	6.4	-4.0
MSRS-074-2	0.18	37.8	0.06	38.0	9.8	3.6
MSRS-075-2	0.18	41.8	0.04	121	5.0	-1.9
MSRS-081-2	0.12	9.7	0.06	462	7.5	-8.6
MSRS-082-2						
MSRS-083-2	0.10	6.3	0.04	265	11.3	-4.9
MSRS-084-2						
MSRS-085-2	0.14	8.8	0.01	72.4	6.6	-1.0
MSRS-086-2	0.12	11.2	0.01	61.4	8.9	1.5
MSRS-091-2	0.14	10.5	0.01	13.8	5.1	2.8
MSRS-092-2	0.19	23.1	0.07	75.2	4.4	-2.1
MSRS-093-2	0.56	70	0.03	57.7	4.7	4.1
MSRS-094-2	0.13	12.1	0.02	16.7	4.4	1.4
MSRS-121-2	0.18	5.0	0.01	2.0		
MSRS-151-2	0.09	4.5	0.00	1.9		

Table A-3-3: Anion chemistry for samples collected during the March 2011 $SO_4^=$ survey. Times, dates, and field parameters are provided in Table A-1-3, while cation chemistry for these samples is provided in Table A-2-3.

ID	F	Cl	Br	SO4$^=$	$^{34}S_{SO4}$	$^{18}O_{SO4}$
MSRS-011-3	0.23	10.5	0.00	203	7.2	-0.1
MSRS-021-3	0.29	9.9	0.00	1080	7.6	-6.5
MSRS-031-3	0.07	3.3	0.00	585	8.7	-3.4
MSRS-032-3	0.77	26.2	0.15	73.3	24.6	9.9
MSRS-033-3	0.25	8.9	0.00	97.8	11.4	1.6
MSRS-035-3	0.14	8.1	0.00	39.6	9.9	2.6
MSRS-061-3	0.18	30.9	0.00	27.5	17.6	6.2
MSRS-073-3	0.41	136	0.07	332	7.0	-4.4
MSRS-075-3	0.31	117	0.06	241	7.2	-3.0
MSRS-081-3	0.18	9.2	0.05	450	9.5	-7.9
MSRS-085-3	0.18	9.2	0.00	81.2	7.9	-3.0
MSRS-086-3	0.19	14.8	0.00	107	10.1	0.9
MSRS-092-3	0.22	95	0.00	69.7	4.0	-0.3
MSRS-094-3	0.23	27.0	0.00	43.0	4.2	1.4

Table A-4-1 Sample ID numbers, dates, times, and flow rates for samples collected from Site 001, just upstream from the Scanlon Dam. Flow rates are from the USGS.

ID	Date	Time	Flow (CFS)
MSRS-001-1	7/7/2010	17:00	1420
MSRS-001-2	7/14/2010	9:00	751
MSRS-001-3	7/20/2010	15:00	613
MSRS-001-4	7/26/2010	12:00	550
MSRS-001-5	8/2/2010	15:10	588
MSRS-001-1A	8/10/2010	8:59	1420
MSRS-001-6	8/11/2010	10:00	1230
MSRS-001-7	8/18/2010	13:25	1100
MSRS-001-8	8/25/2010	14:00	1520
MSRS-001-9	9/1/2010	10:30	814
MSRS-001-10	9/9/2010	14:00	2100
MSRS-001-2A	9/14/2010	9:16	1610
MSRS-001-11	9/24/2010	10:15	1060
MSRS-001-12	10/1/2010	13:30	1120
MSRS-001-13	10/8/2010	14:00	796
MSRS-001-14	10/15/2010	11:00	692
MSRS-001-15	10/21/2010		653
MSRS-001-16	10/29/2010	11:15	10200
MSRS-001-17	11/5/2010	14:00	4080
MSRS-001-18	11/12/2010	11:30	2220
MSRS-001-19	11/19/2010	11:30	1740
MSRS-001-21	12/7/2010	10:10	1350
MSRS-001-22	12/20/2010	9:25	1030
MSRS-001-23	1/5/2011	10:20	1260
MSRS-001-24	1/19/2011	10:10	1290
MSRS-001-25	2/2/2011	10:05	1160
MSRS-001-26	2/16/2011	10:00	1190
MSRS-001-27	3/1/2011	10:10	1060
MSRS-001-28	3/15/2011	10:10	1010
MSRS-001-29	3/29/2011	10:10	1760
MSRS-001-30	4/12/2011	9:50	12800
MSRS-001-31	4/20/2011	3:40	6370
MSRS-001-32	4/27/2011	15:00	5860
MSRS-001-33	5/3/2011	15:00	8750
MSRS-001-34	5/11/2011	14:00	5290
MSRS-001-35	5/18/2011	11:00	3230
MSRS-001-36	5/27/2011	14:15	2520
MSRS-001-37	6/2/2011	14:30	2220

MSRS-001-38	6/8/2011	14:30	1770
MSRS-001-39	6/16/2011	10:00	923
MSRS-001-40	6/23/2011	14:00	3330
MSRS-001-41	6/28/2011	9:30	3070
MSRS-001-42	7/5/2011	14:30	2410
MSRS-001-43	7/11/2011	13:30	1520
MSRS-001-44	7/21/2011	14:30	1110
MSRS-001-45	7/27/2011	14:15	984
MSRS-001-46	8/3/2011	14:30	8820
MSRS-001-5A	8/9/2011	13:45	3340
MSRS-001-48	8/18/2011	9:00	1860
MSRS-001-49	8/24/2011	14:00	1170
MSRS-001-50	9/1/2011	14:00	776
MSRS-001-51	9/7/2011	14:30	665
MSRS-001-52	9/15/2011	15:20	476
MSRS-001-53	9/22/2011	14:30	487
MSRS-001-54	9/28/2011	13:00	390
MSRS-001-55	10/6/2011	13:00	507
MSRS-001-56	10/11/2011	15:00	395
MSRS-001-57	10/19/2011	13:30	581
MSRS-001-58	10/27/2011	14:20	504
MSRS-001-59	11/3/2011	15:00	547
MSRS-001-60	11/10/2011	13:30	505
MSRS-001-61	11/16/2011	14:00	572

Table A-4-2. Cation chemistry for samples collected from Site 001 during this study. Dates and times and flow rates can be found in Table A-4-1 and anion chemistry can be found in Table A-4-3.

ID	Al	Ba	Ca	Fe	K	Mg	Mn	Na	Si	Sr
MSRS-001-1	0.04	0.016	19.7	0.91	1.39	12.3	0.14	6.1	3.9	0.062
MSRS-001-2	0.04	0.016	20.1	1.25	1.38	10.9	0.12	6.4	4.2	0.063
MSRS-001-3	0.04	0.015	21.5	1.18	1.39	11.9	0.12	6.9	4.1	0.067
MSRS-001-4	0.02	0.014	23.0	0.80	1.57	13.8	0.09	8.3	3.7	0.073
MSRS-001-5	0.01	0.014	23.9	0.60	1.78	15.4	0.07	9.3	3.6	0.076
MSRS-001-1A	0.05	0.021	16.7	0.81	1.9	9.3	0.10	6.2	4.6	0.053
MSRS-001-6	0.08	0.016	17.6	0.87	1.97	10.0	0.09	6.8	4.6	0.057
MSRS-001-7	0.04	0.015	22.4	1.24	1.92	13.4	0.12	8.1	5.1	0.071
MSRS-001-8	0.07	0.017	20.1	1.36	1.65	10.5	0.11	6.2	4.9	0.060
MSRS-001-9	0.08	0.017	20.8	1.54	1.51	11.0	0.09	6.3	5.0	0.063
MSRS-001-10	0.06	0.016	21.6	1.66	1.52	11.2	0.13	6.6	5.3	0.062
MSRS-001-2A	0.09	0.018	18.8	1.3	1.5	10.4	0.11	6.2	4.9	0.055
MSRS-001-11	0.07	0.015	20.3	1.16	1.47	12.1	0.10	6.8	4.8	0.059
MSRS-001-12	0.06	0.016	21.3	1.01	1.64	12.9	0.09	7.3	4.6	0.063
MSRS-001-13	0.06	0.015	20.8	0.89	1.60	12.8	0.09	7.4	4.5	0.062
MSRS-001-14	0.06	0.016	21.6	0.91	1.64	13.2	0.11	9.1	4.3	0.064
MSRS-001-15	0.04	0.013	21.8	0.77	1.53	13.4	0.08	7.5	3.8	0.062
MSRS-001-16	0.36	0.027	13.7	1.24	2.68	7.0	0.32	25.4	4.5	0.038
MSRS-001-17	0.14	0.014	12.7	0.79	1.25	6.8	0.05	4.1	4.3	0.034
MSRS-001-18	0.12	0.013	14.4	0.80	1.10	8.1	0.06	4.7	4.3	0.041
MSRS-001-19	0.11	0.012	15.2	0.83	1.06	8.5	0.06	5.1	4.2	0.042
MSRS-001-21	0.09	0.015	18.8	0.77	1.24	10.6	0.09	6.2	4.8	0.056
MSRS-001-22	0.05	0.013	18.2	0.68	1.38	10.3	0.07	6.2	4.8	0.054
MSRS-001-23	0.04	0.012	19.4	0.74	1.43	10.9	0.07	6.3	4.9	0.056
MSRS-001-24	0.04	0.011	19.4	0.72	1.28	11.3	0.06	6.3	4.8	0.055
MSRS-001-25	0.04	0.011	19.3	0.75	1.25	10.7	0.06	6.2	5.1	0.055
MSRS-001-26	0.03	0.011	18.9	0.65	1.24	10.6	0.05	6.8	4.9	0.054
MSRS-001-27	0.04	0.012	20.8	0.78	1.33	11.3	0.07	8.2	5.4	0.059
MSRS-001-28	0.07	0.018	20.5	0.73	1.47	11.3	0.06	7.8	5.1	0.061
MSRS-001-29	0.06	0.021	21.6	0.78	2.55	11.2	0.10	10.8	5.1	0.061
MSRS-001-30	0.10	0.020	10.1	0.63	1.44	4.8	0.12	3.9	3.5	0.031
MSRS-001-31	0.09	0.021	12.9	0.64	1.40	6.7	0.05	5.2	3.6	0.044
MSRS-001-32	0.10	0.020	12.7	0.59	1.34	6.4	0.04	5.3	3.0	0.040
MSRS-001-33	0.13	0.020	11.9	0.54	1.29	5.7	0.04	4.8	2.6	0.036
MSRS-001-34	0.10	0.020	12.9	0.57	1.20	6.6	0.03	4.9	2.3	0.040
MSRS-001-35	0.08	0.017	13.6	0.62	1.21	7.5	0.06	4.9	2.2	0.044
MSRS-001-36	0.09	0.019	15.7	0.71	1.20	8.0	0.06	5.3	2.5	0.049
MSRS-001-37	0.11	0.018	16.2	0.75	1.14	8.5	0.08	5.4	2.6	0.050
MSRS-001-38	0.05	0.018	16.2	0.73	1.18	8.7	0.08	5.7	2.7	0.052

MSRS-001-39	0.04	0.018	16.2	0.73	1.18	8.7	0.08	5.7	2.7	0.052
MSRS-001-40	0.04	0.017	18.5	0.70	1.18	10.2	0.09	6.2	3.2	0.057
MSRS-001-41	0.09	0.019	15.6	0.86	0.90	7.3	0.06	5.0	3.2	0.046
MSRS-001-42	0.06	0.019	17.3	0.91	1.19	9.6	0.08	6.0	3.4	0.055
MSRS-001-43	0.04	0.018	16.5	0.90	1.18	9.3	0.09	5.6	3.6	0.054
MSRS-001-44	0.03	0.019	19.4	0.93	1.33	11.0	0.13	6.6	4.1	0.062
MSRS-001-45	0.03	0.020	20.9	1.01	1.39	12.3	0.11	7.3	4.2	0.064
MSRS-001-46	0.06	0.020	12.1	0.59	1.80	5.9	0.11	3.7	3.1	0.037
MSRS-001-5A	0.12	0.023	17.8	1.45	1.08	7.4	0.15	4.0	4.3	0.050
MSRS-001-48	0.12	0.019	19.6	2.36	1.07	9.5	0.24	4.7	4.9	0.054
MSRS-001-49	0.10	0.017	20.0	2.41	1.03	10.2	0.22	4.9	5.2	0.055
MSRS-001-50	0.08	0.016	20.7	2.07	1.08	11.1	0.14	5.5	5.1	0.057
MSRS-001-51	0.05	0.015	21.3	1.62	1.20	12.5	0.13	6.2	4.9	0.060
MSRS-001-52	0.04	0.014	20.9	0.90	1.25	12.7	0.08	6.5	4.3	0.059
MSRS-001-53	0.02	0.012	20.0	0.54	1.13	11.8	0.06	6.0	3.8	0.055
MSRS-001-54	0.02	0.012	22.0	0.36	1.29	13.5	0.04	6.9	3.4	0.060
MSRS-001-55	0.02	0.013	21.13	0.25	1.62	16.7	0.02	8.8	2.9	0.070
MSRS-001-56	0.01	0.014	25.43	0.20	1.74	17.4	0.01	9.4	2.5	0.073
MSRS-001-57	0.01	0.017	26.70	0.21	2.25	20.1	0.06	10.3	3.4	0.078
MSRS-001-58	0.02	0.015	24.36	0.40	1.84	17.7	0.05	8.9	3.9	0.070
MSRS-001-59	0.01	0.013	25.14	0.38	1.89	19.1	0.06	9.4	3.9	0.074
MSRS-001-60	0.01	0.012	25.88	0.38	1.92	19.9	0.05	10.5	3.7	0.076
MSRS-001-61	0.01	0.012	25.39	0.40	1.81	19.8	0.05	9.4	3.8	0.074

Table A-4-3. Anion Chemistry for samples collected from site OO1 during the present study. Other data for these samples can be found in Tables A-4-1 and A-4-2.

ID	F	Cl	$SO_4^=$	$^{34}S_{SO4}$	$^{18}O_{SO4}$
MSRS-001-1	0.12	5.2	19.3	10.0	3.5
MSRS-001-2	0.13	6.0	12.7	10.0	4.0
MSRS-001-3	0.13	6.2	14.0	9.0	2.7
MSRS-001-4	0.14	7.8	18.3	8.7	3.1
MSRS-001-5	0.14	8.7	20.9	8.6	1.9
MSRS-001-1A	0.13	6.3	9.3	9.2	3.9
MSRS-001-6	0.14	6.3	10.1	8.8	4.3
MSRS-001-7	0.15	7.6	14.7	10.1	3.7
MSRS-001-8	0.11	6.1	9.7	7.9	4.5
MSRS-001-9	0.12	6.0	10.7	8.4	3.8
MSRS-001-10	0.12	6.9	11.0	7.2	4.2
MSRS-001-2A	0.10	6.3	9.5	7.3	1.7
MSRS-001-11	0.11	6.4	14.0	8.0	4.0
MSRS-001-12	0.12	7.1	15.8	7.5	4.3
MSRS-001-13	0.12	7.5	14.1	7.8	4.6
MSRS-001-14	0.13	8.9	16.3	8.1	3.6
MSRS-001-15	0.13	7.3	16.5	8.1	3.3
MSRS-001-16	0.07	10.4	10.6	5.8	5.6
MSRS-001-17	0.08	4.4	8.2		
MSRS-001-18	0.08	4.6	11.3	8.1	5.1
MSRS-001-19	0.09	5.0	10.5	7.5	4.3
MSRS-001-21	0.11	6.0	14.5	8.1	3.5
MSRS-001-22	0.12	5.7	13.4	8.1	3.9
MSRS-001-23	0.11	6.3	14.0	7.9	3.7
MSRS-001-24	0.11	5.8	14.3	7.1	3.4
MSRS-001-25	0.12	5.5	14.0	8.5	4.1
MSRS-001-26	0.13	6.7	13.7	7.6	4.0
MSRS-001-27	0.13	9.3	14.3	7.0	3.8
MSRS-001-28	0.11	7.9	14.6	8.0	2.1
MSRS-001-29	0.10	14.9	13.5	7.3	3.3
MSRS-001-30	0.05	3.9	6.1	6.5	4.5
MSRS-001-31	0.07	5.1	11.6	7.7	5.3
MSRS-001-32	0.07	5.8	8.8	7.1	4.9
MSRS-001-33	0.06	5.4	7.0	7.2	4.7
MSRS-001-34	0.07	4.7	8.8	7.1	3.8
MSRS-001-35	0.08	4.7	10.2	7.3	3.9
MSRS-001-36	0.08	5.1	8.8	7.36	4.5
MSRS-001-37	0.09	5.1	9.9	7.4	3.7
MSRS-001-38	0.10	5.2	10.7	7.9	3.7

MSRS-001-39	0.10	5.5	12.0	7.7	4.5
MSRS-001-40	0.09	6.3	11.7	7.195	4.4
MSRS-001-41	0.08	5.0	6.1	7.8	6.3
MSRS-001-42	0.10	5.4	12.7	8.2	4.1
MSRS-001-43	0.10	4.9	11.8		
MSRS-001-44	0.11	6.1	12.9	8.5	2.1
MSRS-001-45	0.11	6.7	14.7	7.8	2.9
MSRS-001-46	0.06	3.5	5.8	6.7	3.4
MSRS-001-5A	0.07	3.8	4.6	6.12	6.2
MSRS-001-48	0.09	5.0	7.1	6.9	-3.14
MSRS-001-49	0.09	4.9	9.1	7.8	0.38
MSRS-001-50	0.10	5.6	10.6	7.7	-0.06
MSRS-001-51	0.11	5.9	13.3	8.3	-1.23
MSRS-001-52	0.12	6.4	14.1	7.8	-1.48
MSRS-001-53	0.11	5.9	12.4	9.2	-0.12
MSRS-001-54	0.12	6.8	14.6	8.7	0.66
MSRS-001-55	0.14	9.2	19.3	8.0	0.80
MSRS-001-56	0.14	9.9	22.1	8.6	0.14
MSRS-001-57	0.16	10.1	28.0	8.7	0.27
MSRS-001-58	0.14	8.3	25.6	9.6	0.28
MSRS-001-59	0.17	9.5	28.2	9.4	0.78
MSRS-001-60	0.16	11.1	32.3	8.9	-0.19
MSRS-001-61	0.15	9.3	32.3	9.6	1.15

Appendix A3: Concentrations and Loading Rate Figures for Site 001

$$y = 0.0261x + 24.987$$
$$R^2 = 0.9607$$

$$y = 0.0133x + 2.5155$$
$$R^2 = 0.7569$$
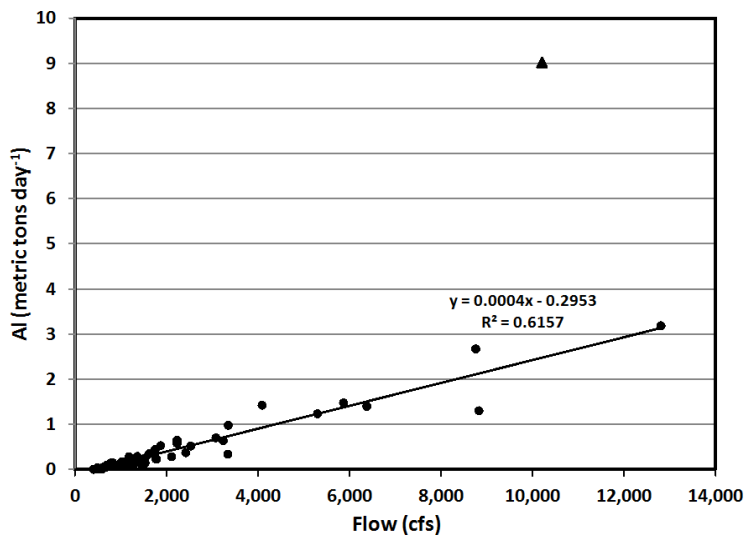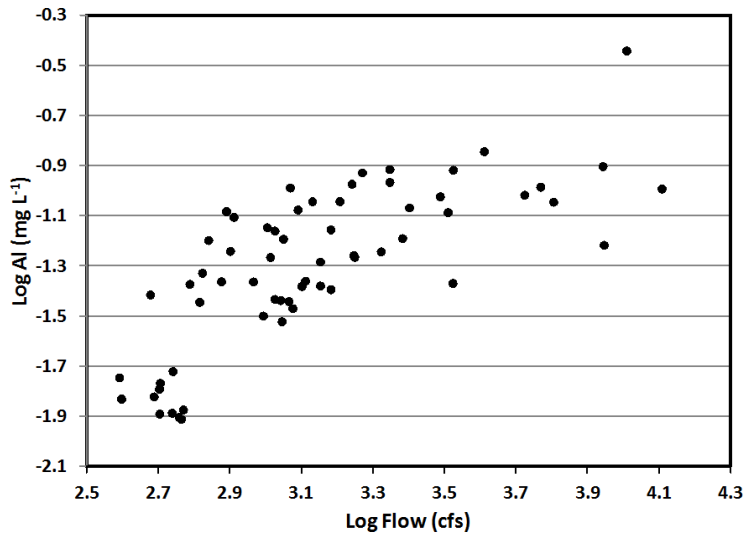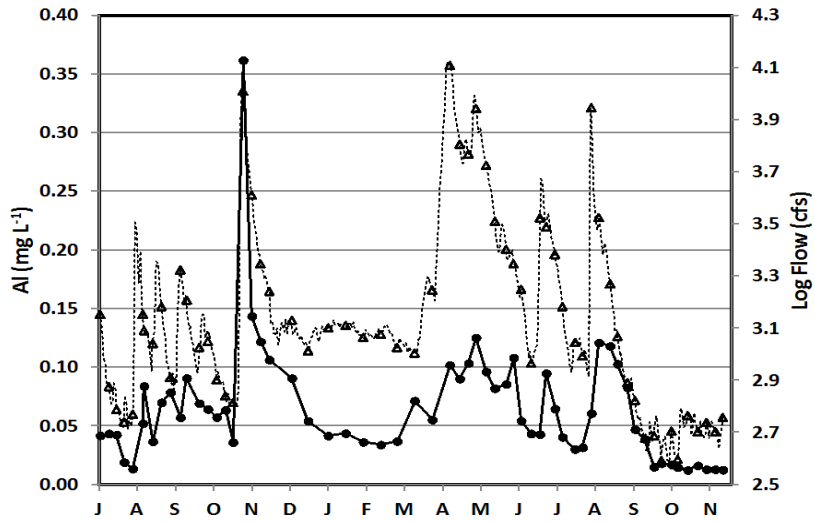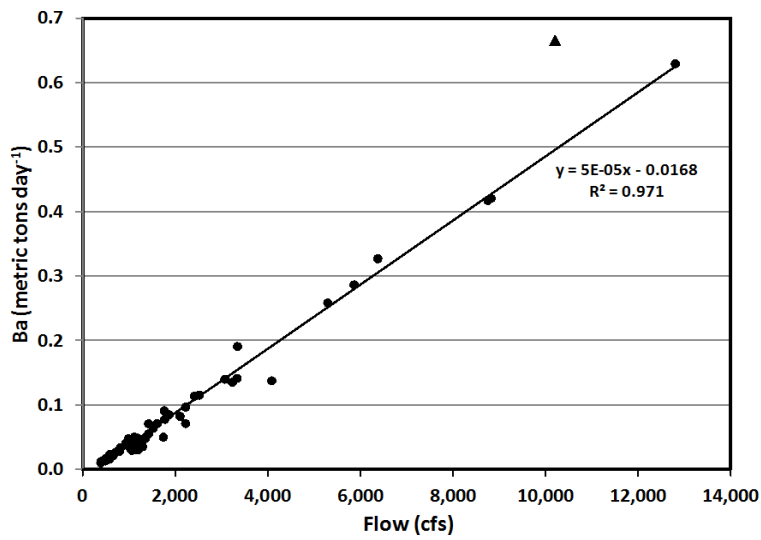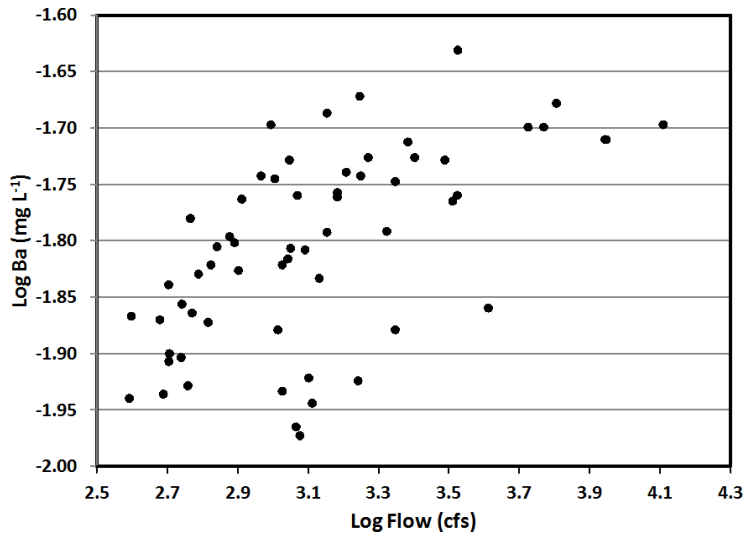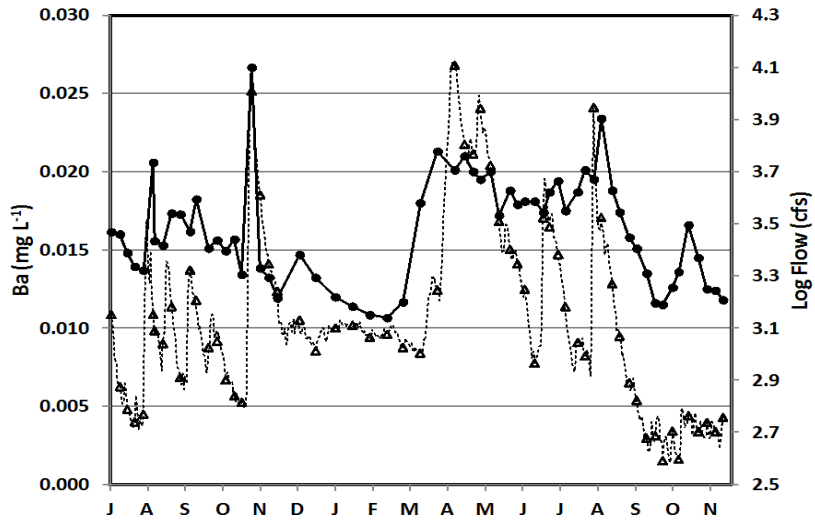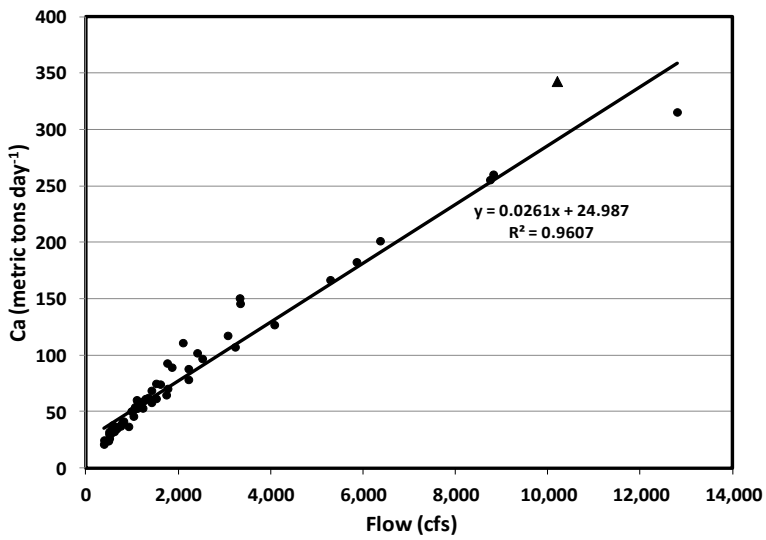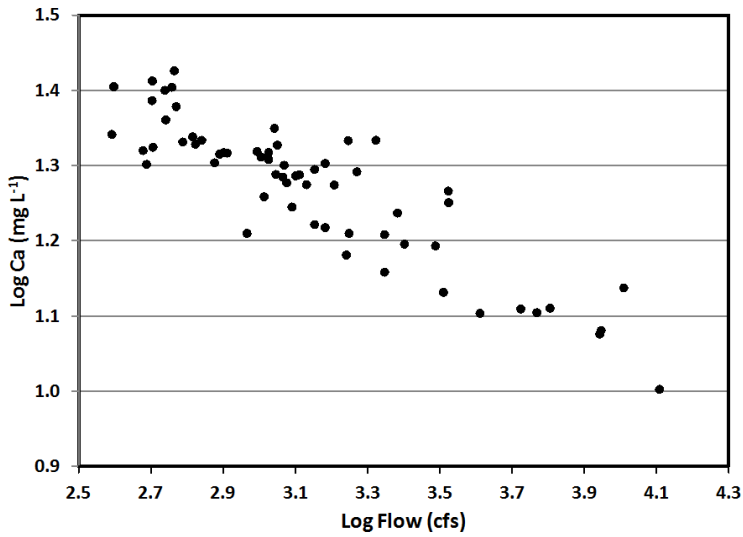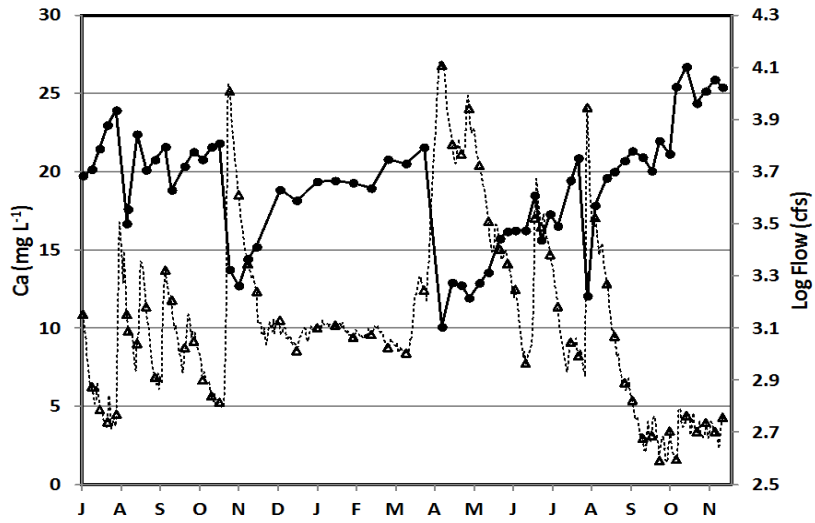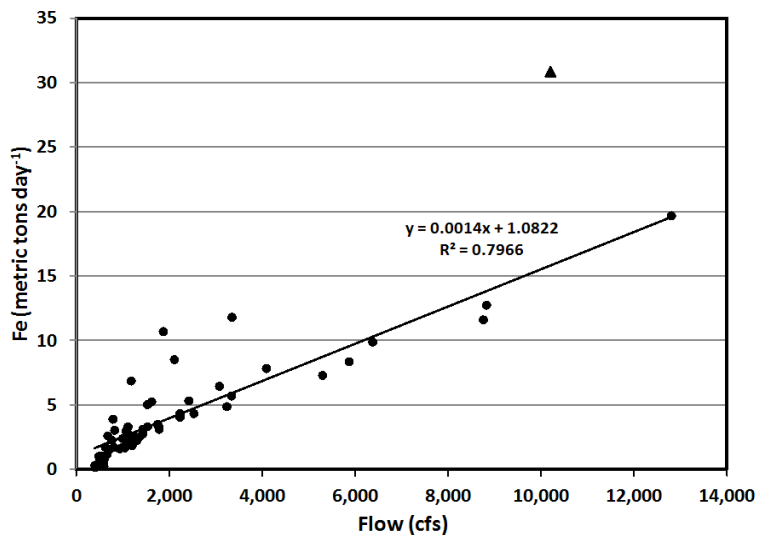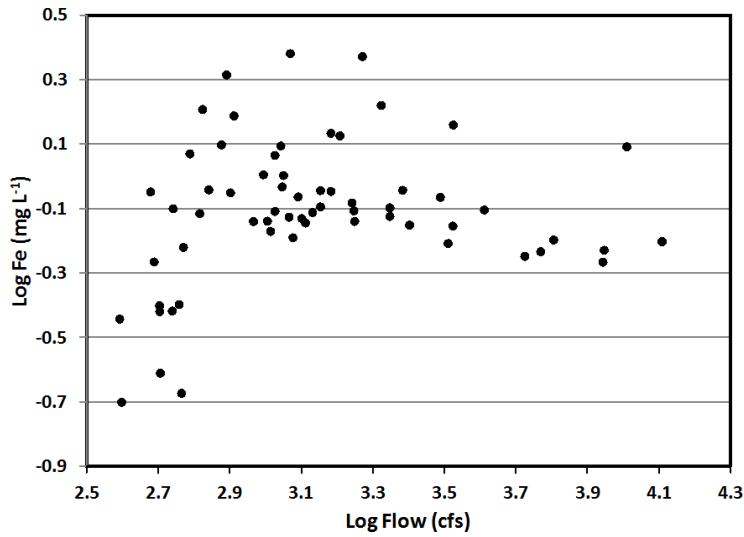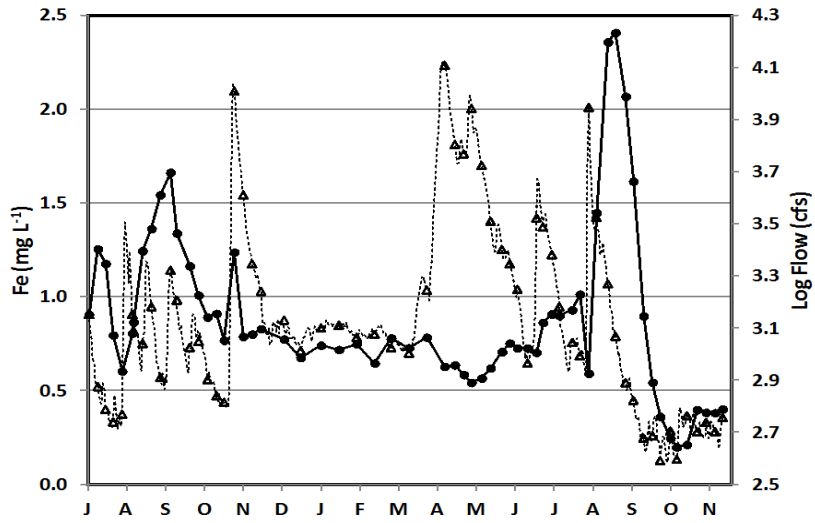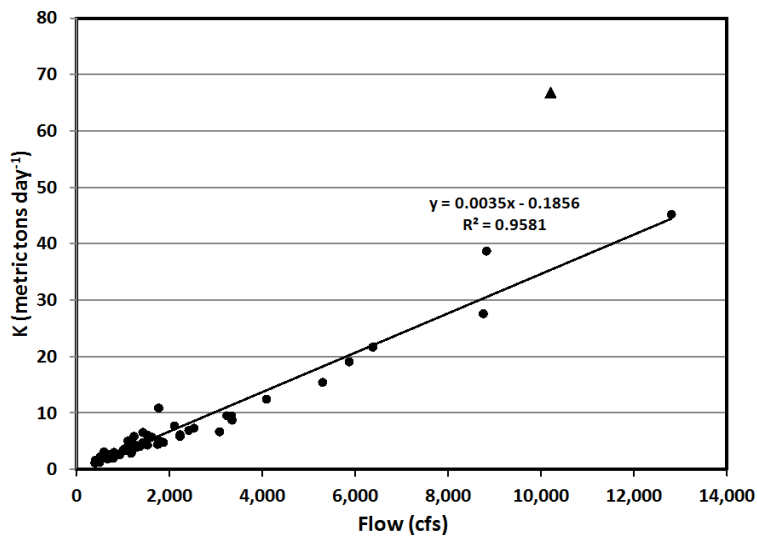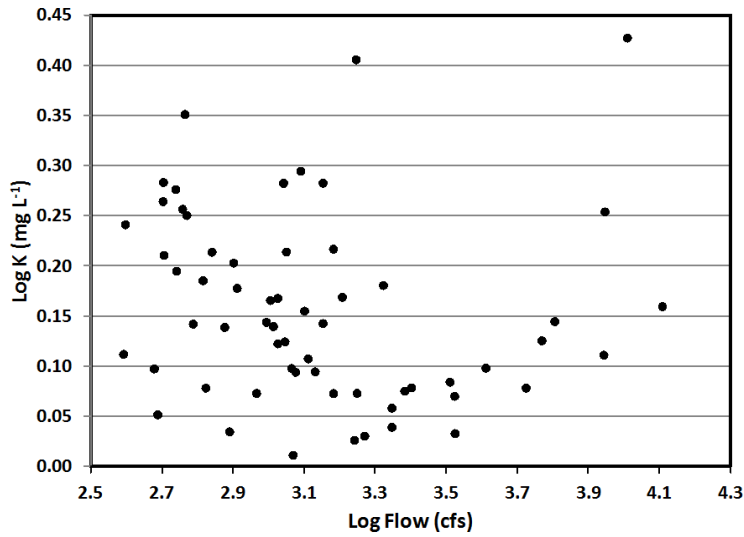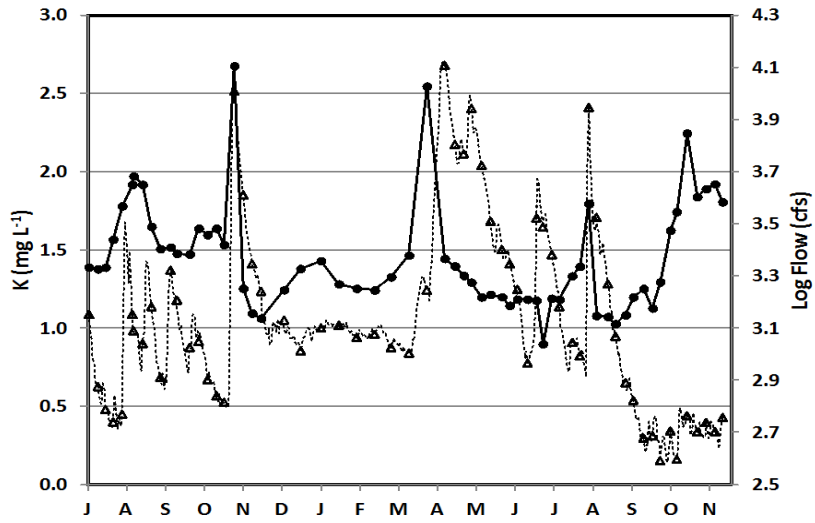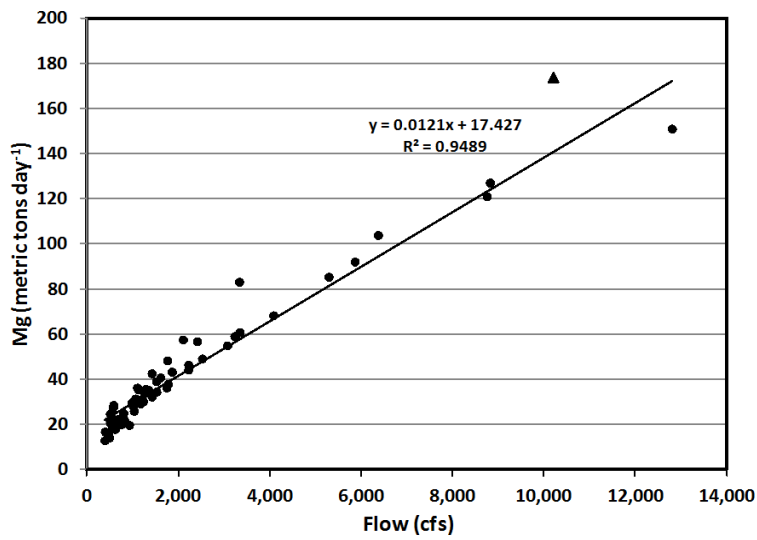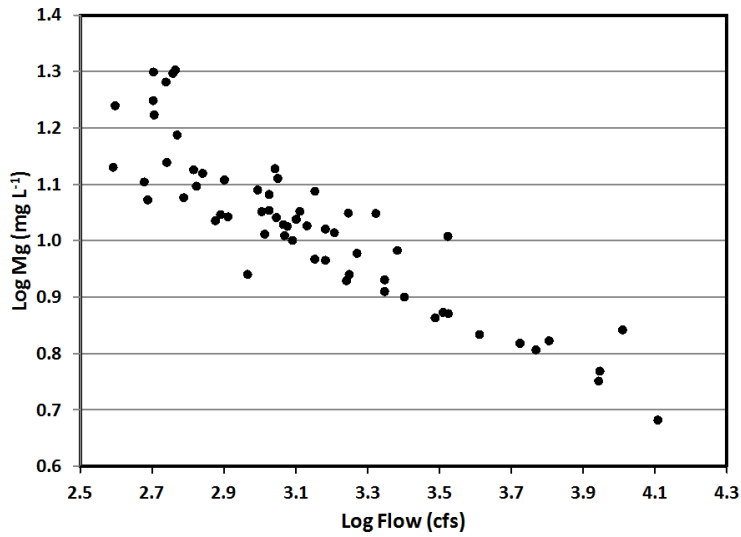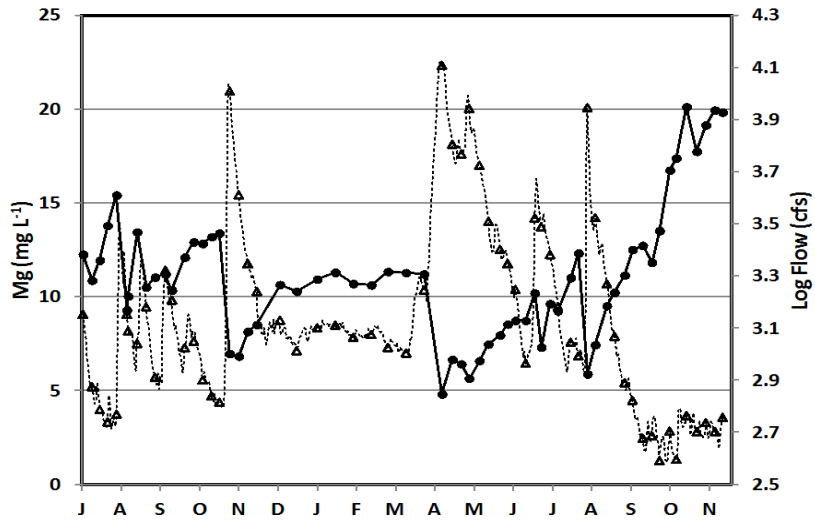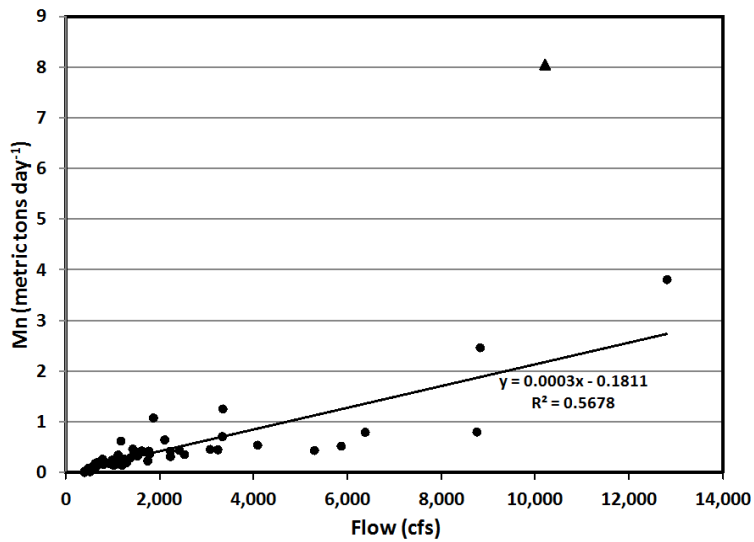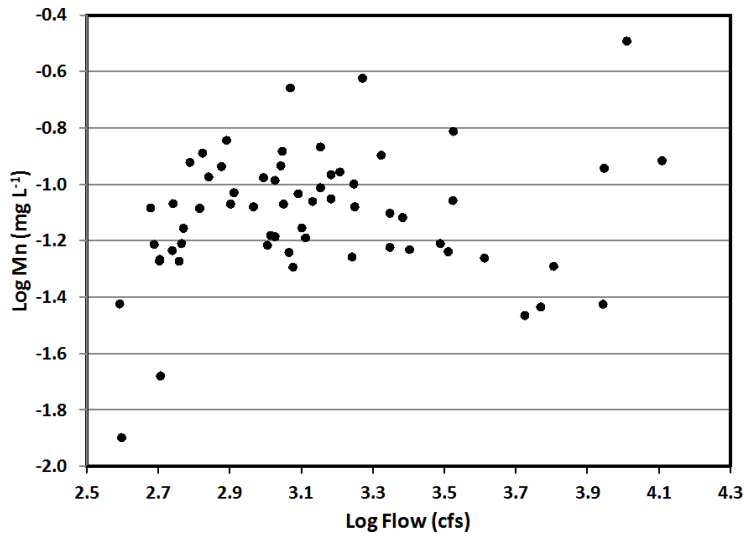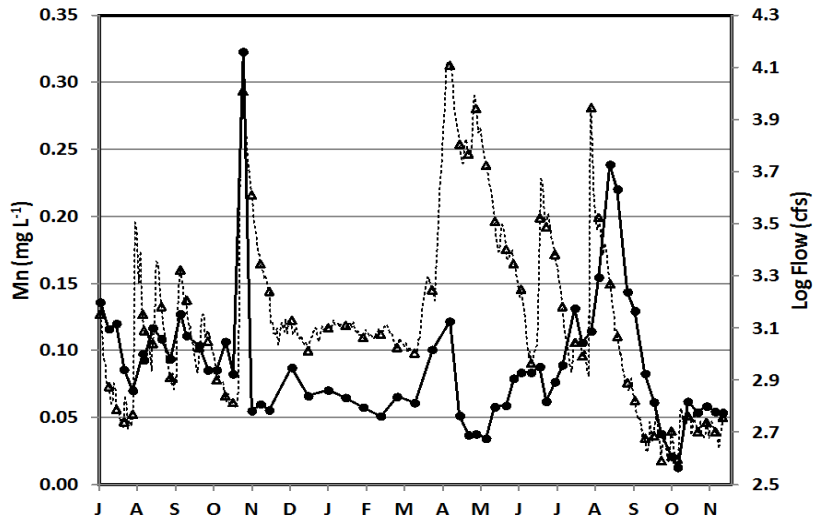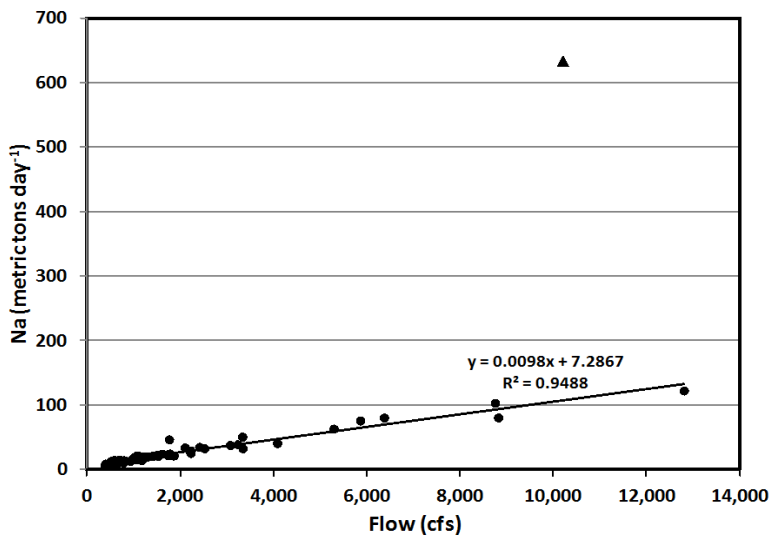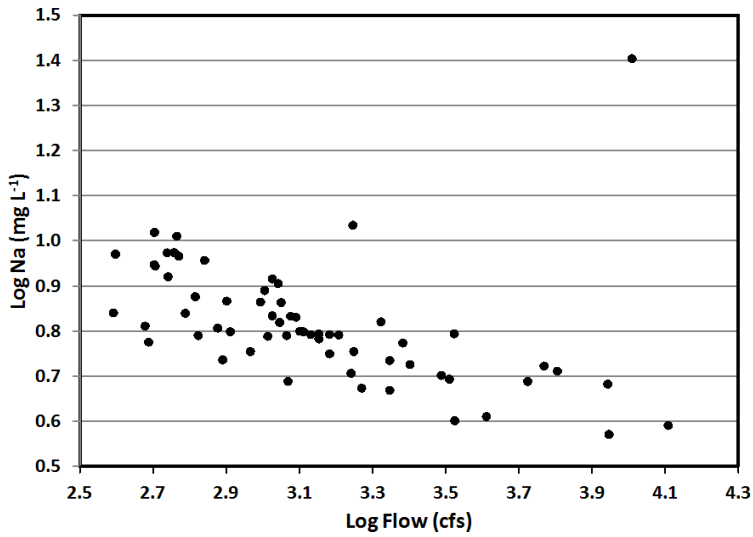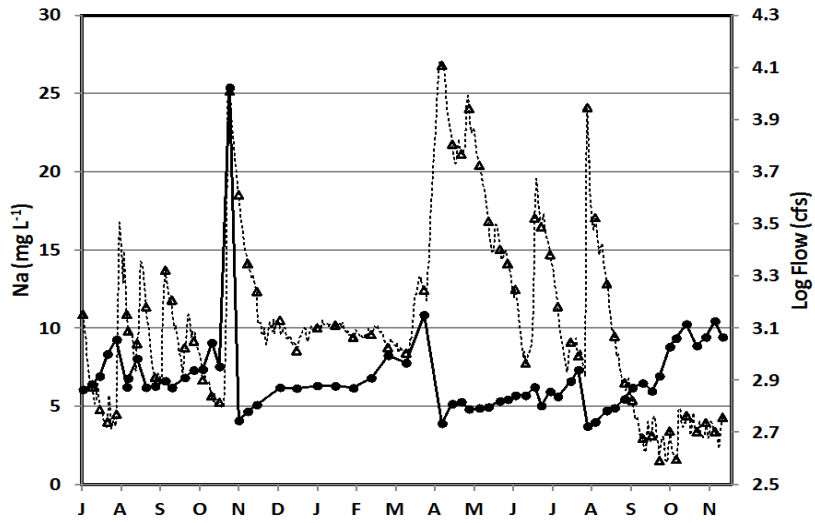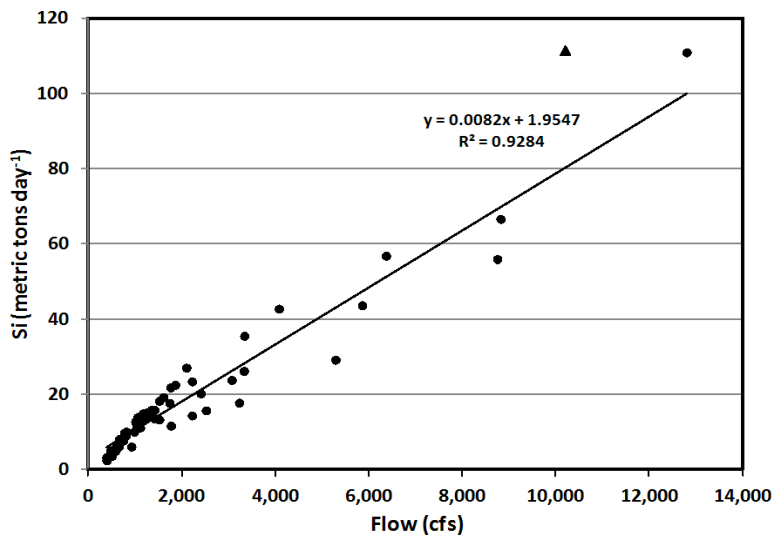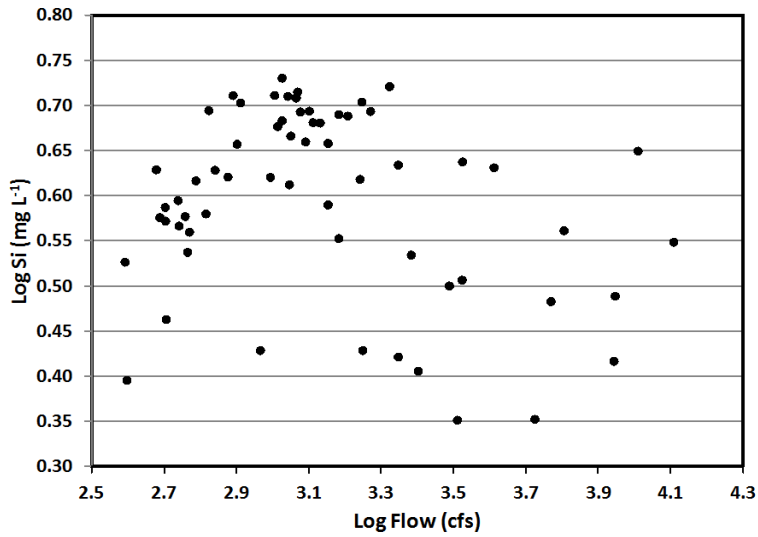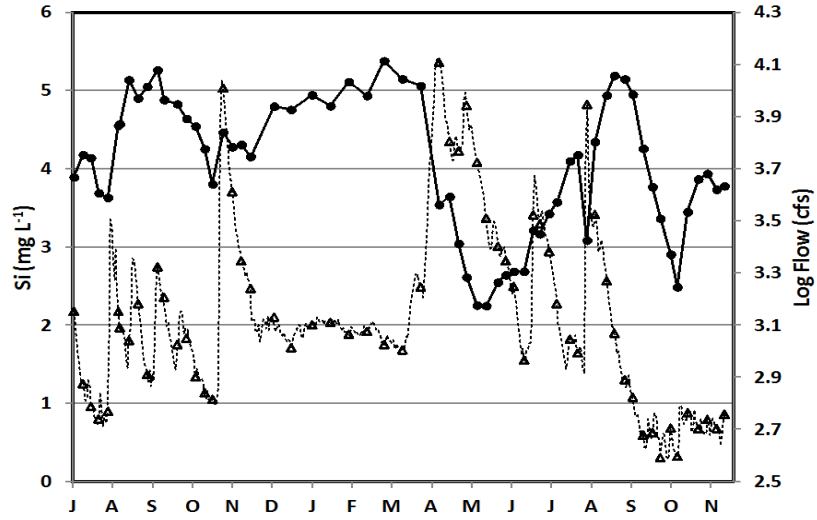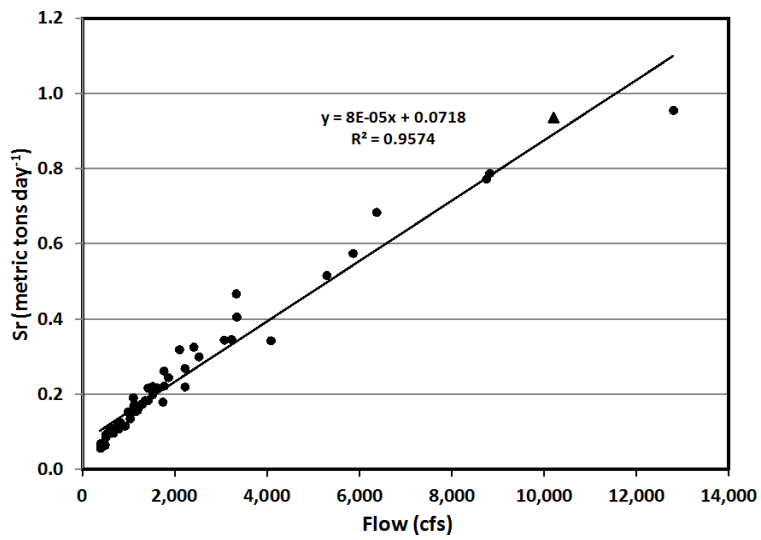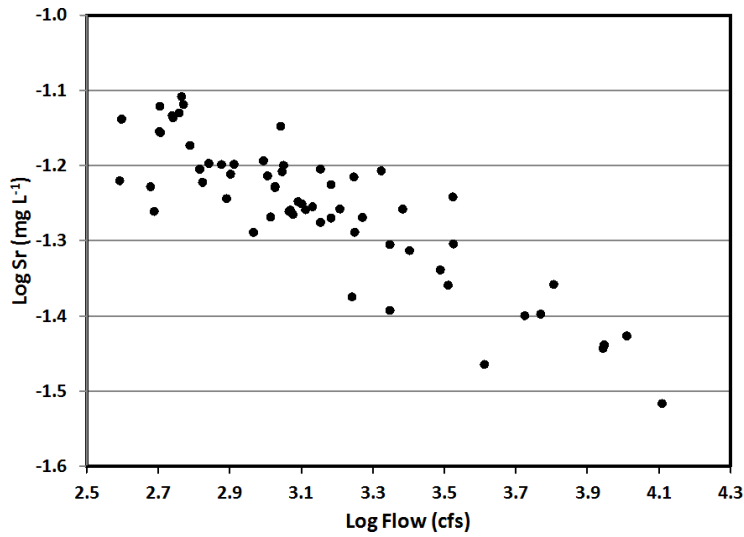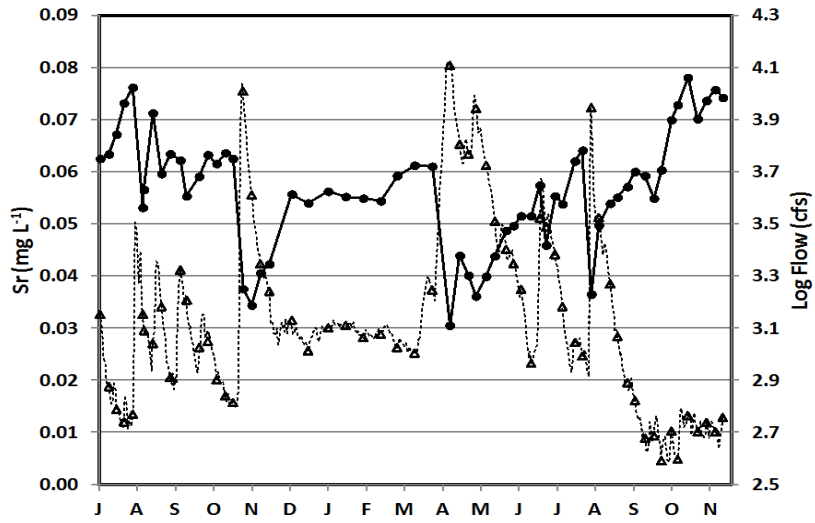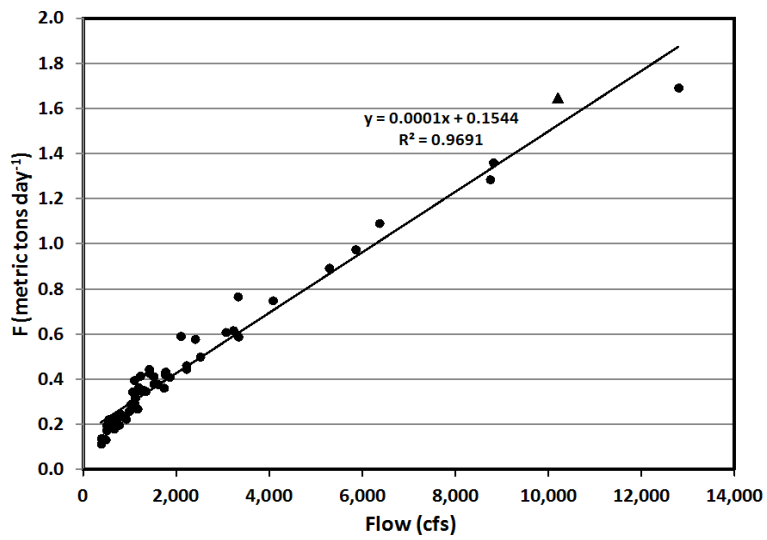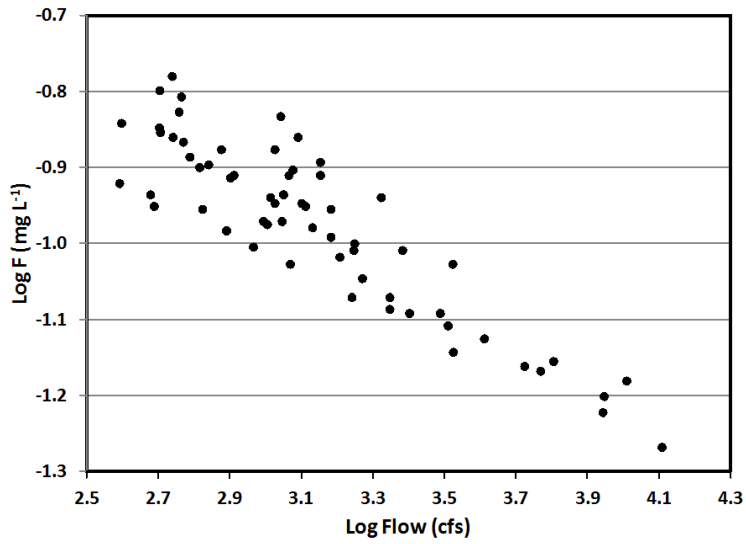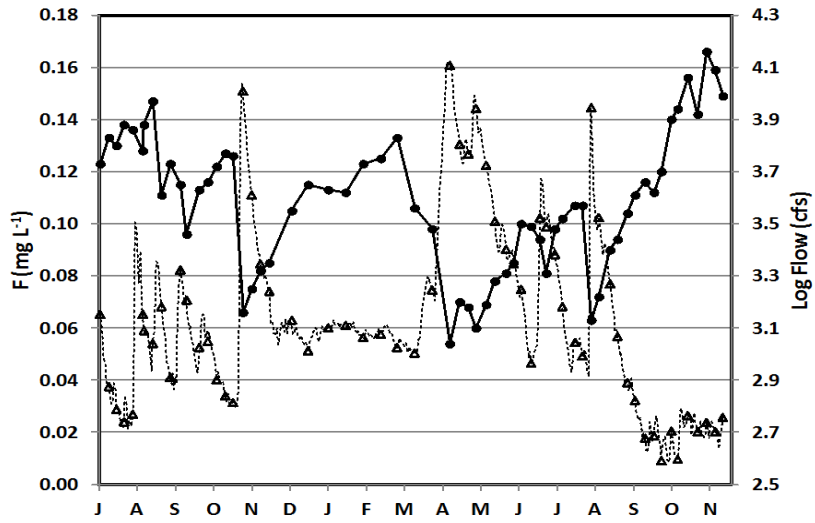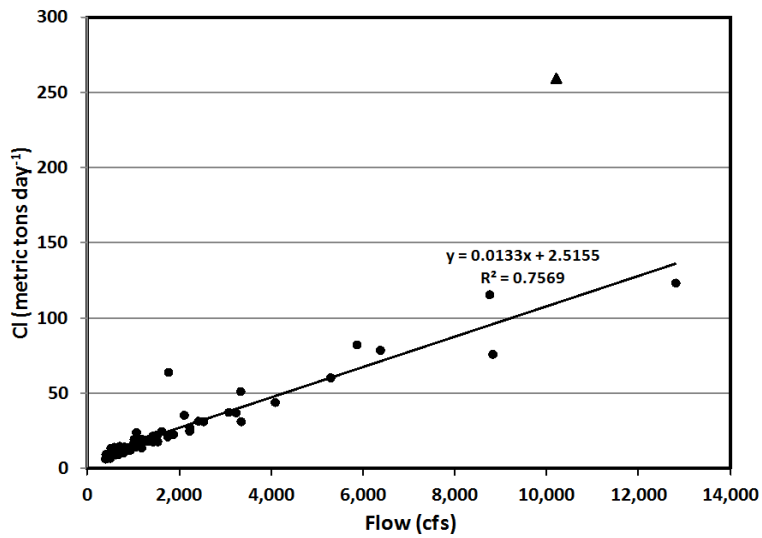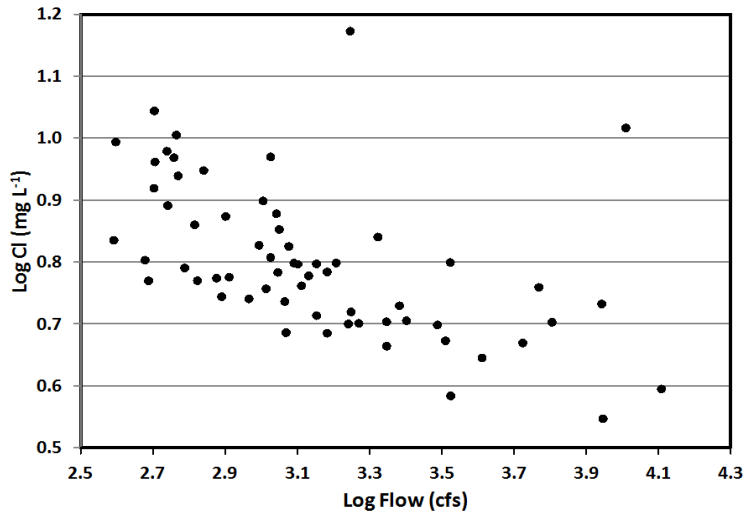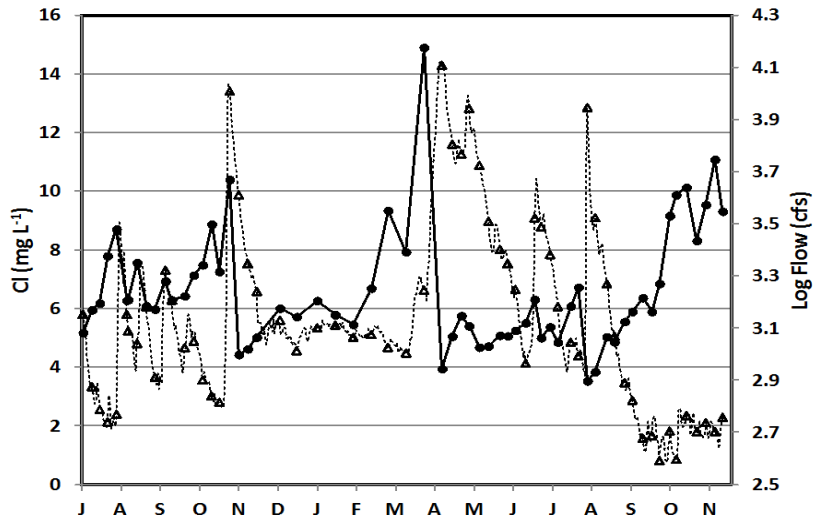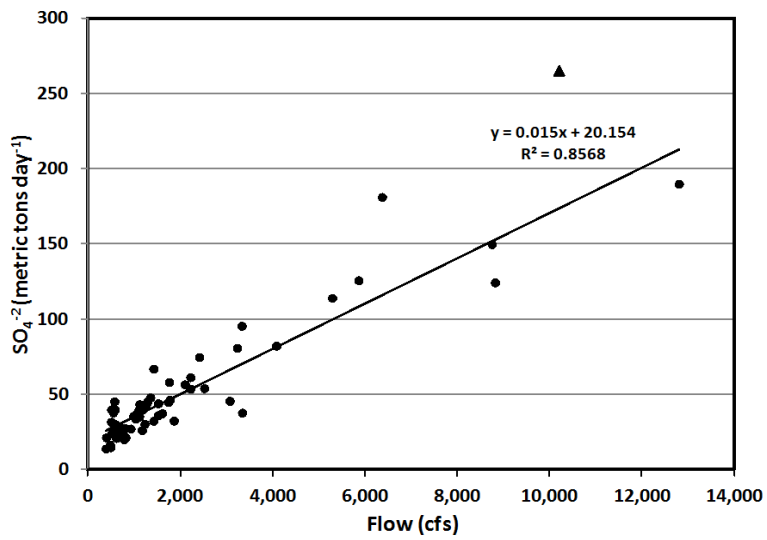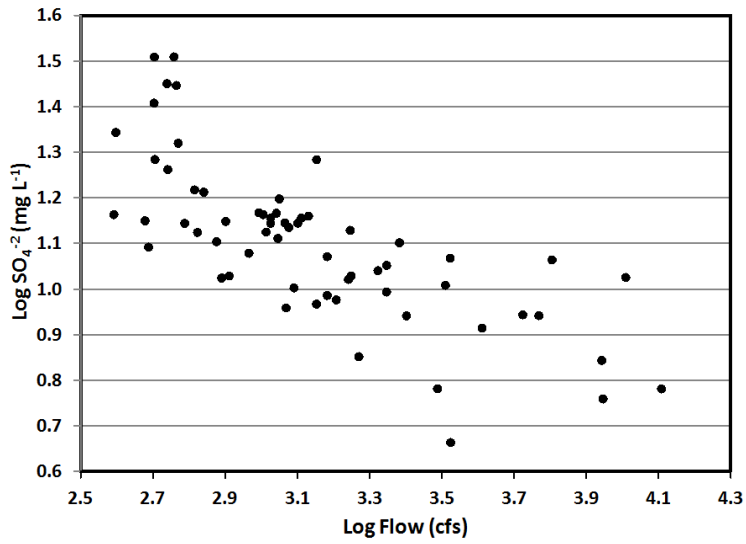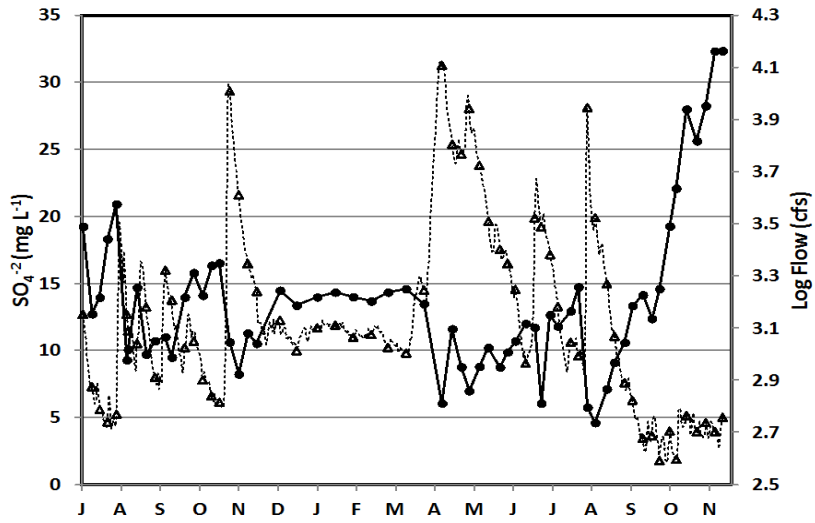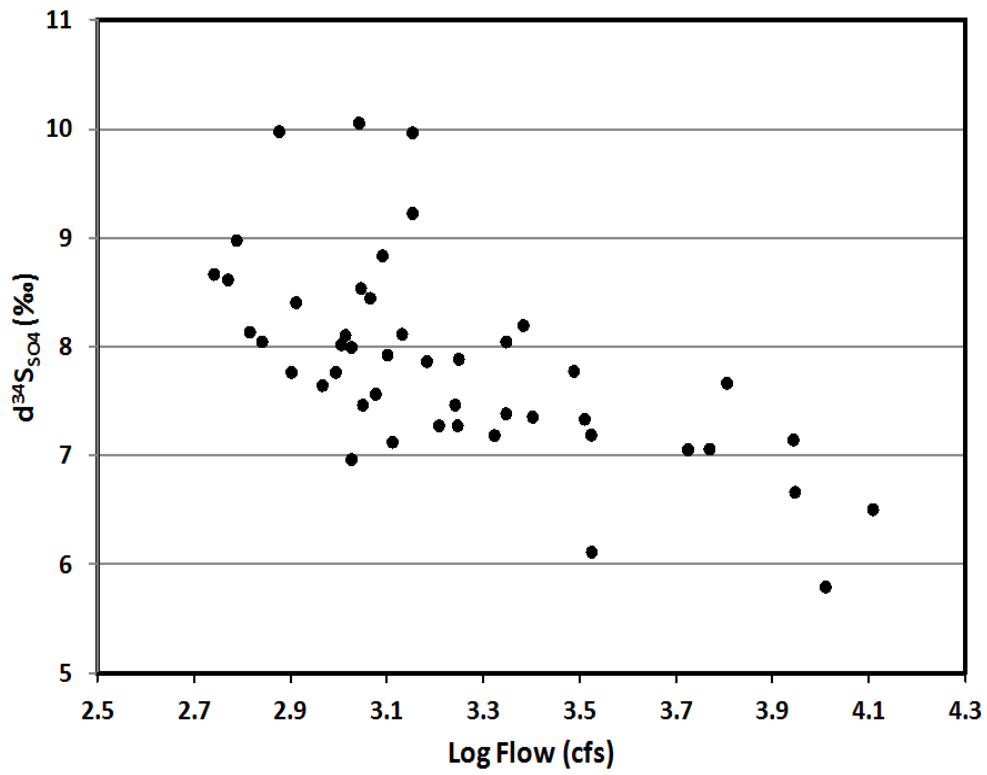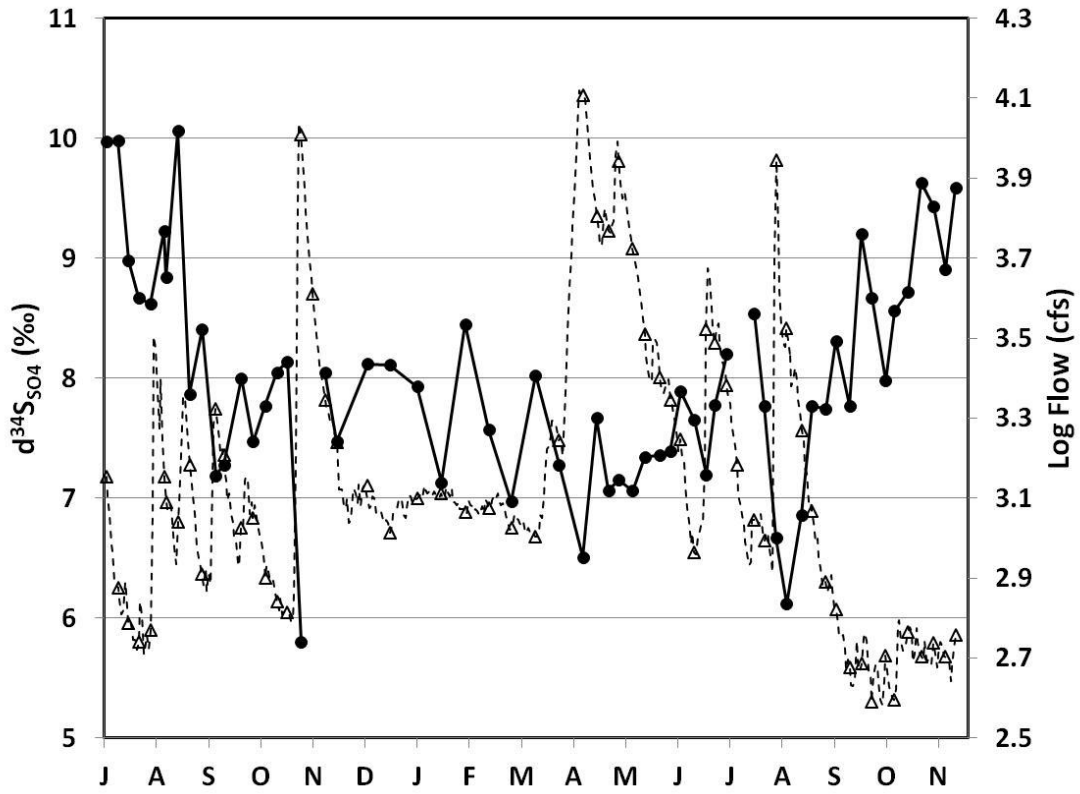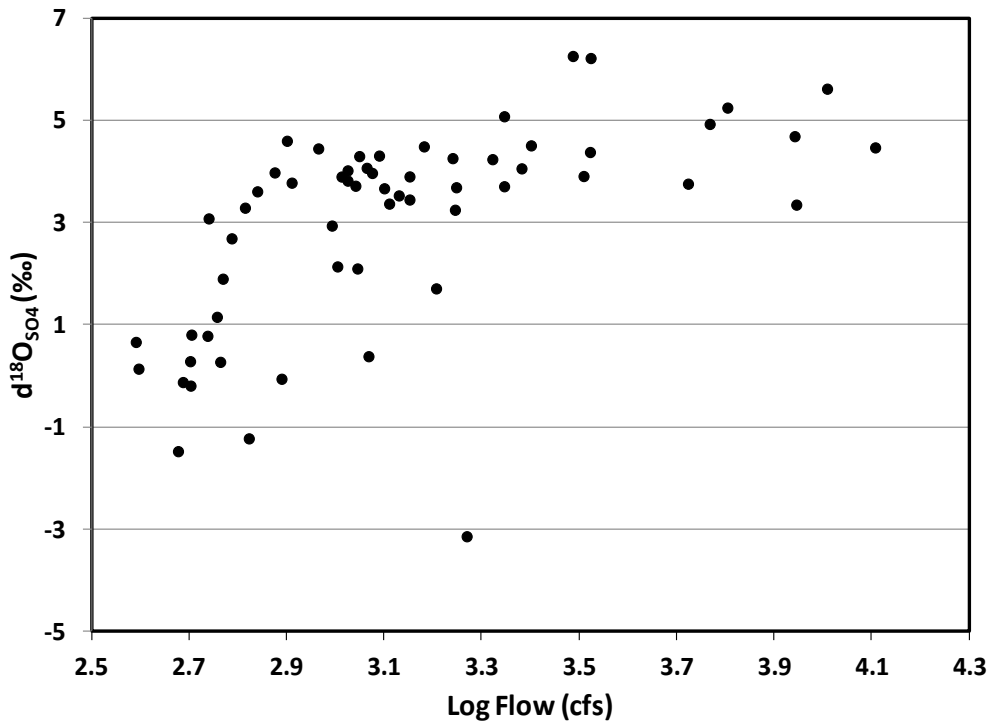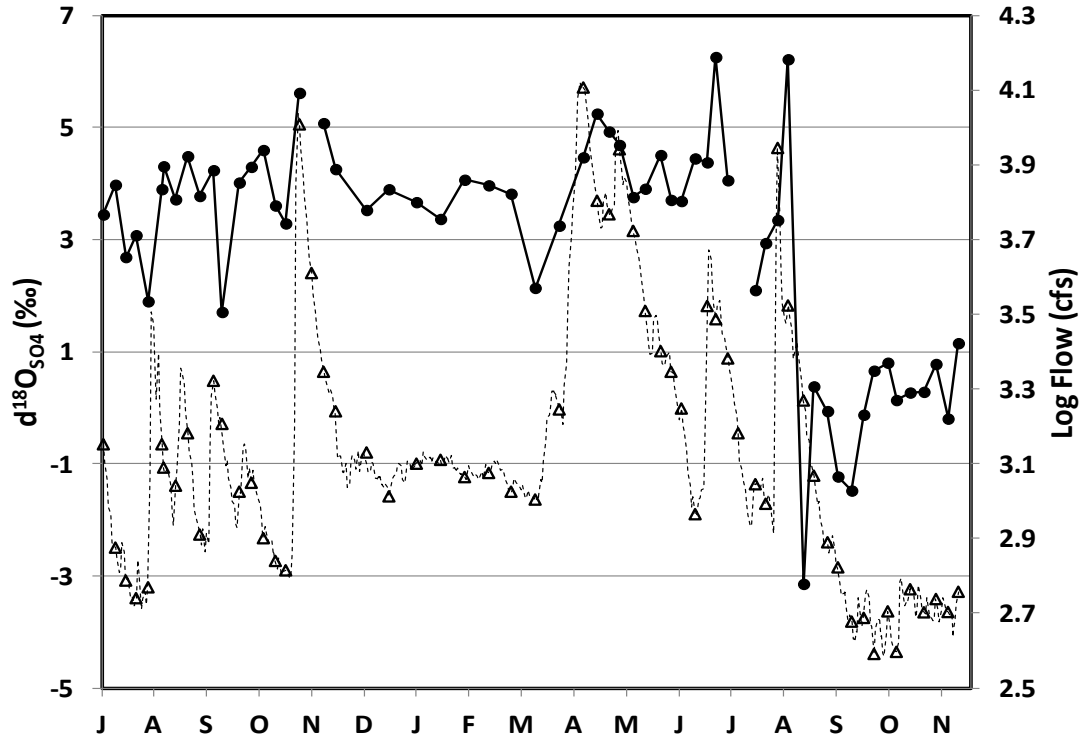
Appendix A4: Sequential Framework Model for $\delta^{34}S_{SO4}$ and $\delta^{18}O_{SO4}$

An interpretive framework for $\delta^{34}S_{SO4}$ and $\delta^{18}O_{SO4}$ in water samples from the St. Louis River Basin

Michael E. Berndt

A Minnesota Department of Natural Resources Memo

June 8, 2011

The Minnesota Department of Natural Resources has recently begun collecting samples and having them analyzed for $\delta^{34}S_{SO4}$ and $\delta^{18}O_{SO4}$ (Berndt and Bavin, 2009, 2011a, 2011b). The detailed changes in $\delta^{34}S_{SO4}$ and $\delta^{18}O_{SO4}$ accompanying sulfur cycling in the watershed are complex and can involve many smaller steps that occur simultaneously and sequentially.   The end result is a distribution that spans from 0 to 40 ‰ for $\delta^{34}S_{SO4}$ and from -12 and +18 ‰ for $\delta^{18}O_{SO4}$ (Figure 1).   However the distribution is unusually shaped in that samples with 0 to 20 ‰ values for $\delta^{34}S_{SO4}$ all have $\delta^{18}O_{SO4}$ values less than about +8, while all but a single sample with $\delta^{34}S_{SO4}$ greater than 20‰ have $\delta^{18}O_{SO4}$ values greater than +8 ‰. Moreover, the population of samples with $\delta^{34}S_{SO4}$ values less than 20‰ forms a triangular shaped patterning in $\delta^{34}S_{SO4}$ - $\delta^{18}O_{SO4}$space, revealing a very narrow range of $\delta^{34}S_{SO4}$ for samples with low $\delta^{18}O_{SO4}$ values, and an ever-expanding range of $\delta^{34}S_{SO4}$ as $\delta^{18}O_{SO4}$ reaches a value of approximately +8 ‰. The purpose of this document is to provide an interpretation for this distribution of samples.

The interpretation begins first by considering the $\delta^{34}S_{SO4}$ that might be expected for $SO_4^=$ derived by oxidation of sulfide minerals in the Biwabik Iron Formation.   Theriault et al. (2011) summarized and provided new sulfur isotopic data for sulfides in the iron formation. Several populations were identified including primary sulfides deposited at the time that the formation was laid down and various secondary mineral populations that occurred as veins, framboids, and euhedral to subhedral pyrite grains. The primary sulfides had $\delta^{34}S_{SO4}$ for sulfides that ranged narrowly from about +2 to   +13 ‰, while the secondary sulfides had $\delta^{34}S_{SO4}$ ranging from -40 to + 80, indicating that post-depositional oxidation and re-reduction processes were widely varying in the formation.

Generally, sulfur isotope fractionation associated with simple oxidation of pyrite is minor and we can, thus, make the approximation that $\delta^{34}S_{SO4}$ in water samples found close to the site where oxidation is taking place represents the average $\delta^{34}S$ of Fe-sulfides (e.g., $\delta^{34}S_{pyrite}$) being oxidized at the site. In practice, waters sampled at sites closest to the Iron Range and with the least chance of interacting with organic-rich wetlands have $\delta^{34}S_{SO4}$ values that range typically between about +4 and +9 ‰. This range is consistent with derivation from primary sulfides in the Iron Formation (or of secondary sulfides with average $\delta^{34}S_{pyrite}$ that falls within the range of the primary sulfide field).   In the framework shown in Figures 1 and 2, we assume that $\delta^{34}S_{pyrite}$ = 5.0 ‰, although it is recognized that the observed range is between +4 and +9 ‰. If the primary sulfide had a value of +4 or +9 ‰, the entire frame can be

shifted horizontally by -1 or right by +4 ‰, respectively, to account for cycling of sulfate derived from lower or higher $\delta^{34}S_{pyrite}$, respectively.

In contrast to $\delta^{34}S_{SO4}$, the $\delta^{18}O_{SO4}$ value produced when Fe-sulfides are oxidized does not depend at all on $\delta^{34}S_{pyrite}$ but depends, rather, on the mechanism of oxidation and the source of oxygen.   Toran and Harris (1989) point out that eight separately electron transfers must occur if sulfur in an oxidation state of -2 is converted $SO_4^=$ where sulfur has a +6 charge.   In addition, the central sulfur molecule obtains four oxygen atoms, each with its own separate potential source and fractionation factor that can affect the $\delta^{18}O_{SO4}$ value.   In terms of oxygen exchange reactions with water and the atmosphere, there are three broad types of oxidation reactions possible:

Type 1: $S^= + 2O_2 = SO_4^=$ (O_2 is oxidizing agent, and O in SO4 all comes from O_2)

Type 2: $S^= + 2O_2^* + 4H_2O = SO_4^= + 4H_2O^*$ (O_2 is oxidizing agent, but O in SO_4 is from H_2O)

Type 3: $S^= + 8Fe^{+++} + 4H_2O = SO_4^= + 8H^+ + 8Fe^{++}$ (Fe^{+++} is oxidizing agent, and O in SO_4 is all from H_2O)

Although mineral-derived O_2 could potentially be incorporated in the $SO_4^=$ molecule, this type of exchange is almost never observed.   Depending on the relative importance of each type of reaction, a different fraction of the oxygen in $SO_4^=$ will be derived from either atmospheric O_2 or H_2O. $\delta^{18}O_{SO4}$ for the wide range of processes can be computed from the following equation:

$$\delta^{18}O_{SO4}(‰) = f_{H2O} (\delta^{18}O_{H2O} + E_{H2O}) + f_{O2}(\delta^{18}O_{O2} + E_{O2})$$

where f_{H2O} and f_{O2} are the fraction of sulfate oxygen atoms derived from ambient water and atmospheric oxygen, respectively. E_{H2O} and E_{O2} are the per mil (‰) fractionations for $SO_4^=$ and the subscripted component, ambient water or atmospheric oxygen, respectively.   Toran and Harris reviewed two biologic pathways and one abiologic process that resulted in f_{O2} values of 0, 0.75, and 0.875, respectively. E_{O2} values ranged from -4.3 to -11.4 ‰ while E_{H2O} values ranged from -6 to 4.1 ‰, depending on the assumptions made in their derivation.

Meteoric water in this region has $\delta^{18}O_{SO4}$ of approximately -10 ‰, which corresponds closely to values for water sampled close to the mining region.   This suggests oxidation in the Iron Range is commonly dominated by Type 2 or Type 3 reactions, such that $f_{O2}=0$, $f_{H2O} = 1$, and further that E_{H2O} may be close to 0 ‰.   This is interpreted in Figure 1, primarily as a Type 3 process, whereby oxidation of pyrite in the Biwabik Iron Formation results in waters containing $SO_4^=$ with $\delta^{18}O_{SO4}$ values close to the meteoric water value of -10 ‰ and $\delta^{34}S_{SO4}$ values set by that of the primary sulfide minerals.

As another possible means to oxidize sulfides in the iron formation, we consider a second Toran and Harris case, where $f_{O2}=0.75$, $f_{H2O} = 0.25$, $E_{O2}= -4.3$ to -11.4 ‰, and $E_{H2O} = 4.1$ to -6.1 ‰.   By this process and using a value of +23.5 ‰ to represent atmospheric O_2 and -10 ‰ for meteoric water, we calculate $\delta^{18}O_{SO4}$ values ranging from 4.6 to 12.7‰.   For samples with low $\delta^{34}S_{SO4}$ (indicative that $\delta^{18}O_{SO4}$ was less impacted by sulfate reduction, as discussed below) the maximum $\delta^{18}O_{SO4}$ values found in the

DNR studies are in the +6 to +8 ‰ range, consistent with having been derived by an O_2-mediated process (combined Type 1 and Type 2 processes) with f_{O2} around 0.75. The final $SO_4^=$ oxidation process discussed by Toran and Harris (1989) (with the fraction of O_2 derived from the atmosphere equal to 0.875) generates $\delta^{18}O_{SO4}$ values ranging from +8 to +16 ‰ using meteoric water and atmospheric oxygen.   This value is above all of the values measured for low-$\delta^{34}S_{SO4}$ that were sampled in the watershed.

In summary, for water samples containing low $\delta^{34}S_{SO4,}$ a diverse set of oxidation mechanisms appears to be active in the watershed with f_{O2} ranging from 0 to 0.75 – and constraining the resulting $\delta^{18}O_{SO4}$ values to fall between -12 and +8 ‰. It is noted, further, that waters sampled close to the Iron Range sites tend to fall closer to the "Fe-mediated oxidation" point and samples collected far downstream in the St. Louis River have $\delta^{18}O_{SO4}$ values that is always ranges from +2 to +6. Though mass balance considerations indicate that most of the $SO_4^=$ in the St. Louis River at Mile 36 is derived from the Iron Range mining district, it is apparent that the $\delta^{18}O_{SO4}$ value shifts considerably as the $SO_4^=$ released from the waste rock piles and pits on the Iron Range migrates through the wetlands, lakes, and streams downstream from the mining region.   This process of oxygen isotope re-equilibration for $SO_4^=$ without a corresponding change in sulfur isotopic values is not understood, but similar effects have been previously noted by Caron et al. (2003) in a similar region and by Turchyn and Schrag (2004) on a global scale for seawater. To re-equilibrate the $SO_4^=$, the central sulfur atoms in the original $SO_4^=$ molecules must be stripped of their original oxygen atoms (e.g., reduced) and have them replaced by a different set of oxygen atoms (e.g., re-oxidation of the sulfide). This behavior has been observed by Berndt and Bavin (2011b) on both the watershed and sub-watershed scales.

The left edge of the frame, extending directly upwards from the Fe-mediated BIF sulfide point, indicates the changes in $\delta^{18}O_{SO4}$ that could be expected for 0 to 100% re-equilibration of the oxygen atoms in the $SO_4^=$ as it travels from the iron formation to Mile 36 in the St. Louis River. The vast majority of samples collected from the watershed have $\delta^{34}S_{SO4}$ as $\delta^{18}O_{SO4}$ that lie distinctly to the right of this, indicative that significant sulfate reduction occurs in the watershed.

Sulfate reduction is a process that affects both $\delta^{34}S_{SO4}$ and $\delta^{18}O_{SO4}$ at the same time, because the bacteria that drive sulfate reduction preferentially use $SO_4^=$ atoms containing the lighter atoms.   In Figure 1, the line extending upward and to the right from the Fe-mediated oxidation point is drawn with a slope of 1.0, representative of a sulfate reduction process whereby the isotope fractionation factor is considered to be exactly the same for both O and S (e.g., the fractionation is determined only by the weight of the molecule and not based on the identity of the atom causing the greater molecular weight). The $SO_4^=$ reduction process was, in this case, assigned a fractionation factor ($\Delta^{34}S_{SO4-Sulfide}$) of +17‰, consistent with data from Berndt and Bavin (2011a) for subsurface bacterial sulfate reduction observed near a tailings basin on the Iron Range. That is, it was assumed that the sulfide that forms is 17‰ lighter than the $SO_4^=$ from which it is derived. Once the sulfide forms, the $\delta^{34}S_{SO4}$ of the residual sulfate becomes elevated. A Rayleigh distillation process is assumed, whereby sulfide formed early in the process becomes instantaneously isolated from the system.

By this process, the $\delta^{34}S_{SO4}$ would shift from +5 to approximately +33 while $\delta^{18}O_{SO4}$ shifted from -10 to 18 if 80% of the sulfate released by oxidation was reduced elsewhere in the environment. Subsequent re-equilibration of the oxygen isotopes in the residual sulfate would cause the $\delta^{18}O_{SO4}$ values to shift downward, approaching a value near 6‰. It is noted that $\delta^{34}S_{SO4}$ as $\delta^{18}O_{SO4}$ distribution in samples collected so far imply that sulfate reduction generally precedes the oxygen isotope equilibration process. If the reaction sequence occurred in the opposite order, we might expect to find samples in the 5 to 20‰ $\delta^{34}S_{SO4}$ range with $\delta^{18}O_{SO4}$ values between +8 and +18. The distribution also suggests that the majority of the sulfide oxidation in the watershed must occur by an Fe^{+++} mediated process. $SO_4^=$ reduction following an O_2 mediated process would also be expected to produce some samples in the +5 to +20‰ $\delta^{34}S_{SO4}$ range with $\delta^{18}O_{SO4}$ values between +8 and +18 ‰. Extensive sampling in the watersheds has turned up no such samples so far.

Although the framework interpretation displayed in Figure 1 can be used to account for the distribution of isotopic data from samples so-far collected in and near the St. Louis River basin, considerable caution is urged for strict numeric application. In particular, it is possible, if not likely, that more than one type of sulfate-reducing bacterial process is occurring in the watershed. If so, then the sulfur and oxygen fractionation factors could be different from the values used to construct the frame in Figure 1 (see Detmers et al (2001) for list of $\Delta^{34}S_{SO4\text{-}Sulfide}$ values as function of different sulfate reduction processes). The percentages of sulfate removed would be shifted upwards or downwards, depending on the actual fractionation factor used. Moreover, the framework assumed a starting value of +5 for $\delta^{34}S_{SO4}$. The entire frame will shift left or right depending on what the actual starting value is for a particular situation within the watershed.

The interpretation is, however, believed by the author to be representative of the overall processes that dominate SO_4 cycling in the watershed – as illustrated in Figure 2. $SO_4^=$ in the Iron Range is most commonly released from primary sulfides, likely by an Fe^{+++}-mediated oxidation process.   This $SO_4^=$ is variably reduced, sometimes by more than 90% (confirmed using alternate method in one case). Once released into the open water flow system, the $\delta^{18}O_{SO4}$ in the $SO_4^=$ that remains following the reduction process is re-equilibrated without much further change in $\delta^{34}S_{SO4.}$

Berndt, M. E. and Bavin, T. K. (2009) Sulfate and Mercury Chemistry of the St. Louis River in Northeastern Minnesota: A Report to the Minerals Coordinating Committee. Minnesota Department of Natural Resources, Division of Lands and Minerals. St. Paul, MN, USA. 83 p.

Berndt, M. E. and Bavin, T. K. (2011a) Sulfate and Mercury Cycling in Five Wetlands and a Lake Receiving Sulfate from Taconite Mines in Northeastern Minnesota: A Report to Iron Ore Cooperative Research Program. Minnesota Department of Natural Resources, Division of Lands and Minerals. St. Paul, MN, USA.

Berndt, M. E. and Bavin, T. K., (2011b) A preliminary assessment of sulfate release and sulfate cycling processes in the St. Louis River watershed. An Environmental and Natural Resources Trust Fund Progress Report. Minnesota Department of Natural Resources Submitted Report.

Caron, F., Tessier, A., Kramer, J. R., Schwarz, H. P., Rees, C. E. (1986) Sulfur and oxygen isotopes of sulfate in precipitation and lakewater, Quebec, Canada. Applied Geochemistry 1: 601-606.

Detmers, J., Bruchert, V., Habicht, K. S., and Kuever, J (2001) Diversity of sulfur isotope fractionations by sulfate-reducing proakaryotes. Appl. Environ. Microbiol. 67, 888-894.

Theriault, S. A., Miller, J. D., Berndt, M. E., and Ripley, E. M. (2011) The mineralogy, spatial distribution, and isotope geochemistry of sulfide minerals in the Biwabik Iron Formation. Institute for Lake Superior Geology, Abstract. 2 pages.

Toran, L. and Harris, R. F. (1989) Interpretation of sulfur and oxygen isotopes in biological and abiological sulfide oxidation. Geochim. Cosmochim. Acta. 53, 2341-2348.

Turchyn, A. V. and Schrag, D. P. (2004) Oxygen isotope constraints on the sulfur cycle over the past 10 million years. Science. 303, 2004-2007.
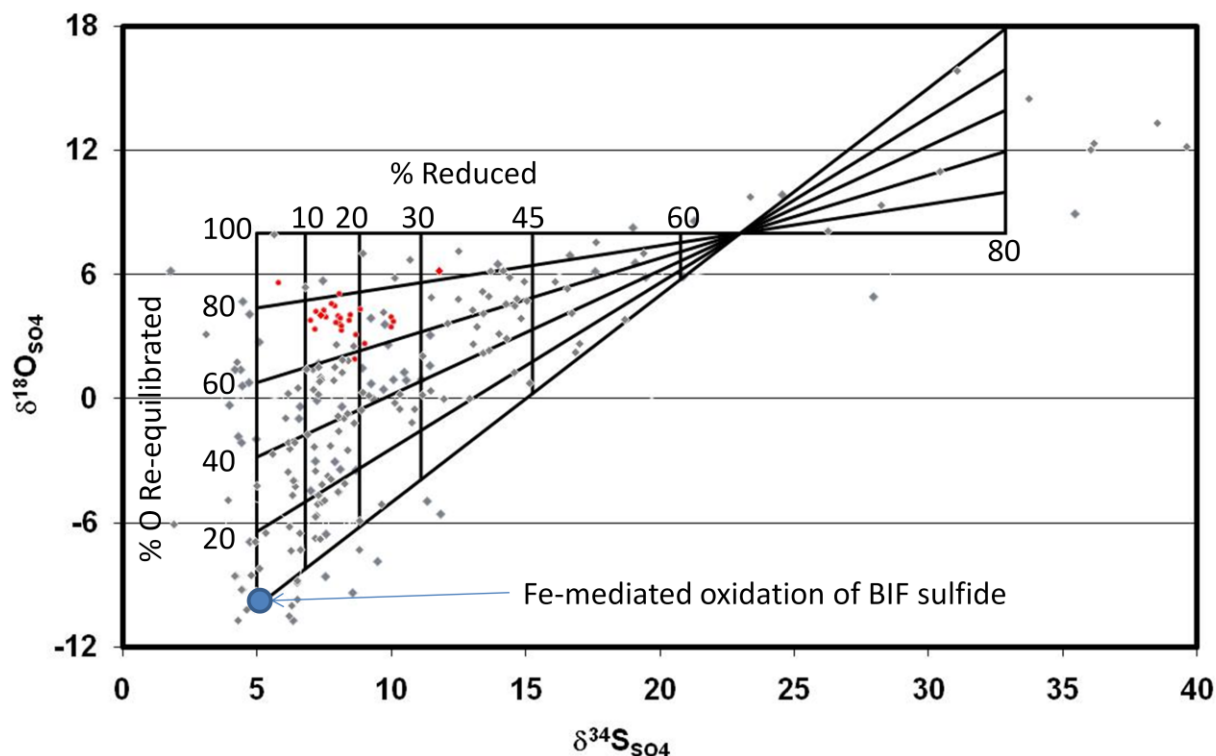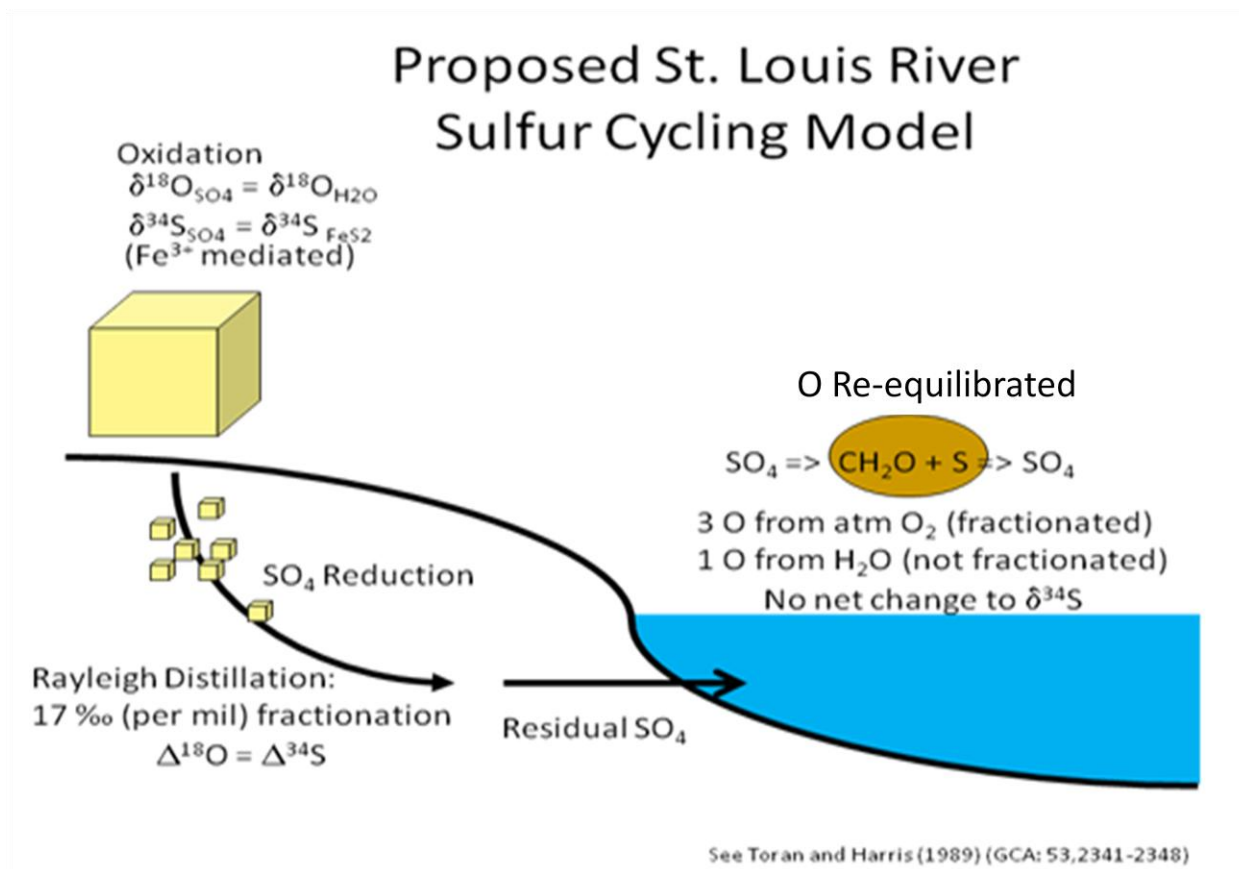
Figure 1. $\delta^{34}S_{SO4}$ and $\delta^{18}O_{SO4}$ data collected through July 2011 by the Minnesota Department of Natural Resources in or near the St. Louis River watershed.   Dark gray points are assorted data from

lakes, streams, rivers, and wells. Red points are from the St. Louis River at Mile 36. See the text and Figure 2 for a description of the framework model used to interpret the isotopic data from this watershed.

Proposed St. Louis River Sulfur Cycling Model

Oxidation
$\delta^{18}O_{SO4} = \delta^{18}O_{H2O}$
$\delta^{34}S_{SO4} = \delta^{34}S_{FeS2}$
(Fe^{3+} mediated)

O Re-equilibrated

$SO_4 \Rightarrow CH_2O + S \Rightarrow SO_4$

3 O from atm O_2 (fractionated)
1 O from H_2O (not fractionated)
No net change to $\delta^{34}S$

SO_4 Reduction

Rayleigh Distillation:
17 ‰ (per mil) fractionation
$\Delta^{18}O = \Delta^{34}S$

Residual SO_4

See Toran and Harris (1989) (GCA: 53,2341-2348)

Figure 2. Preliminary sequential model used to account for isotopic data in the St. Louis River watershed. See text.